

# BLOCK CAVE MINE INFRASTRUCTURE RELIABILITY APPLIED TO PRODUCTION PLANNING

by

ENRIQUE RUBIO

B. Eng., Universidad de Chile, Chile, 1998  
M.A.Sc., The University of British Columbia, Canada, 2002

A THESIS SUBMITTED IN PARTIAL FULFILLMENT OF  
THE REQUIREMENTS FOR THE DEGREE OF

DOCTOR OF PHILOSOPHY

in

THE FACULTY OF GRADUATE STUDIES  
(Mining Engineering)

THE UNIVERSITY OF BRITISH COLUMBIA  
February 2006

©Enrique Rubio, 2006

## ABSTRACT

The production promise of a mine should reflect the fundamental models that sustain the mining system. Commonly this promise is formalized by the production schedule of a mine which is a bankable document that supports the decision of whether or not to pursue (or continue to pursue) the mining venture. Currently there are several computer based applications that enable mining engineers to compute a production schedule for a block cave operation. However, several operational upsets such as hang ups, oversize material, wet muck and rock instability affect the availability of mining infrastructure jeopardizing the original production estimates. These upsets can be related to geotechnical properties and caving processes in the rock mass. The current schedulers do not incorporate or account for geotechnical properties and caving processes. Thus, they often overestimate the production capacity of the mine.

In this dissertation, a methodology has been devised for using observations of the failure frequency of mining infrastructure such as draw points, production drifts and ore passes to assess the reliability of this infrastructure to sustain a given production schedule. The novel aspect of measuring draw point reliability in this way is that it effectively subsumes complex geotechnical phenomena that lead to draw point failure such as geological conditions, stress concentration, or coarse fragmentation. The research found that the rate of occurrence of failure of a draw point can be characterized by a "bathtub curve" whose shape changes with the geotechnical characteristics of the rock mass, mining system and stress regime.

The final phase of the research integrated the estimated mining infrastructure reliability into production scheduling through a reliability model. This integrated model provided the ability to generate from a number of draw points, a production plan in which a subset of the draw points will yield the requested tonnage with an associated degree of reliability based on the reliability of individual components of the mining infrastructure. Validation of the reliability model demonstrated that it does reproduce the tonnage distribution curve and consequently estimates the technical uncertainty of a production schedule related to mining infrastructure availability.

## TABLE OF CONTENTS

<b>ABSTRACT.....</b>	<b>ii</b>
<b>TABLE OF CONTENTS .....</b>	<b>iii</b>
<b>LIST OF TABLES .....</b>	<b>v</b>
<b>LIST OF FIGURES .....</b>	<b>vi</b>
<b>ACKNOWLEDGMENTS .....</b>	<b>ix</b>
<b>1 INTRODUCTION.....</b>	<b>1</b>
1.1 Statement of the Problem.....	4
1.2 Research Question .....	7
1.3 Contribution of the Thesis .....	8
1.4 Organization of the Work .....	9
<b>2 LITERATURE REVIEW .....</b>	<b>10</b>
2.1 History of Block Caving .....	14
2.2 Fundamental Models of Block Caving .....	16
2.3 Block Cave Production Scheduling .....	20
2.4 Uncertainty in Block Cave Production Scheduling .....	25
<b>3 FAILURE BEHAVIOUR OF MINING INFRASTRUCTURE .....</b>	<b>28</b>
3.1 Operational Database .....	28
3.1.1 Daily tonnage records .....	29
3.1.2 Daily status records .....	31
3.1.3 Convergence records.....	32
3.1.4 Records of draw point hang up .....	33
3.1.5 Records of oversize draw points .....	36
3.1.6 Production schedules .....	36
3.2 Effect of Geotechnical Events on Production Performance .....	36
3.2.1 Effect of hang ups on production performance.....	37
3.2.2 Effect of production performance on induced stresses .....	40
3.3 Failure of mining infrastructure .....	47
3.3.1 Data Analysis for computing draw point ROCOF curve.....	55
3.4 Draw point ROCOF curve as a function of geotechnical domains.....	56
3.5 Draw Point Reliability as an Indicator of Geotechnical Events .....	59

3.5.1	Measurements of draw point reliability .....	60
3.5.2	Effect of hang up frequency on draw point reliability .....	63
3.5.3	Effect of induced stress on draw point reliability .....	63
<b>4</b>	<b>PRODUCTION SCHEDULING INTRODUCING THE CONCEPT OF RELIABILITY .....</b>	<b>65</b>
4.1	Definition of System Reliability .....	65
4.2	Reliability of a System with Redundancy at the Component Level .....	68
4.3	Block Cave Reliability Model .....	70
4.3.1	Draw point productivity as a function of draw point yield and draw cycle.....	76
4.4	Production Scheduling Integrating Draw Point Reliability .....	78
4.5	Production Schedule Reliability .....	83
4.6	Sensitivity of Different Inputs to the Reliability Model .....	87
4.7	Using the Reliability Model to Assess the Value of Overdrawn Draw Points .....	89
4.8	Using the Reliability Model to Support Tactical Decisions .....	90
4.9	Definition of Production Capacity of a Block Cave Mine using Reliability .....	91
4.10	Expected Tonnage versus Adjusted Draw Rate to Assess Production Capacity .....	93
<b>5</b>	<b>MODEL VALIDATION .....</b>	<b>95</b>
5.1	Reliability Model Calibration Using Absolute Reliability .....	96
5.2	Reliability Model Calibration Using Tonnage Distribution .....	98
5.3	Calibration Based On Expected Tonnage per Period .....	101
<b>6</b>	<b>DISCUSSION AND CONCLUSIONS .....</b>	<b>103</b>
6.1	Discussion .....	103
6.2	Conclusions .....	106
6.3	Recommendations .....	108
	<b>REFERENCES.....</b>	<b>110</b>
	<b>APPENDICES .....</b>	<b>120</b>
<b>A</b>	<b>Proposed Operational Database in Block Cave Mines.....</b>	<b>120</b>
<b>B</b>	<b>Recursive Algorithm for the Reliability of a k-out-of-n System.....</b>	<b>123</b>
<b>C</b>	<b>Proposed Production Scheduler Workflow .....</b>	<b>127</b>



## LIST OF TABLES

Table 3.1 Geotechnical information of the mine operations.....	28
Table 3.2 Features of the mining system .....	29
Table 3.3 Operational and planning data collected from the mines .....	29
Table 3.4 Example of daily tonnage record from Mine M1 .....	30
Table 3.5 Example of cumulative monthly tonnage drawn from Mine M1 .....	31
Table 3.6 Example of Height of Draw (HOD) calculation.....	31
Table 3.7 Example of draw point status extracted from database of mine M1 .....	32
Table 3.8 Convergence measurements taken along production drift 13 from mine M1 .....	33
Table 3.9 Example of monthly hang up records from mine M2.....	35
Table 3.10 Example of monthly tonnage from mine M2.....	35
Table 3.11 Calculation of hang ups/ton based on hang up and tonnage records.....	35
Table 3.12 Counting failures as a function of the daily draw point status records.....	48
Table 3.13 Counting process of failures for draw point D54 .....	49
Table 3.14 Estimation of Draw Point Rate of Occurrence of Failure.....	50
Table 3.15 Average draw point ROCOF for Mine M1.....	53
Table 4.1 Draw point reliabilities to compute the entries .....	73
Table 4.2 Intermediate entry reliability table, $R_e(i, j)$ .....	74
Table 4.3 Estimation of crosscut production capacity based on reliability estimates .....	83
Table 4.4 Production profile at 85% reliability .....	86
Table 5.1 Comparison of actual versus computed reliability .....	100
 Table B.1 Draw point reliabilities to compute the entries $R_e(i, j)$ .....	 126
Table B.2 Intermediate entry reliabilities $R_e(i, j)$ .....	126

## LIST OF FIGURES

Figure 1.1 Chuquicamata mine, Codelco – Chile (Flores et al, 2004).....	2
Figure 1.2 Production profile of eight operating block cave mines.....	3
Figure 1.3 Actual versus forecast production of an existing operation .....	5
Figure 1.4 One month of tonnage reconciliation per draw point.....	5
Figure 2.1 Mechanized panel caving at Henderson mine (Doepken, 1982).....	10
Figure 2.2 Layout of the panel cave mining system (Flores, 2004) .....	12
Figure 2.3 Production level geometry (Moss et al, 2004).....	13
Figure 2.4 Undercutting method used in block caving (Barraza and Crorkan, 2000).....	14
Figure 2.5 Fundamental models that affect the planning parameters of a block cave mine (Rubio et al, 2004) .....	17
Figure 2.6 Typical production schedule from an operating mine.....	21
Figure 2.7 Current mine planning process in block cave mining (Rubio et al, 2004).....	23
Figure 3.1 Draw point blockage in block caving (Barlett, 2000) .....	34
Figure 3.2 Oversize at a draw point of mine M2 .....	37
Figure 3.3 Hang up frequency as a function of draw point maturity.....	39
Figure 3.4 Draw point monthly productivity as a function of hang up frequency.....	40
Figure 3.5 Illustration of the angle of draw in a draw profile along a production drift.....	41
Figure 3.6 Effect of angle of draw on the normalized deviatoric stress experienced at the cave front (Rubio et al, 2004).....	42
Figure 3.7 Drift collapse due to a shallow angle of draw .....	43
Figure 3.8 Drift collapse due to a steep angle of draw .....	43
Figure 3.9 Drift collapse due to a sudden change on the angle of draw .....	44
Figure 3.10 Draw point minor apex pillar deformation as a result of uneven draw at mine M4..	46
Figure 3.11 Total crosscut deformation as a function of the draw cycle.....	47
Figure 3.12 Operational records of draw point status data .....	48
Figure 3.13 Cumulative number of failures for a single draw point.....	50
Figure 3.14 Experimental draw point ROCOF for draw point D54 .....	52
Figure 3.15 Draw point ROCOF curve for mine M1.....	54
Figure 3.16 Bathtub curve for a mechanical component (Hoyland and Rausand, 1994) .....	55
Figure 3.17 Draw point ROCOF curve for different production areas of mine M1 .....	57

Figure 3.18 Draw point ROCOF curve comparison between two operating block cave mines ...	58
Figure 3.19 Average monthly draw point availability from mine M1 .....	62
Figure 3.20 Comparison of draw point reliability versus draw point availability .....	62
Figure 3.21 Effect of hang up frequency on draw point reliability .....	63
Figure 3.22 Effect of convergence on draw point reliability .....	64
Figure 4.1 Components of a traditional mining system (Kazakidis and Scoble, 2002).....	66
Figure 4.2 System reliability based on the reliability of the components $r_1, r_2, r_3$ (Hoyland and Rausand, 1994) .....	67
Figure 4.3 Comparison between series parallel and parallel series for 3 components with 100% component redundancy .....	68
Figure 4.4 Selection of 10 out of 15 components to compare with the performance of 10 components connected in series.....	70
Figure 4.5 Reliability comparison between a series and a $k$ -out-of- $n$ system.....	70
Figure 4.6 Reliability block diagram of a block cave production system .....	71
Figure 4.7 Redundancy versus system reliability .....	75
Figure 4.8 Impact of draw point selection on crosscut reliability.....	76
Figure 4.9 Draw point yield as a function of height of draw .....	77
Figure 4.10 Draw cycle time as a function of $k$ .....	78
Figure 4.11 Expected evolution of actual tonnage distribution .....	79
Figure 4.12 Proposed mine planning model including reliability model.....	80
Figure 4.13 Scheme to compute the reliability of a given production schedule.....	82
Figure 4.14 Assessment of reliability based on a computed production schedule .....	84
Figure 4.15 Production schedules including reliability as a target .....	85
Figure 4.16 Production schedules with integrated reliability .....	86
Figure 4.17 Effect of redundancy at the draw point and crosscut level.....	87
Figure 4.18 Sensitivity of the reliability model to the ROCOF curve .....	88
Figure 4.19 Sensitivity to crosscut productivity .....	88
Figure 4.20 Assessing the effect of overdrawn draw points in the production schedule.....	90
Figure 4.21 Reliability model used to prioritize secondary blasting .....	91
Figure 4.22 Evolution of the production capacity distribution throughout a production schedule .....	92

Figure 4.23 Stochastic definition of production capacity of a block cave mine.....	93
Figure 4.24 Expected tonnage computed using the reliability model and the fudge factor approach.....	94
Figure 5.1 Data flow to compute the reliability of the original production schedules of mines M1 and M2 .....	96
Figure 5.2 Calibration of computed reliability using a constant crosscut production capacity ....	97
Figure 5.3 Calibration of computed reliability using variable crosscut production capacity across the active layout .....	98
Figure 5.4 Dataflow used to estimate actual reliability of a 60 days period based on the tonnage distribution curve .....	99
Figure 5.5 Actual reliability as a function of actual tonnage distribution for a period of 60 days	99
Figure 5.6 Reliability model calibration using mine M1 data set.....	100
Figure 5.7 Reliability model calibration using mine M2 data set.....	101
Figure 5.8 Comparison between expected tonnage versus actual tons mined from mine M2....	102
Figure A.1 The reconciliation model.....	121
Figure B.1 Intermediate reliability calculation .....	125
Figure C.1 Process flow for the proposed scheduler including reliability.....	127
Figure C.2 Draw point list used in the reliability model.....	128
Figure C.3 Status matrix used in the reliability model .....	128
Figure C.4 Tonnage matrix used in the reliability model .....	129
Figure C.5 Draw point yield curve used in the reliability model.....	129
Figure C.6 Draw point ROCOF curve used in the reliability model .....	130
Figure C.7 Draw point database used as part of the reliability model .....	130
Figure C.8 Tonnage targets per period used in the reliability model.....	131

## ACKNOWLEDGMENTS

I would like to express my gratitude to The Universidad de Chile Departamento de Ingeniería de Minas, the institution that made possible my MASc and PhD studies at UBC:. In particular I would like to thank the individuals that constantly supported my graduate studies in Canada: Francisco Brieva, Bruno Behn, Aldo Casali, Jaime Chacon and Hans Goefert.

My research had been aided financially by Codelco – Chile through its support to the mining technology group at the Universidad de Chile. I would like to express my gratitude to Juan Enrique Morales, Fernando Geister and Octavio Araneda for enabling my research.

Faculties at The University of British Columbia, Mining Engineering Department who were always willing to support my research and to contribute to the concepts presented in this dissertation. My supervisor Dr. Scott Dunbar for the amazing way of keeping the balance between science and engineering application on his continuous contributions made to this research. Also I would like to acknowledge the rest of the committee members Dr. Malcolm Scoble, Dr. Tony Diering and Dr. Rob Hall for their constant effort to contribute on their best to the success of the research presented in this dissertation. To my colleagues graduate students at UBC for their patience to listen many times about block cave production planning and reliability theory.

To Gemcom software international for giving me the opportunity to collaborate in engineering several block cave mines operating around the world. In particular I would like to acknowledge Dr. Tony Diering not only on his quality as a committee member but also as boss, leader and friend. Many of the concepts expressed in this dissertation have been derived out of discussions and work that has been done in the last five years as part of the Gemcom team.

There are many mining companies and especially engineers that have contributed with data, expertise and discussion over the years to make this research applicable to the actual stage of block cave mining. PT Freeport Indonesia personnel: Eddy Samosir, Rudy Prasetyo, Cahya Kurniawan, Chuck Brannon, Dave Flient, Widyo Yudanto, Daulat Napitupulu, Eman Widijanto, Fourmarch Sinaga, Tad Szwedzicki, Husni Sahupala. Palabora Mining Company: Sheperd Dube,

Sergei Diachenko, Sam Ngidi, Lessane Sennanye, Lammie Nienaber, Jaggard Russell and Matt Gili. Rio Tinto technical services: Allan Moss and Mark Howson. Codelco Chile: Mario Vickuña, Augusto Aguayo, Gabriel Valenzuela, Patricio Vergara, Jorge Baraqui, Francisco De La Huerta, Mauricio Barraza, Rigoberto Muñoz. I would like to acknowledge specially to my good friends Mauricio Melendez and Alejandro Moyano for being always willing to collaborate and discuss mining concepts and ideas. Mauricio has contributed in a great deal specially to the concept of angle of draw and damage in block cave mines. Alejandro Moyano has shown me what a real mining engineer is by always bringing applied concepts and solutions to the operation and planning of a mine.

I would like to specially thank my parents for their constant encouragement to finish my studies at UBC. Dad your help has been invaluable in the many trips you made to Vancouver to assist me keeping the balance between my work and family. Finally I would like to thank my children Natalia and Matias for giving me the energy to continue and ultimately finish my dissertation.

This dissertation is dedicated to my outstanding wife Alex for her awesome way of expressing her love and support to me over the years. Many of the accomplishments on my career have been the product of having you as a wife with your understanding and patience over the many trips in which you had to stay by yourself taking care of everything especially our children. So I dedicate this work to you.

# 1 INTRODUCTION

Mine planning consists of defining the source, destination and timing of extraction of every single unit of mineral resource during the life of the mine. The mine plan plays a significant role in linking the strategic objectives of a mining company to the operation of the mine. The production schedule is most likely one of the most important components of the production plan since it defines the tonnages and grades to be mined throughout the life of the mine. This document is often used by bankers, share holders and other stake holders to assess the potential benefits of a mining venture. In consequence, the production schedule delineates the business promise of a mining company. If the production schedule of a company is weak, the economics of this venture will be rather questionable. Also, if the strategic objectives are not reflected in the day to day operational performance, it is because the mine plan has been misleading.

Several operations around the world are looking to apply low cost and highly productive mining methods that could work in a low grade, competent rock mass and deep ore bodies. In particular several open pit mines around the world such as Chuquicamata mine in Chile shown in Figure 1.1 Chuquicamata mine, Codelco – Chile (Flores et al, 2004) are looking to postpone the closure of the mine by introducing underground mining methods. In order to maximize the utilization of existing infrastructure such as power and production plants, the chosen methods need to be highly productive and cost effective. Thus massive underground mining methods will most likely be used. One such method, block caving, has gained popularity in recent years due to its productivity and economic characteristics. Nevertheless, very little research has been conducted on geotechnical principles which dictate how the mining system works. Thus there is a considerable amount of uncertainty related to the way how a rock mass behaves in a caving environment and this leads to uncertainty in planning block cave mines.



**Figure 1.1 Chuquicamata mine, Codelco – Chile (Flores et al, 2004)**

Many definitions of block caving can be found in the literature, however one of the most conceptual as well as practical is given by Laubscher (1994) “*cave mining refers to all mining operations in which the ore body caves naturally after undercutting its base. The caved material is recovered using draw points*”. One of the main conclusions that one can make from this definition is that block caving relies mainly on the interaction between the rock mass and the stresses induced by the cave propagation to surface and on the movement of large quantities of rock.

Since the knowledge of rock mass behaviour such as caveability, fragmentation, stresses, flow mechanisms, in block caving is limited, the planning methods used in block caving should account for the uncertainty in the geotechnical behaviour of the rock mass. However the current methods used for scheduling block cave mines are rather deterministic and do not include such uncertainty. This leads to production schedules that do not account for operational upsets triggered by geotechnical events. In consequence, the current scheduling methods often compute production targets that are too optimistic and which are difficult or impossible to fulfill during the operation of the mine. The resulting production schedule computed as part of the production plan often differs from the actual tonnage mined. Figure 1.2 shows a chart of actual production from five different mines during an eight to twelve year period. This chart has been constructed



as part of the research presented in this dissertation, to show that there is a wide range of possible production profiles for a given deposit during the life of the mine, depending on the rock mass properties, size of the footprint, ore body geometry, stress behaviour, availability of capital and ultimately the strategic objective of the company.

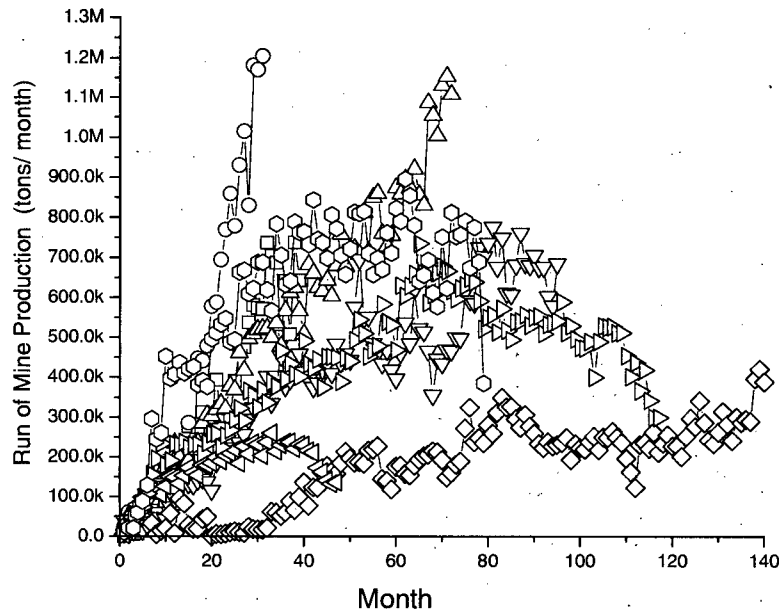


**Figure 1.2 Production profile of eight operating block cave mines**

The research presented in this dissertation aims to develop a methodology and a tool to account the effect of uncertain geotechnical factors in production scheduling by introducing the reliability of mining infrastructure. This reliability is meant to subsume all or a considerable part of the geotechnical events that trigger operational upsets on tunnels, ore passes and draw points. Incorporating the reliability of mining infrastructure in production planning will lead to an estimation of the system reliability, which represents a measure of the confidence embedded in the production schedule. Furthermore redundancy will be added to the mining system in order to plan the amount of resources needed to achieve a certain level of reliability for a given production plan. Finally, system reliability together with the production schedule redefines the concept of production capacity of the mine reflecting the underlying uncertainty of geotechnical events on mining infrastructure.

## 1.1 Statement of the Problem

Block caving has gained increased popularity in recent years due to its ability to produce large tonnages at low operating cost. However, there are several issues that add considerable uncertainty to the mining method such as: caveability in competent and highly stressed ore bodies (De Nicola and Fishwick, 2000); seismicity due the presence of high stresses that could adversely affect the mining method (Dunlop and Gaete, 1995); stress redistribution due to a particular draw strategy (Rubio et al, 2004); ultimate rock mass fragmentation that may have been poorly estimated (Hustrulid, 2000); lack of precision in estimating the grade distribution within the ore body (Aguayo et al, 2004); and dilution or the manner in which waste is included in the caved rock mass as it moves toward the draw points (Dolipas, 2000). Inadequate recognition and understanding of these issues may lead to disruption of production performance. The ability to integrate the above mentioned issues in production planning plays a significant role in the success of a block caving operation. The way in which the uncertainty of the block caving components is treated within the planning stage is crucial to estimate the production targets that will drive the operation to be a great success or a catastrophic failure (Carew, 1992). Figure 1.3 shows an operating mine performing with a high compliance between the original production schedule and the actual production using traditional scheduling methods.

However, the difference between forecast and actual production of a particular draw point reveals a different performance. For the same mining operation shown in Figure 1.3, Figure 1.4 compares forecast and actual tonnage at individual draw points within an active production area during one month of production. Note that even though the total production forecast has been achieved, an even distribution of tonnage per period across the active area has not been achieved. This tonnage variance induces two well known operational draw point performances: under-pulling and over-pulling. Under-pulling means that the actual tonnage is less than the production forecast and over-pulling means that actual production has exceeded the forecast production.

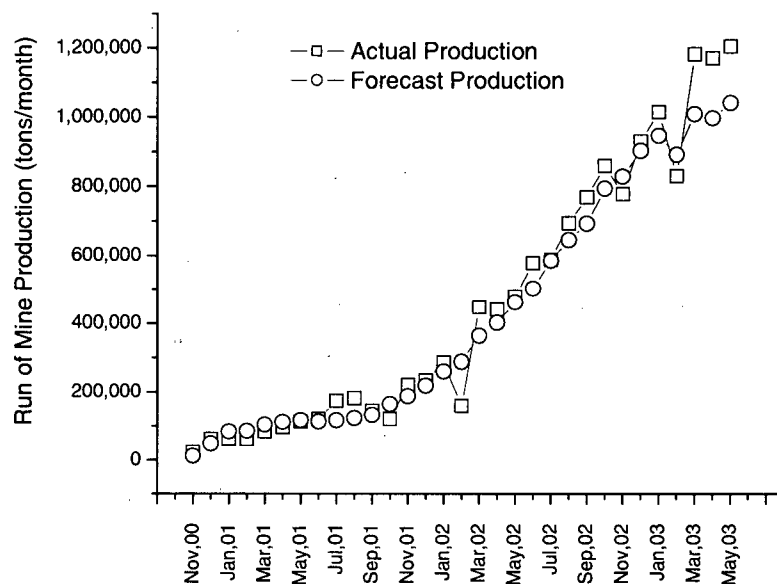


**Figure 1.3 Actual versus forecast production of an existing operation**

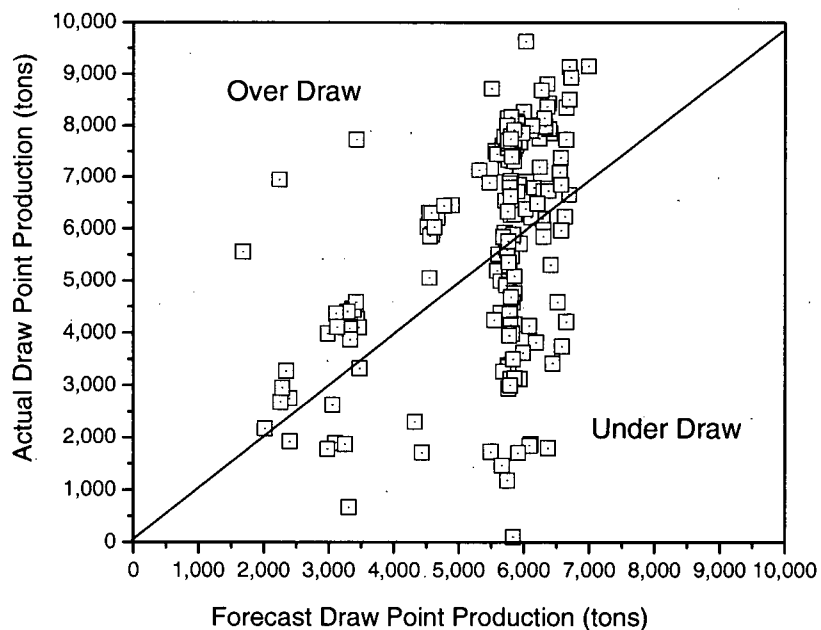


**Figure 1.4 One month of tonnage reconciliation per draw point**

It is generally accepted that under-draw and over-draw behaviour leads to early dilution entry, excessive induced stresses, and loss of planning abilities (Heslop and Laubscher, 1981). Usually the simulated mine plans are based upon a production strategy that includes several draw rules, which tend to draw down the caved ore as evenly as possible. If the production strategy is broken because under or/and over draw performance, those draw rules would also be broken. Uneven draw within an active production area creates zones of low or under draw which allow compaction to occur within the fragmented ore overlying the production level. Frictional forces are also induced at the boundaries of the under draw zones as a result of the differential draw between the under and over drawn zones (Rubio et al, 2004). The compaction and the frictional forces combine to produce high stresses in zones of low or under draw. The gradual compaction of the under draw zones leads to a density gradient within the fragmented ore, which induces non uniform movement of particles creating channeling and other oriented flow that may result in early dilution entry.

There are many reasons for the under and over draw performance. Some authors have attributed the variance between actual and plan to the “stealing ore” phenomenon which is known as the operational tendency to extract more ore from productive draw points, near the ore pass, in order to achieve the production target (Guest et al, 2000). This can be minimized by application of an appropriate production control system such as underground dispatch (Prasetyo et al, 2004). However, if the production forecast for a given draw point exceeds its natural capacity, the draw point will be unable to meet the forecast production and will not be used or will be under-drawn. To meet the overall production target, a few draw points will have to be over-drawn to compensate.

Currently production targets are the result of production schedules computed with mine planning parameters that do not evolve as a function of the operational performance and are not linked to fundamental models that describe the geotechnical behaviour of the rock mass. These issues lead to production schedules that do not reflect the actual rock mass behaviour within the mining system, in particular, they do not incorporate the operational upsets triggered by geotechnical events that affect the availability of mining infrastructure. Infrastructure availability is directly related to the production capacity of the mine. Thus a production scheduling methodology that

does not integrate the geotechnical behaviour of the rock mass within the block cave mining system will lead to optimistic production schedules. Optimistic production schedules would usually force the use of more resources than planned jeopardizing the original value of the mine. For example, when a production plan is computed, all draw points have the same chance of being part of the schedule. However the likelihood of a draw point being available when a plan is in operation varies across the layout due to rock mass properties and production performance. Consequently there will be draw points that tend to achieve their production target more easily than others. Therefore the treatment of draw points within the production scheduling algorithm should reflect the rock mass variability across the layout.

In summary a robust production planning tool should incorporate actual mine behaviour and make full use of the production data such as production records, infrastructure status records, stress indicators, fragmentation and geotechnical mappings of the rock mass. If such data can be shown to reflect geotechnical behaviour, then the uncertainty of a production schedule induced by geotechnical events would be reduced.

## **1.2 Research Question**

The following research question drives this dissertation

Can empirical observations in block cave mines be used to represent geotechnical effects on production performance and thus improve the performance of production planning?

Several numerical models for predicting block cave behavior are described in this dissertation. The effective integration of such models in a dynamic production scheduling environment is difficult due to uncertainties in the geotechnical models and, more fundamentally, due to the inability of such models to capture true rock mass behaviour. It is proposed that draw point reliability could subsume the most important geotechnical events that affect the production performance of a draw point. Different block cave mines facing operational upsets due to geotechnical factors have experienced a lack of productivity affecting their ability to meet the production targets. The reliability model will be used to test the ability to reproduce the production performance observed at these mines.

The integration of draw point reliability together with the mine planning parameters such as draw cycle and draw point yield in a mine wide reliability model enables the insertion of infrastructure redundancy of different components of the mining system such as drifts, production crosscuts, draw points. The introduction of redundancy in the mining system leads to a set of planning decisions that generate different production schedules with different reliabilities. The redundancy approach to production planning will be tested using the proposed mine reliability model. It is expected that a production schedule with a high reliability would tend to minimize the variance between actual and forecast draw point production, since the production forecast would have been computed as a function of the true mining infrastructure reliability.

As a result of this research new aspects related to production planning are defined such as system redundancy, which becomes a planning variable, production schedule reliability, which becomes the main outcome of the research presented in this dissertation.

### **1.3 Contribution of the Thesis**

The main contributions of this thesis are:

- The demonstration that the rate of occurrence of failure curve at a draw point can subsume the most important geotechnical effects that lead to production losses. The life cycle of a draw point is demonstrated to be characterized by a bathtub curve, similar to an aging component in a mechanical system.
- The system reliability reflects the level of certainty of a given production schedule. It is demonstrated that neither the draw point productivity nor the crosscut productivity affect the reliability of a production schedule. It is rather the combination of draw point productivity, crosscut productivity and infrastructure reliability which dictates the certainty of a production schedule.
- The reliability of a production schedule is integrated with the components of a production schedule such as draw point development sequence, draw rate and development rate. These parameters combined with the system reliability redefine the production capacity of a block cave mine. This definition includes, the probability of achieving the production targets stated as part of the production schedule of the mine.

## **1.4 Organization of the Work**

This dissertation is organized in six chapters. Chapter 1 has briefly introduced the research topic and stated the research question and objective. Chapter 2 reviews the background of the block cave mining system as well as planning methodologies used in block caving and other underground mining methods. Chapter 3 reviews the geotechnical factors affecting production performance, also introduces the concept of reliability as a function of the rate of occurrence of failure of mining infrastructure. Chapter 3 also introduces the bathtub curve as a representation of a the rate of occurrence of failure of a draw point during its life. Chapter 4 develops the model in which the block cave mine infrastructure reliability is used to quantify the reliability of a production schedule of a given mining system to achieve a given production target. Chapter 4 also reviews several applications of the model to planning problems and describes how the model can be used to improve mine planning decisions. Chapter 5 presents several analyses in which the reliability model is validated against observed production performance from two operating mines. Finally, Chapter 6 summarizes the conclusions and recommendations made as a result of this work.

## 2 LITERATURE REVIEW

Cave mining refers to all mining operations in which the ore body caves naturally after undercutting and the caved material is recovered through draw points (Laubscher, 1994). In this method the full block or an approximately equi-dimensional block is fully undercut to initiate caving. The undercut is drilled and blasted progressively and some broken ore is withdrawn to create a void into which initial caving of the overlying material can take place. As material is extracted from draw points located on the production level, the caving propagates upwards throughout the ore body until the overlying rock also caves and surface subsidence occurs. Figure 2.1 shows a diagrammatic representation of panel caving at the Henderson molybdenum mine in Colorado.

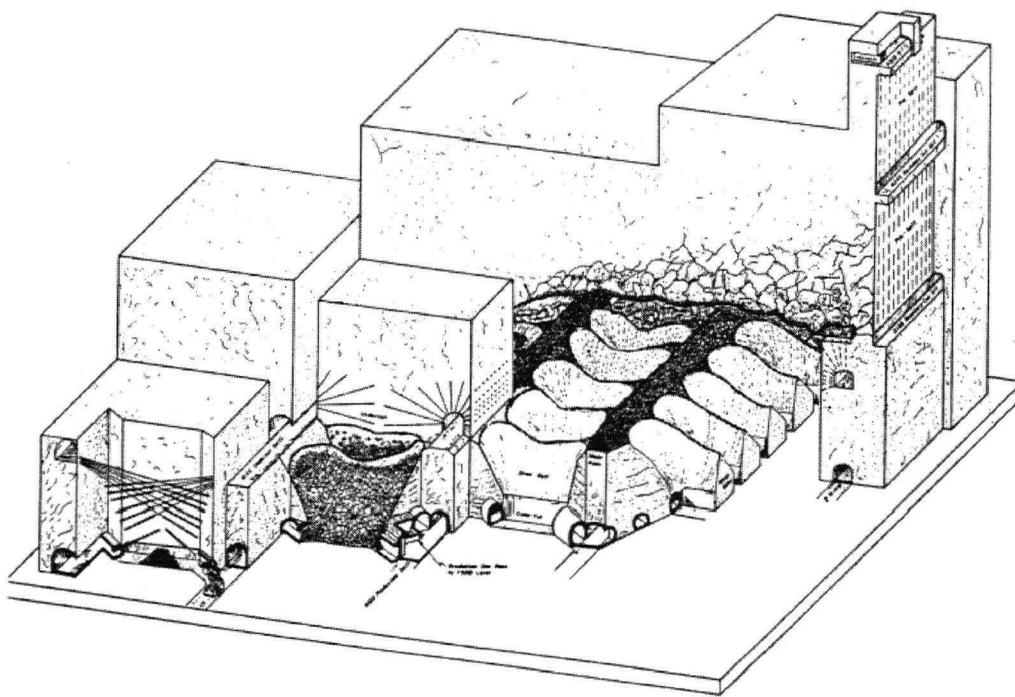


**Figure 2.1 Mechanized panel caving at Henderson mine (Doepken, 1982)**

The size of broken material will dictate which ore-handling system is suitable. For fine ore fragmentation the full gravity system (Grizzly) is most suitable. For somewhat coarser material, a slusher system should be implemented. For coarse material, the Load – Haul – Dump (LHD) system might be the best option. Other parameters should be taken in the selection of an ore-handling system such as work force sophistication, cost labor, availability and capital cost of equipment and any other factors that may be unique to the particular mine (Tobie, 1982).



Historically, block caving has been used for massive, low strength, and low grade ore bodies which produce fine fragmentation (Lewis and Clark, 1964). It is a low cost mining method which is suitable for automation to emulate the concept of a "rock factory" (Tota, 1997). Nevertheless block caving is highly capital intensive, requiring considerable investment in the development and preparation of the mine before production begins. Nowadays there is a trend to use block caving in competent rock masses which results in coarser fragmentation than the traditional application of the method.

Peele (1941) distinguishes three forms of block caving:

- a) Division of the footprint of the deposit into regular squared or rectangular blocks, drawing evenly to maintain a horizontal plane of contact between broken ore and caved waste cap.
- b) Division of the horizontal area into panels retreating from one end of a panel to the other, maintaining an inclined plane of contact between broken ore and caved waste cap.
- c) No division of the horizontal area of the ore body into blocks or panels, retreat mining from one wall to the other, maintaining an inclined plane of contact between broken ore and caved waste cap.

Nowadays a block cave mining is sub-divided into block caving and panel caving. Block caving is used for small size footprints that can be undercut in a short period of time compared to the life of the mine. In this case an inclined plane is maintained while undercutting the ore body as specified according to the second definition of the above list. On the other hand panel caving is used mainly for large footprints in which undercutting is performed throughout 50-70 % of the life of the mine. Operations using panel caving also keep an inclined plane to control dilution entry. deWolf (1981) described a planning technique to control the position of the plane that define the interface between ore and dilution as a function of the amount of draw. The author introduced the concept of draw charts that forced the extraction to follow a given draw profile across the active area.



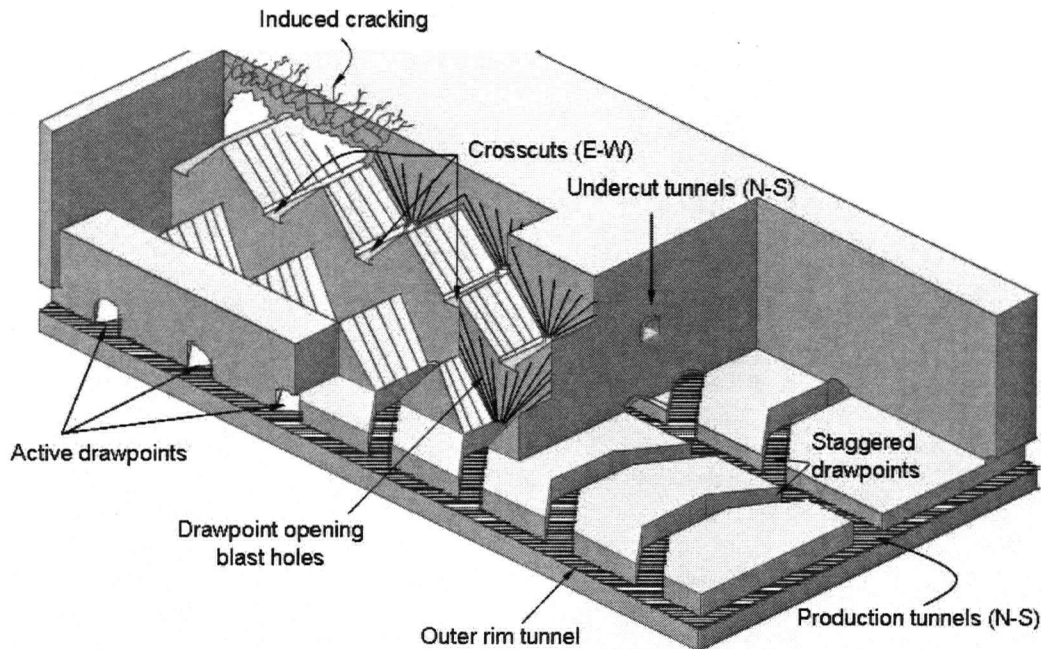


**Figure 2.3 Production level geometry (Moss et al, 2004)**

The ventilation level contains a set of parallel drifts running in the same direction and orientation as the production drifts, along a ventilation drift several crosscuts are created to inject fresh air to the production level and exhaust contaminated air from the production level using vertical raises that connect the ventilation with the production level. The haulage level contains a set of tunnels that connect with the production level through ore passes. The main purpose of the haulage level is to efficiently haul the ore produced to surface using underground trucks, trains, conveyor belts or skips. When using conveyor belts or skips underground crushing would be required which is done either on the crusher level or on the production level.

The mine layout described above is very general and there are variations of the layout which depend on the size of the ore body and the ultimate productivity of the mining system. For example there are operations that have neither ventilation nor haulage level. In this case the ventilation is performed via the production level and the LHDs would dump directly to the crushers located outside of the access drift surrounding the ore body without ore passes.

Based on the undercutting sequence a block cave mine is classified into conventional undercutting, advanced undercutting or pre-undercutting as illustrated in Figure 2.4. (Barraza and

Crorkan, 2000). The conventional undercutting method consists of blasting the undercut level once the development and construction of the production level has been finalized. The advanced undercutting method was introduced to reduce the exposure of the draw points to the abutment stress zones induced as a result of the undercutting process. For the advanced undercutting method just the production drifts are developed in advance to the blasting of the undercut. The pre-undercutting method is such that no development or construction takes place on the production level before the undercut has been blasted.

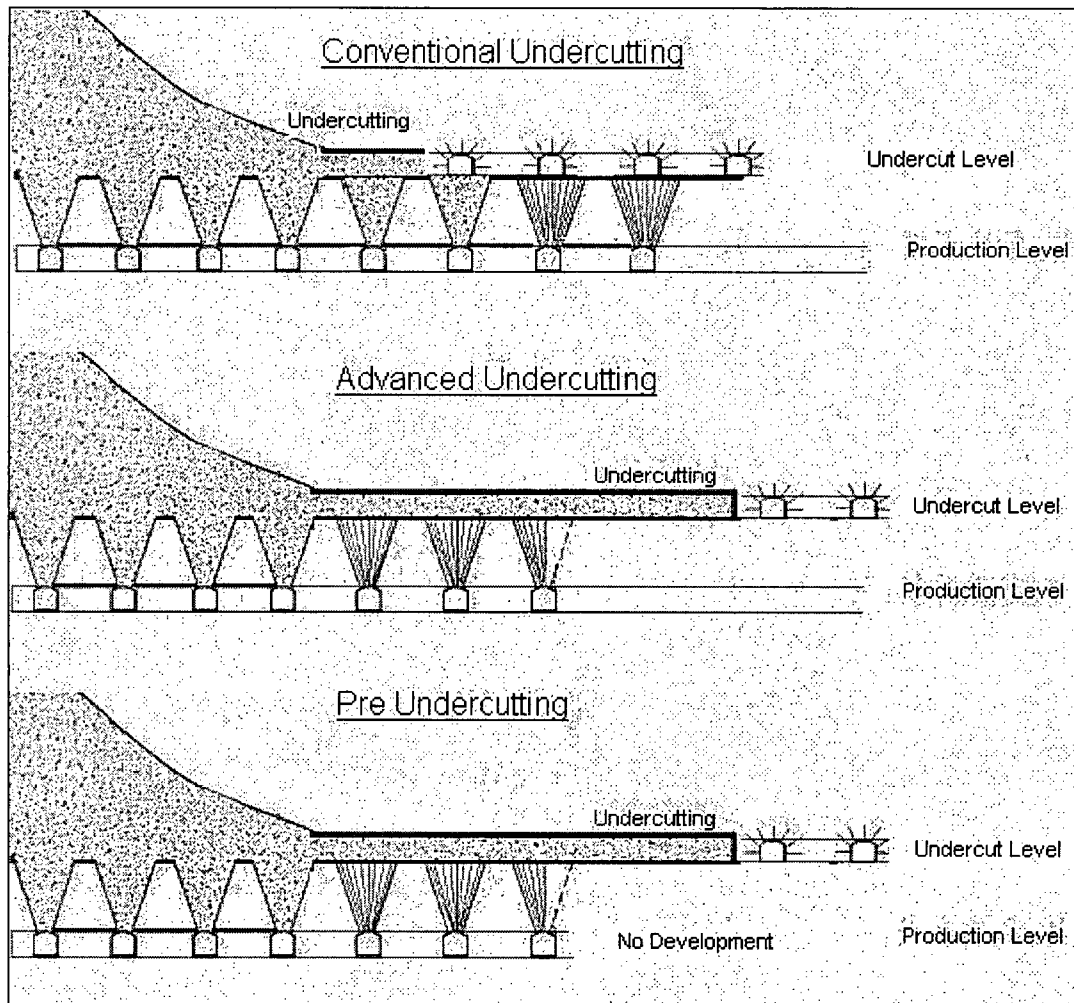


**Figure 2.4 Undercutting method used in block caving (Barraza and Crorkan, 2000)**

## 2.1 History of Block Caving

The first block caving operation recognized as such was the Pewabic mine, Menominee Range, Michigan (Peele, 1941). The method was crude and the only similarity to present day operations

was the ore handling. The production level was conditioned as a room and pillar mine in which the pillars were reduced in size to induce the caving. Desired fragmentation was achieved after six months of caving. Several other operations in Arizona used a modified Pewabic method such as the Nowry mine, the Tobin mine and the Detroit Copper Co. The Humboldt mine was probably the first block cave operation to separate the undercut level from the production level. It is interesting to see that at this stage there was a clear understanding of the effects of block confinement and the implication of confinement on the final production performance since the block was separated from the hangingwall and footwall using drilling and blasting techniques.

The Miami mine in Arizona showed an interesting application of the gravity method that included an undercut level, a grizzly level, a set of raises for ore handling purposes and a haulage level. For a drawing strategy the Miami mine used a panel caving concept in which they would undercut from one end to the other of an entire  $120\text{m} \times 140\text{ m}$  block. The angle of contact between ore and waste was planned to be between 40 and 60 degrees from horizontal to minimize dilution and over stress on the crown pillar.

Ore extraction in block caving has two related effects described by Peele (1941). More tonnage and lower grade than expected is extracted due to dilution of ore from the waste cap. Draw control tends to minimize dilution entry. Draw control concepts were first introduced by McClennan (1930) at the Humboldt mine aiming to minimize the amount of dilution as part of the ore extraction. The author summarized the application of draw control as shown below:

- a) the ore should be drawn evenly so that the contact between the broken ore and the broken waste cap is a horizontal plane and
- b) regulate drawing to reduce induced stresses on production openings.

Since 1950 De Beers has used block cave methods for its operations in South Africa (Owen and Guest, 1994). Not all methods introduced at De Beers operations were successfully initiated and often plans had to be reviewed and modified according to the performance of the mine. Mechanized panel caving was introduced at Premier mine in 1990 (Bartlett, 1992).

The Henderson mine was the first block cave operation to introduce fully mechanized equipment. The mine started in 1976 using 4 yd<sup>3</sup> LHDs. The design has evolved to utilize 7 yd<sup>3</sup> equipment (Rech et al, 2000) and the productivity of the mining system has increased from 136 tonnes/hour to 376 tonnes/hour. The LHD fleet size has been reduced from 30 to 7 while maintaining the same production rate. Nowadays the Henderson mine also uses underground haul trucks of 72 tonnes capacity.

The El Teniente mine first used LHDs in the early 1980s (Chacón et al, 2004) and introduced a novel way of designing the production level layout that is nowadays called the El Teniente layout. Stationary hammers (Moyano and Vienne, 1994) and different alternatives of caving, such as advance undercut caving, were introduced at the Sub 6 mine part of the El Teniente complex (Rojas et al, 2000).

Even though the technology and the methods applied in block caving have evolved dramatically over the years, concepts for mine planning have not followed the same path of evolution. In recent years much attention has been given to understand the principles of gravity flow and rock mechanics without considering mine planning as an important part of the mining system.

## **2.2 Fundamental Models of Block Caving**

Block caving is a mining method that relies on natural processes for its success. Therefore more detailed geotechnical investigations of the ore body are required than with other methods where conventional drilling and blasting are employed as part of the production of the mine. The main geotechnical parameters affecting the planning of the block cave are presented by Brown (2003) as follows:

- Caveability
- Cave initiation
- Cave propagation
- Fragmentation
- Stress performance surrounding the cave boundary

The list of geotechnical parameters presented earlier supports the definition of several aspects related to the planning of the mine such as undercut sequence, draw rate and development rate. The ability to represent the variability of the geotechnical parameters throughout the ore body would result in decreasing the risk of the mining method as well as increasing the ability to forecast production (Summers, 2000).

An illustrative representation of the link between the geotechnical and the mine planning parameters of block caving has been proposed (Rubio et al, 2004) in order to understand the influence of rock mass, stress regime and mining system in production performance. As shown in Figure 2.5, the fundamental models of fragmentation, geomechanical, geological and reconciliation are used to determine mine planning parameters, such as draw rate, undercut sequence, development rate, tonnage, draw method and production targets.

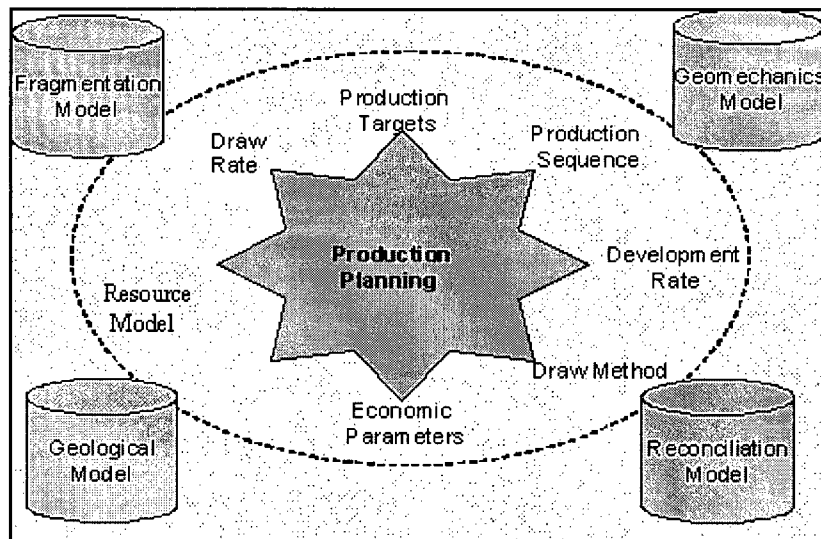


**Figure 2.5 Fundamental models that affect the planning parameters of a block cave mine (Rubio et al, 2004)**

The **geomechanical model** affects the following aspects of the design and planning of a block cave mine:

- Draw point sequence will be affected by the structural pattern. Usually, the undercut sequence will be oriented perpendicular to the major structures in order to produce blocks that can enhance the caveability of the rock mass. (Rojas, 2000).

- Abutment stress at the cave front will be a function of the pre mining stresses and the angle of draw. This will affect the stability of the excavations located on the undercut, production level and haulage level immediately below the front of the caving boundary (McKinnon and Lorig, 1999).
- Seismicity is the response of the rock mass to the stresses developed at the cave back as the cave propagates to surface and also the response of the rock mass surrounding the excavations exposed to the abutment stress such as undercut, production, ventilation and haulage drifts and rib tunnels. By measuring the properties of the seismic events an estimation of the energy released can be performed to assess the stresses acting on those events. This can be useful for forecasting caveability and other caving activity related.(Glazer and Hepworth, 2004).
- Induced stresses due to uneven draw. By performing uneven draw high stresses are transferred to the zones of low draw due to the compaction of the broken rock overlying the production level (Febrian et al, 2004). It has been shown that the draw performance influences the distribution of stresses surrounding a draw point (Rubio et al, 2004).

The **fragmentation model** affects several aspects of the planning of a block cave mine, the most important aspects are as follows:

- Dilution entry point which is the result of mixing of fragmented material along the draw column (Heslop and Laubscher, 1981). Large variance of fragmentation along the draw column leads to an increased amount of chaotic movement of rock within the broken rock induced by the large density gradient. Gravity will tend to move finely fragmented material towards the low density areas or coarse fragmented areas until equilibrium is reached within the broken rock.
- Draw point spacing is the result of the draw column diameter which is believed to be a function of the ultimate fragmentation of the draw column (Kvapil, 1965). The draw point spacing is designed in such manner that the material overlying the production level can be drawn without leaving static areas that may transfer stresses to the production level infrastructure.
- Draw point secondary breakage activity is the result of the frequency of oversize boulders, typically larger than 2 m<sup>3</sup> that can not be handled by the LHD.



- Hang up frequency is produced by boulders larger than the draw bell opening. Oversize and hang up frequency will severely affect the productivity of the mining system has been presented by Moss et al (2004) and Barraza and Crorkan (2000).
- Draw point yield is the maximum productivity of a draw point in the free flow state. As the draw point matures the fragmentation becomes finer due to secondary fragmentation. Therefore the void ratio decreases as the draw point matures leading to an increase in LHD bucket capability, consequently achieving higher draw point productivity (Esterhuizen et al, 2004).

The **geological model** links data relating to structure, lithology and mineralogy with the ultimate metallurgical recovery. This model aims to build a geometallurgical model that can provide a reasonable estimate of the metallurgical recovery based on the combination of the composite lithologies. Didyk and Vasquez (1981) showed the effect of different rock types on metallurgical recoveries at El Salvador mine.

The **reconciliation model** captures the production performance of the mine. If this model is available it is used to feedback key performance indicators to the fundamental models in order to calibrate their behavior. The reconciliation model is also used to check the validity of different assumptions made regarding to a production schedule. Thus this model will be used as a guide to frame the production planning of the mine based on historical performance. The reconciliation model affects the following aspects of the design and planning of a block cave mine:

- Draw rate is adjusted based on the historical production performance of draw points located in a given rock mass domain. Usually the adjustment factor will be taken as a form of draw point availability depending of its history of oversize and hang up frequency, potential wet muck and potential instability for a given rock mass domain.
- Development rate is adjusted depending on the rock mass stress regime in which the construction will take place. Actual mine development performance is important since it captures the bottlenecks in the mining system that affect the construction cycle of mining infrastructure.

- Draw strategy is compared against the historical performance of the mine. Based on the production objective, the draw strategy will be modified in order to compute a schedule that is realistic and consistent with the production promise.

It is important to note that the reconciliation model has not yet been introduced at the operating mines, rather it has been conceptualized as the research unfolds over the years. Thus, at this time there will be some mines applying parts of the reconciliation model as a result of informal discussion or technical advice. An interesting example of a reconciliation model was presented by Kraushacer (1987) who used operational databases as a main source of operational performance indicators for construction planning. The reconciliation model allowed the calculation of different operational performance parameters that can be used as feedback for future construction plans.

A considerable amount of numerical modeling has to take place in order to achieve a comprehensive understanding of the interaction between the rock mass and the mining system (Flores et al, 2004). The modeling is normally used to estimate parameters such as: stress distribution at the front cave to decide upon the mining sequence; stress re-distribution on the cave back to estimate ultimate fragmentation; fragmentation models to estimate draw point productivity. Despite the amount of modeling performed at the feasibility stage of a block cave mine, very few of the results are carried forward and integrated into the ongoing mine planning activities.

### **2.3 Block Cave Production Scheduling**

The main task of production planning is to define the production rates of a mining system. This decision will ultimately define the value of the mining project. Scheduling the extraction and rates of production for an underground mine operation is a common task carried out during the life of the mine from feasibility through to the final production phase (Russel, 1987). In the case of a block cave mine, the production schedule mainly defines the amount of tonnage to be mined from the draw points in every period of the plan to achieve a given planning objective. The mine plan also defines the number of new draw points that need to be constructed and their sequence to sustain a given production target. To compute this production schedule many decisions need

to be made with regards to accessibility and infrastructure, mine and plant capacity and mining sequence. Figure 2.6 shows an example of a mine plan in which the tonnage and grade are predicted during the mine life.

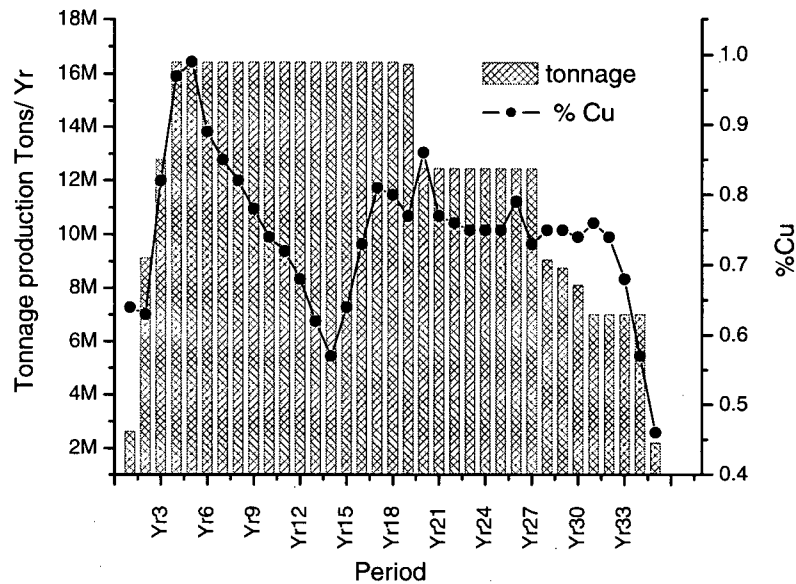


**Figure 2.6 Typical production schedule from an operating mine**

The planning parameters used to compute a production schedule of a block cave mine have been presented by Rubio (2001) as follows:

- Development rate defines the maximum feasible number of draw points to be opened at any given time within the scheduled horizon. This constraint is usually based on the footprint geometry, the geotechnical behaviour of the rock mass and the existing infrastructure of the mine, which will typically define available mining faces.
- Draw point construction sequence defines the order in which the draw points will be constructed. This sequence is usually defined as a function of the undercut sequence. This constraint usually acts on the draw point status activating those that are at the front of the production face. Commonly the undercutting sequence is defined once the elevation and horizontal dimension of the footprint has been decided.
- Maximum opened production area at any given time is an operational constraint that depends on infrastructure and equipment availability as well as on ventilation resources. A large number of active draw points might lead into serious operational problems such

as excessive haulage distance and problems related to the movement of equipment within the active draw points.

- Draw rate limits the production yield of a draw point at any given time within the production schedule. The draw rate is a function of the fragmentation and the caveability model. The draw rate needs to be fast enough to avoid compaction and slow enough to avoid air gaps.
- Draw ratio defines a temporary relationship in tonnage between one draw point and its neighbors. It is believed that this parameter controls the dilution entry point and the damage of the production level due to induced stresses.
- Period constraints force the mining system to achieve the desired production target usually keeping it within a range that allows flexibility for potential operational variations.

The planning parameters shown in Figure 2.7 perform as operational constraints in the planning stage of a mine. These planning parameters should be based upon the fundamental models described in Section 2.2 of this dissertation. However, the link between the fundamental models, particularly the geomechanical model, and the planning parameters has not been formalized or documented. For example it is often found, in practice, that draw rate is exaggerated to achieve the desired production targets, which disregards the relationship between draw rate and rock mass fragmentation.

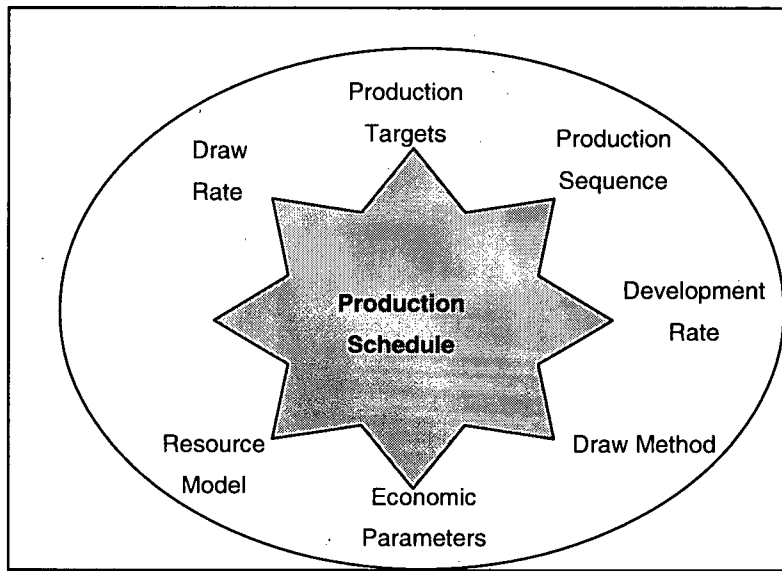


**Figure 2.7 Current mine planning process in block cave mining (Rubio et al, 2004)**

Several methods are currently used to compute production schedules in a block cave mine. They can be classified in two main categories heuristic methods and operations research methods. The original heuristic methods were the manual draw charts used at the beginning of block caving. These methods evolved to the form presented by deWolf (1981) at Henderson where a way to avoid early dilution entry was described by constraining the draw profile to an angle of draw of 45 degrees. A significant breakthrough was presented by Heslop and Laubscher(1981) who described a volumetric algorithm to simulate the mixing along the draw column. Carew (1992) described the use of a commercial package called PC-BC to compute production schedules at Cassiar mine. Diering (2000) showed the principles behind the commercial tool PC-BC to compute production schedules, providing several case studies where different draw methods have been applied depending on the ore body geometry and rock mass behaviour. An alternative model was also presented by Kear (2000), in which a floating surface method is used to find the optimal draw strategy for the Palabora mine using an iterative algorithm.

The application of operations research methods to the planning of a block cave mine was first described by Riddle (1976). This development intended to compute mining reserves and define the economic extent of the footprint. The final algorithm did not reflect the operational constraints of block caving described above since it worked with the block model directly instead of defining the concept of draw column as an individual entity of the optimization process. Other

authors such as Caccetta and Giannini (1988), Wilke et al (1984), and Gershon (1987) have attempted to develop methodologies to optimize production schedules, but none of them has satisfactorily produced a robust technique which has an acceptable level of success in block caving. One of the main reasons for this unsuccessful history has been the difficulty of defining a multi-period objective function over different mine planning horizons that integrates the gravity flow mechanism present in block caving. Chanda (1990) developed a model to optimize production from a slusher block cave method using scrapers as production machines. Chanda concentrated on a short term planning problems that cover a time horizon of a few weeks to a few months applying single step optimization rather than multi period optimization.

More sophisticated algorithms have been developed by Guest (2000) to analyze and compute long term plans. Guest postulates that by following a set of surfaces that conceptually define a draw control strategy, dilution can be minimized and therefore net present value (NPV) can be maximized. This algorithm does not integrate the concept of gravity flow as part of the optimization process. Also Guest assumes that a draw strategy can be summarized by the definition of a set of surfaces which may be a very difficult task to perform in metal mining due to grade variability. It is interesting to note that Guest stated the importance of the draw strategy on dilution control as part of the production scheduling process. Rahal et al (2003) used a dual objective mixed integer linear programming algorithm to minimize the deviation between the actual state of extraction (height of draw) and a set of surfaces that tend towards a defined draw strategy. This algorithm assumes that the optimal draw strategy is known. Nevertheless it is postulated that by minimizing the deviation to the draw target the disturbances produced by uneven draw can be mitigated. Diering (2004) presented a non linear optimization method to minimize the deviation between a current draw profile and the target defined by the mine planner. Diering emphasizes that this algorithm could also be used to link the short with the long term plan. The long term plan is represented by a set of surfaces that are used as a target to be achieved based on the current extraction profile when running the short term plans. Rubio et al (2004) presented an integer programming algorithm and an iterative algorithm to optimize long term schedules in block caving integrating the fluctuation of metal prices in time.

The main problems associated with the methods presented above can be summarized as follows:

- The methods do not incorporate the variability and the dynamic behaviour of the fundamental models throughout the ore body.
- The methods do not have a rational way to link the mine planning parameters with the fundamental models.
- The methods do not integrate the operational upsets that affect productivity. Therefore the current systems do not adapt as a function of the historical performance.
- The methods do not incorporate, in a routine basis, operational performance to adjust the medium and the long term plans.

The issues with the current production scheduling methods listed above reflect that the current methods do not integrate the technical uncertainty inherent to the mining method. Thus, the production targets computed with the existing methods lead to unrealistic production targets, forcing the operation of the mine to break the rules integrated in the original production schedules. This motivates the development of a methodology that could integrate operational performance of the mine, as a reflection of the rock mass behaviour to the mining system, into production planning to compute realistic production targets per draw point during the life of the mine.

## **2.4 Uncertainty in Block Cave Production Scheduling**

The lack of a formal link between the fundamental models and the planning parameters leads to a considerable amount of uncertainty in the planning process. Summers (2000) described the main sources of uncertainty in block cave mining pointing out that there are no clear methodologies to incorporate the natural variability of the rock mass in the process of design and planning the mining system.

The treatment of uncertainty in production planning as generally being discussed by several authors such as Samis and Poulin (1997), who proposed the insertion of contingency plans associated with parameters that have high level of uncertainty in the long term production strategy that could aim to avoid production shortages and/ or an increase of production costs. Singh and Skibniewski (1991), Kajner and Sparks (1992) have also looked at the flexibility needed in mineral resource industry as a function of the level of uncertainty. Commonly

simulation of the mining system has been the main tool used to assess the amount of flexibility needed in a mine design or a mine plan. The main problem with this approach is that often simulation models do not integrate the fundamental models such as stress distribution, caveability and gravity flow. In other mining methods in which the production outcomes are controlled by drilling and blasting activities discrete event simulation has been used to plan tactical decisions (Dessureault et al, 2000).

Flexibility or the ability to deal with changes and upsets has often been proposed as a response to uncertainty in mine planning. Real options have been used to estimate the value of flexibility (Dunbar et al., 1998; Trigeorgis, 1998). Kazakidis (2003) proposed a flexibility index that uses simulation to quantify the value of the operational flexibility. However real option concepts do not provide a methodology to quantify the amount of flexibility needed in a production schedule nor do they integrate operational performance observations to dynamically adjust the production schedule.

There are several methods developed to quantify the impact of uncertainty on the financial valuation of the mine. Often Monte Carlo simulations have been used to quantify the risk related to metal price uncertainty. Smith (1999) and Dimitrakopoulos (2002) have developed methods to quantify uncertainty related to ore body modeling and its impact on the production schedule for open pit mines.

The methods summarized above concentrates mainly in uncertainty derived from metal prices and grades. These methods do not appear to be the correct approach for quantifying the system uncertainty involved in block caving. Xiaotian (1989) introduced the concept of caving parameters to describe the process of caving. The caving parameters have associated probability distribution to affect different mine planning parameters such as sequence and undercutting rate. The mine plan is computed using simulation integrating the probability distribution of the caving parameters. This paper does not discuss how the distributions are constructed and whether or not those distributions would be stationary.



Krantz and Scott (1992) recognized that planning a mine is a dynamic rather than a static activity. One of the main mine planning activities should be the comparison of actual vs. planned production and use this comparison to modify the initial assumptions. The mine needs to be built with enough flexibility to integrate the potential improvements resulting from this comparison. Thus success of the plan will depend upon the ability of the mine to react to the current operational situation.

More than 12 operating block caves and projects have been visited during the time that this research has taken place and none of them reports the production forecasts in a form of a range, band or confidence interval to represent the technical uncertainty of these forecasts. The uncertainty of a production schedule is missing in the process of planning a block cave mine. If the uncertainty could be quantified, different decisions could be made in order to integrate flexibility in the mining system that could mitigate the risk caused by the underlying uncertainty.

The uncertainty related to rock mass behaviour within the mining system leads to unplanned operational upsets such as infrastructure failure that tend to jeopardize the original production estimates. Thus a natural approach would be to incorporate the infrastructure failure characteristics of a mining component as part of the planning process. Even though this approach does not integrate a model of rock mass behaviour within the planning process, it does include the effects of that behaviour in mining infrastructure. This is an empirical approach that will be reviewed in the following chapter.

### 3 FAILURE BEHAVIOUR OF MINING INFRASTRUCTURE

Mining infrastructure may fail due to geotechnical events that tend to reduce its physical availability. In particular, there are two geotechnical events, coarse fragmentation and over stress, that affect the productivity of block cave mining infrastructure. Coarse fragmentation at the draw point leads to the formation of hang ups and oversize, reducing the effective time that the draw points have available to achieve a given production target (Barraza et al, 2000). Over stress on the crown pillar leads to closure that often ends in the collapse of a production area (Rubio et al, 2004).

In this section the characteristics of infrastructure failure as a result of these two geotechnical events will be studied. Then a methodology will be devised to quantify the reliability of draw points as a function of the rate of occurrence of failure. Finally, it will be shown that draw point reliability correlates well with the underlying geotechnical events that triggered mining infrastructure failure.

#### 3.1 Operational Database

An important component of the research was the collection of different pieces of information recorded at different mines in order to be able to demonstrate the fundamental concepts presented in this dissertation. A summary of the geotechnical information recorded at four mine operations, labeled M1 to M4 to maintain confidentiality, is shown in Table 3.1. These four operations represent 80% of the worldwide block cave underground mine production.

**Table 3.1 Geotechnical information of the mine operations**

	<b>M1</b>	<b>M2</b>	<b>M3</b>	<b>M4</b>
RMR (Laubscher, 1989)	45	80	70	65
Fracture frequency per meter	-	0.1-0.8	1-2	3-4
Fragmentation	10% >2m <sup>3</sup>	45% >2m <sup>3</sup>	40% >2m <sup>3</sup>	15% >2m <sup>3</sup>

The geotechnical information presented above was taken from technical reports found at the operations. It may be seen from Table 3.1 that the four mines are operating in different rock mass environments. For example M2 and M3 are challenging the traditional application of block

caving based on their highly competent rock mass environment while M1 and M4 are operating in a rock mass environment that is considered to be ideal for block caving.

The main features of the mining systems at these mines are shown in Table 3.2. The number of draw points and crosscuts constructed at these mines is an indication of the scheduling complexity required to coordinate all the production units in order to meet the production target.

**Table 3.2 Features of the mining system**

	<b>M1</b>	<b>M2</b>	<b>M3</b>	<b>M4</b>
Undercutting Method	Advanced Undercutting	Advanced Undercutting	Pre Undercutting	Traditional Undercutting
Mining Method	Panel Caving	Block Caving	Panel Caving	Panel Caving
Depth (m)	850	1200	500	500
Production (tons/day)	38,000	30,000	32,000	23,000
Draw points	300	320	250	365
Production Crosscuts	14	20	26	20

The operational and planning data used to illustrate the concepts exposed in dissertation are summarized in Table 3.3.

**Table 3.3 Operational and planning data collected from the mines**

	<b>M1</b>	<b>M2</b>	<b>M3</b>	<b>M4</b>
Amount of data collected	4 years	3 years	3 years	2 years
Tonnage records	X	X	X	X
Status records	X	X	X	
Convergence records	X	X		
Hang up records	X	X		
Oversize records	X	X		

The different components shown in Table 3.3 are explained in the following sections of the dissertation.

### **3.1.1 Daily tonnage records**

Tonnage records correspond to the daily records of tonnage drawn from every active draw point across the mine layout. Usually this data is collected by production systems such as Underground

Dispatch (Barraza et al, 2004) which operate interactively with the LHD operator to record the number of buckets drawn from a given draw point at a given time. The number of buckets is converted to tonnage based on the weight reported by the mill.<sup>1</sup> An example of daily tonnage records is shown below in Table 3.4.

**Table 3.4 Example of daily tonnage record from Mine M1**

Date	Draw Point Name	Tonnage (tons)
5/1/2003	D1	108.8
5/1/2003	D2	97.4
5/1/2003	D3	97.4
5/1/2003	D4	129.9
5/1/2003	D5	97.4
5/1/2003	D6	120.2
5/1/2003	D7	175.5
5/1/2003	D8	129.9
5/1/2003	D9	129.9
5/1/2003	D10	129.9
5/1/2003	D11	108.8
5/1/2003	D12	107.1
5/1/2003	D13	107.1
5/1/2003	D14	129.9
5/1/2003	D15	129.9
5/1/2003	D16	129.9
5/1/2003	D17	129.9
5/1/2003	D18	99.1
5/1/2003	D19	148.1

The daily tonnage records are used to compute the cumulative tonnage drawn per draw point per month as shown in Table 3.5. This tonnage is commonly used to represent draw point maturity. The cumulative tonnage drawn from a draw point can be converted to Height of Draw column (HOD) at a given period by dividing the cumulative tonnage drawn by the in situ density and the effective draw point area. For example using the cumulative tonnage shown in Table 3.5 the HOD is computed in Table 3.6 using a draw point area of 280 m<sup>2</sup> and an in situ density of 2.7 tonnes/m<sup>3</sup> (values associated with mine M1). HOD will be used extensively to represent draw point aging.

---

<sup>1</sup> The actual trend is to install weightometers on the LHD buckets to measure the tonnage drawn from a draw point in real time. However, this system has not yet been delivered to operations since the weightometers are still too sensitive to the oscillations of the hydraulic system of the LHD (van Hout et al, 2004).

**Table 3.5 Example of cumulative monthly tonnage drawn from Mine M1**

Draw Point Name	Apr,01	May,01	Jun,01	Jul,01	Aug,01	Sep,01
D1	10,182	10,843	13,132	13,969	14,918	16,346
D2	11,481	12,181	13,660	14,472	15,625	17,736
D3	16,482	17,067	18,576	19,094	21,766	23,236
D4	15,379	16,255	17,868	18,276	19,451	21,408
D5	12,512	13,581	15,155	17,204	20,291	22,529
D6	13,039	14,011	16,331	18,552	20,184	22,830
D7	16,355	18,149	21,251	23,188	27,404	32,340
D8	10,946	12,851	16,874	19,080	25,497	29,889
D9	13,143	16,245	22,551	25,207	30,900	35,248
D10	20,945	25,497	30,308	32,351	39,728	44,951
D11	20,612	33,594	36,418	40,236	47,161	51,266
D12	27,194	39,263	41,411	47,563	53,461	56,752
D13	1,969	2,167	4,330	11,042	21,422	30,813

**Table 3.6 Example of Height of Draw (HOD) calculation**

Draw Point Name	Apr,01	May,01	Jun,01	Jul,01	Aug,01	Sep,01
D1	13	14	17	18	20	22
D2	15	16	18	19	21	23
D3	22	23	25	25	29	31
D4	20	22	24	24	26	28
D5	17	18	20	23	27	30
D6	17	19	22	25	27	30
D7	22	24	28	31	36	43
D8	14	17	22	25	34	40
D9	17	21	30	33	41	47
D10	28	34	40	43	53	59
D11	27	44	48	53	62	68
D12	36	52	55	63	71	75
D13	3	3	6	15	28	41

### **3.1.2 Daily status records**

Status records correspond to information collected daily on regarding the physical status of the draw points. Table 3.7 shows an example of the draw point status data collected from mine M1. Currently there is a trend in the industry to implement the recording of draw point status as part of the Underground Dispatch system so that every time a LHD is dispatched to a draw point the LHD operator would have to communicate the initial and the final status of the draw point. Also the secondary breakage equipment and crews would be dispatched by the Underground Dispatch system in order to keep records of the draw points that have been blasted. Usually the information recorded by the Underground Dispatch system is checked at the beginning of the day

as part of the production control tasks. If there is a difference between the information recorded by the system and what is seen in the field, the status is corrected and imported manually into the production database. The draw point status recorded at the draw points can be classified as active, oversize, wet muck, hang up, and closure (high deformation). Currently there is one draw point status recorded per day, although a drawpoint may experience different status conditions within a day. For instance a draw point could change from active to oversize and return to active status within a day. In this case the draw point would be recorded as active, thus ignoring the draw point repair that took place during the day. More sophisticated systems will be needed to record the changes of draw point status during the day in order to more accurately capture the actual availability of a draw point.

**Table 3.7 Example of draw point status extracted from database of mine M1**

Draw Point\ Day	1	2	3	4	5	6	7	8	9	10	11	12	13	14
D1	A	A	A	A	A	A	A	A	A	A/H	A/H	A/H	A/H	A/H
D2	B/H	B/H	B	B	B	B	B	B	B	B	B	B	B	B/H
D3	A	A	A	A	A	A	A	A	A	A	A	A	A	A
D4	A	A	A	A	A	A	A	A	A	A	A	A	A	A
D5	A	A	A	A	A	A	A	A	A	A	A	A	A	A
D6	A	A	A	A	A	A	A	A	A	A	A	A	A	A
D7	-	-	-	-	-	-	-	-	-	-	-	-	-	-
D8	-	-	-	-	-	-	-	-	-	-	-	-	0	0
D9	-	-	-	-	-	-	-	-	-	-	-	-	0	0
D10	-	-	-	-	-	-	-	-	-	-	-	-	0	0
D11	A/H	A/H	A	A	A/H	A/H	A/H	A/H	A	A/H	A/H	A/H	A/H	A/H
D12	C	C	C	C	C	C	C	C	C	C	C	C	C	C
D13	A/H	A/H	A/H	A	A/H	A/H	A/H	A	A/H	A	A	A/H	A/H	A
D14	A	A	A	A	A	A	A	A	A	A	A	A	A	A

The draw point status conditions shown above are: active draw point (A), oversize draw point (B, B/H), temporarily closed due to high convergence draw point (C) or hanged up draw point(A/H).

### **3.1.3 Convergence records**

Convergence records result from the monitoring of displacements at different locations along the production drift using a tape extensometer (Febrian et al, 2004). Table 3.8 shows an example of convergence data collected from mine M1. The purpose of convergence monitoring is to provide

an early warning of excessive displacement of the back of drifts located on the undercut and production levels. Another benefit of this monitoring is to provide information to assess the state of the induced stresses and rock behavior during undercutting and production stages, providing valuable information for mine planning and operations to maintain ground stability (Febrian et al, 2004). Several convergence stations are installed along production and undercut drifts and are monitored at least once per week. If a station showed high convergence, daily monitoring would be performed in this area.

**Table 3.8 Convergence measurements taken along production drift 13 from mine M1**

Date	Station	Hz_Incr(mm)
3/16/2000	P13C01	-0.30
3/16/2000	P13C02	0.05
3/16/2000	P13C03	0.20
3/16/2000	P13C04	-0.30
3/16/2000	P13C05	-0.60
3/16/2000	P13C06	0.95
3/22/2000	P14C01	0.50
3/22/2000	P14C02	0.25
3/22/2000	P14C03	0.10
3/22/2000	P14C04	-0.55
3/22/2000	P14C05	-0.10
3/22/2000	P14C07	-0.10
3/22/2000	P15C02	-0.85
3/22/2000	P15C03	0.10

#### **3.1.4 Records of draw point hang up**

Hang up records are extracted from the draw point status database. Figure 3.1 shows an illustration of hang ups and oversizes experienced at draw points. Hang ups are stable arches formed inside the draw bell as a result of the movement of a large boulder. Oversize is considered to be any boulder at a draw point greater than  $2\text{m}^3$ , which seems to be the maximum size that a LHD bucket can load (Moss et al, 2004).

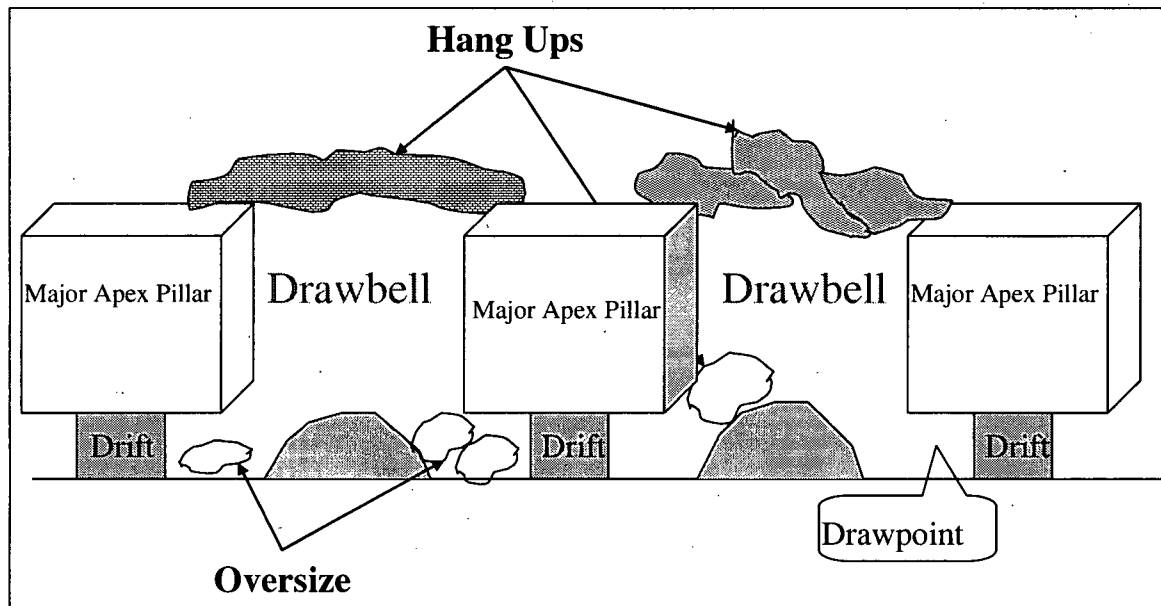


**Figure 3.1 Draw point blockage in block caving (Barlett, 2000)**

The hang up status is of such importance that it is usually stored in a separate database in order to keep track of the amount of explosives used to remove the hang up as well as the machines used to drill and place the explosives. Given these records, a list of hang ups per draw point per month could be constructed as shown in Table 3.9. The tonnage drawn per draw point in the same period of time could be computed using the daily tonnage records. An example of monthly tonnages from mine M2 is shown in Table 3.10. By combining the number of hang ups with the tonnage drawn per period, it is possible to compute the hang up frequency, hang ups/ton, for a given period of time as shown in Table 3.11. For the periods in which there is no tonnage drawn this calculation is disregarded. This indicator is extremely important for the study of the effect of hang ups on production performance.



**Table 3.9 Example of monthly hang up records from mine M2**

Draw Point Name	Jan,02	Feb,02	Mar,02	Apr,02	May,02	Jun,02	Jul,02
P1	7	4	4	1	6	7	13
P2	1	-	-	-	1	1	2
P3	1	2	1	-	10	10	8
P4	3	2	5	-	6	9	9
P5	4	2	2	-	4	7	5
P6	2	3	4	-	2	1	8
P7	1	5	5	-	2	11	3
P8	5	4	2	-	2	2	9
P9	2	2	-	-	-	4	7
P10	-	-	-	-	1	3	4
P11	-	-	-	-	5	6	8

**Table 3.10 Example of monthly tonnage from mine M2**

Draw Point Name	Jan,02	Feb,02	Mar,02	Apr,02	May,02	Jun,02	Jul,02
P1	116	1,573	1,384	243	2,363	1,196	2,192
P2	379	45	455	117	1,505	1,141	887
P3	163	2,067	1,303	-	1,798	2,254	2,572
P4	2,423	1,842	1,263	88	2,626	2,529	2,660
P5	511	2,525	1,808	-	2,151	3,274	1,637
P6	1,091	2,229	1,798	-	1,283	2,391	789
P7	472	2,525	2,414	-	1,929	2,502	468
P8	2,539	1,195	1,475	-	1,060	1,766	97
P9	968	144	152	10	959	2,502	536
P10	1,780	162	1,313	126	2,212	3,495	419
P11	1,788	-	-	-	3,787	2,548	2,173

**Table 3.11 Calculation of hang ups/ton based on hang up and tonnage records**

Draw Point Name	Jan,02	Feb,02	Mar,02	Apr,02	May,02	Jun,02	Jul,02
P1	0.0603	0.0025	0.0029	0.0041	0.0025	0.0059	0.0059
P2	0.0026	-	-	-	0.0007	0.0009	0.0023
P3	0.0062	0.0010	0.0008		0.0056	0.0044	0.0031
P4	0.0012	0.0011	0.0040	-	0.0023	0.0036	0.0034
P5	0.0078	0.0008	0.0011		0.0019	0.0021	0.0031
P6	0.0018	0.0013	0.0022		0.0016	0.0004	0.0101
P7	0.0021	0.0020	0.0021		0.0010	0.0044	0.0064
P8	0.0020	0.0033	0.0014		0.0019	0.0011	0.0924
P9	0.0021	0.0139	-	-	-	0.0016	0.0131
P10	-	-	-	-	0.0005	0.0009	0.0095
P11	-				0.0013	0.0024	0.0037

### **3.1.5 Records of oversize draw points**

Oversizes are treated in the same manner as hang ups, given their relevance to production performance. By combining the number of oversizes with the tonnage drawn from a draw point, it is possible to compute the oversize frequency, number of oversizes/ton, for a given period of time.

### **3.1.6 Production schedules**

The original production schedules are the original production estimates per draw point through the life of the mine completed as part of the feasibility study of the mine. This information was not found at the mines M1 to M4. It was usually found that the mines had kept the original global production targets per year or per quarter. However the detail per draw point was not available. This information was reconstructed based on the production targets reported in the feasibility study, draw point undercut sequence derived from the draw point status, draw rate reported in the feasibility study, development rate from draw point status and mine design (draw point spacing) from the feasibility study. The result was the tonnage planned per draw point per month during the life of the mine.

It was observed that there was no standardized way of recording operational upsets, besides the draw point status, that could be used for detailed back analysis or for general study of production performance. Considering that block caving is a complex mining method, more attention should be paid to capturing different operational and geotechnical situations that could assist mining engineers and geologists to understand the phenomenon of caving and its production implications. A proposed design for an operational database to be used in block cave mining is presented in Appendix A.

## **3.2 Effect of Geotechnical Events on Production Performance**

Production activities in a block cave mine are continuously interrupted due to infrastructure damage as a result of geotechnical events. One of the most significant interruptions is the secondary breakage activity to clear either a hang up or an oversize event at a draw point. Since secondary breakage usually involves the use of a drill and explosives to remove a hang up or an oversize, to clear one or several draw points along a crosscut, an entire production drift may be

closed to avoid hazards. Another important operational upset triggered by geotechnical events is the damage of the production infrastructure due to cracking or rock sloughing, or the collapse of the production drift due to induced stresses. The damage produced by induced stresses requires repair that could cease production from that drift for a period ranging from a few weeks to several months. It has also been found that usually after a few weeks without drawing from a production drift, damage occurs, sometimes resulting in the collapse of the production drift. This phenomenon is the result of rock mass compaction and subsequent stress transfer from the material overlying the production level to the production crown pillar. The fragmentation and the pillar convergence geotechnical events will be studied in the following sections, with a view to understand their implications on production performance.

### ***3.2.1 Effect of hang ups on production performance***

The secondary breakage activities taking place in an underground mine constantly interact with the production activities of the mine. In a block caving environment every production drift is usually engaged in production, secondary breakage or rework at any given time. Secondary breakage activity is often viewed as a bottle neck to reach production goals. Oversize events, as shown in Figure 3.2, are usually cleared within a shift and with production resuming immediately after blasting or breaking the boulder with mobile hammers.



**Figure 3.2 Oversize at a draw point of mine M2**

The situation is very different with hang ups which usually require a day or at least two shifts to clear. At the moment there is no a single rule regarding how many draw points should hang up until the status of a production crosscut is changed to secondary breakage. There are at least two strategies to attack the problem: the first is to wait for a given number of hanged up draw points in a crosscut, the second is to have a fixed secondary breakage sequence in which, regardless of the number of hanged up draw points, the status of the crosscut is changed to secondary breakage at a certain time. At the moment there is no clear evidence to say which strategy is more productive. Most likely the strategy to follow would depend upon the changes on rock mass fragmentation during the life of the mine.

Mine M2 has experienced extremely coarse fragmentation as a result of the geotechnical environment (high RMR) in which block caving has been applied. Consequently the scheduling of secondary breakage activities has been crucial to the productivity of the mine. The mine is divided into three geotechnical domains: D1, D2, D3 which lead to different fragmentation characteristics across the layout. Figure 3.3 shows the hang up frequency (hang ups/1000 tons) of these three areas as a function of draw point maturity. The cumulative tonnage drawn from a draw point converted to a height of draw column (HOD) is used as a proxy for draw point maturity in this case.

Figure 3.4 shows that the hang up frequency decreases as the draw point matures for the three geotechnical domains. This shows that material drawn from higher up in the draw column will have more secondary fragmentation than material located at the bottom. The second interesting observation from Figure 3.4 is that the hang up frequency tends to be fairly uniform across the active layout once a particular value of HOD is achieved, about 100 m in this case. This will lead to a totally different production scenario that could eventually facilitate expansion of the current production rates. Given that the hang up frequency will become uniform, the strategy to treat hang ups should evolve accordingly.

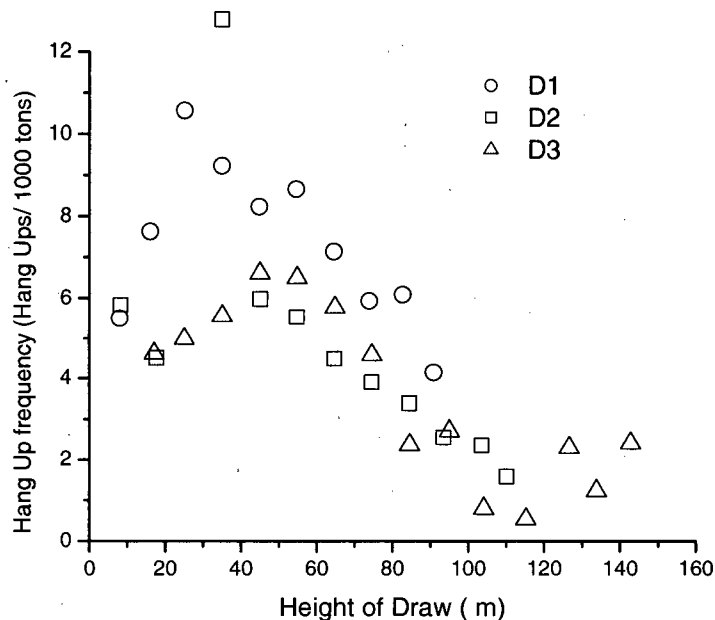


**Figure 3.3 Hang up frequency as a function of draw point maturity**

The second analysis performed at mine M2 was to correlate hang up frequency with draw point productivity per month with the objective of illustrating the impact of this geotechnical event on draw point productivity. Figure 3.4 shows the results of this analysis. There is little doubt that productivity is inversely correlated to hang up frequency. The more hang ups a draw point experiences in a given time period, the less time each draw point will be available for production. Figure 3.4 shows that hang up frequency, as an indicator of geotechnical events, affects draw point productivity. Consequently it could be expected that hang up frequency would affect the productivity of the whole mining system.

It should be noted that sometimes the correlation between hang up frequency and draw point productivity is positive. This can be explained by the fact that a draw point that is excessively drawn (i.e., yields high production) leads to differential draw with its neighbors and facilitates the development of a hang up in the draw bell.

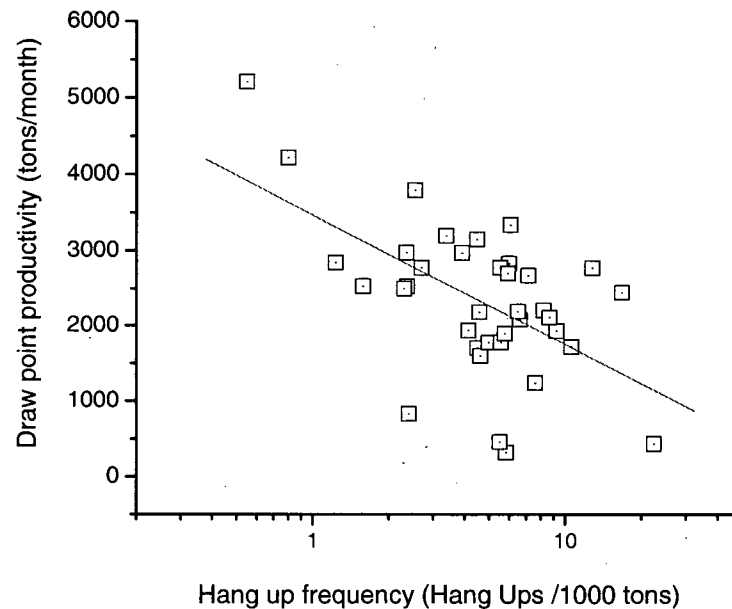


**Figure 3.4 Draw point monthly productivity as a function of hang up frequency**

### ***3.2.2 Effect of production performance on induced stresses***

There are several operational aspects that could lead to stress redistribution across the active layout. However a distinction should be made between stresses observed at the cave front and stresses observed within the active production area. A discussion of the nature of these two stress redistributions is given below.

#### ***Stress at the cave front***

The main cause of over stresses at the cave front is related to the angle of draw which affects the stress pattern at the cave front. The angle of draw is commonly measured in a vertical cross section perpendicular to the mining sequence displaying the height of draw (HOD) of the draw points as shown in Figure 3.5. A line is fitted to intersect the HOD of all draw points shown on this section. Then the angle of draw is measured from the horizontal to the fitted line.

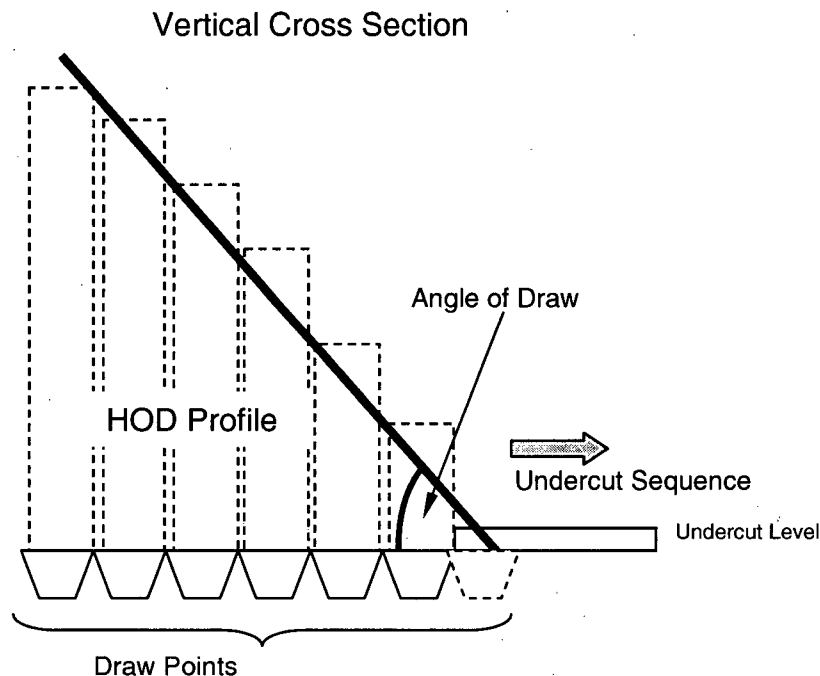


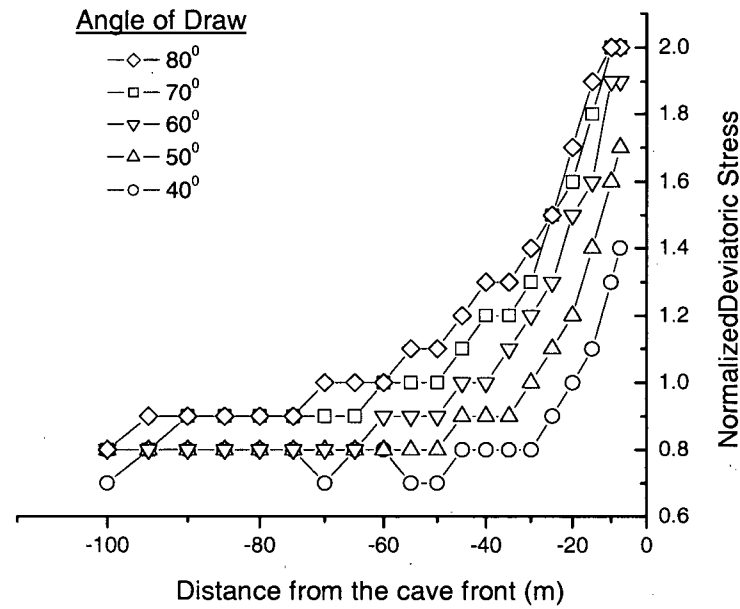
**Figure 3.5 Illustration of the angle of draw in a draw profile along a production drift**

Mine M3 had experienced a significant number of collapses at the cave front. As part of their production database this mine has recorded the time and location of the collapses for the first five years of operation. These data together with the production records were used to back-analyze the angle of draw in association with the historical collapses experienced at this mine. Collapse of the cave front was found to occur under three conditions:

- Shallow angle of draw: A shallow angle of draw would produce an open span that exceeds the rock mass strength and thus the roof of the undercut level would collapse as a result of the stress acting on the back of the undercut area.
- Steep angle of draw: As shown below a steep angle of draw induces a rotation of the stress tensor as well as increases the deviatoric stress (difference between principal stresses) experienced at the cave front (Rubio, et al, 2004).
- Sudden changes of the angle of draw between periods: This is explained below.

Figure 3.6 shows the effect of different angles of draw on the deviatoric stress which has been normalized by the deviatoric stress experienced at the pre mining stage. For a steep angle of draw the cave front will experience a significant increase in deviatoric stress with respect to the

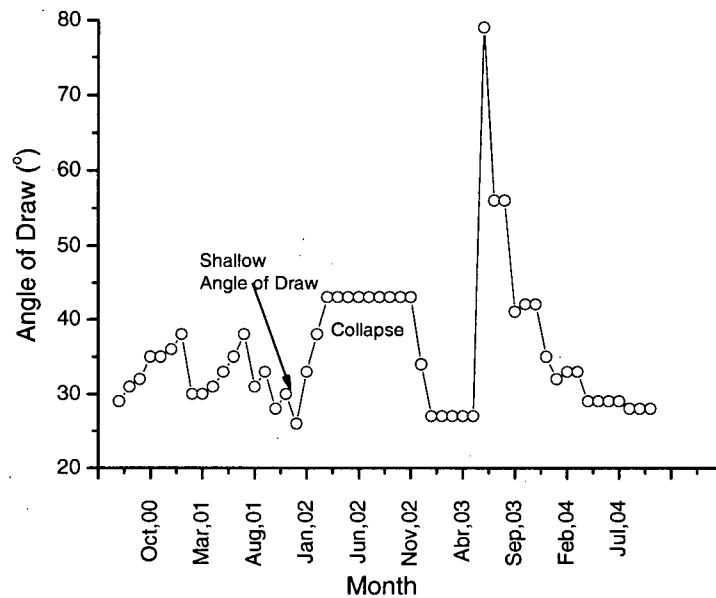
pre mining stage. The change in deviatoric stress will induce shear stress which, depending on the rock mass strength, could produce the collapse of the cave front. A collapse of the cave front would affect the productivity of the mining system since draw points could not be commissioned.



**Figure 3.6 Effect of angle of draw on the normalized deviatoric stress experienced at the cave front (Rubio et al, 2004)**

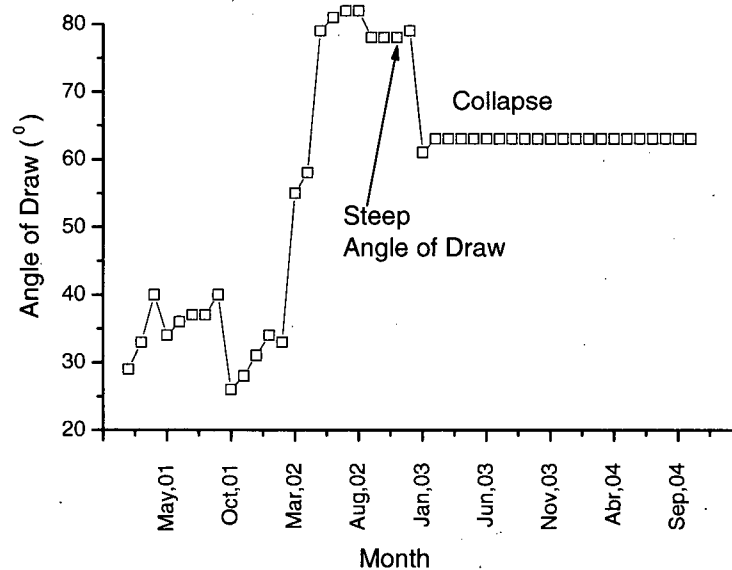
To show that such collapses occur, the data available from Mine M3 was used to compute the monthly angle of draw at each production crosscut for an approximate four year period. Then the angle of draw was correlated with the collapses experienced at this mine. It was shown that shallow or steep angles of draw induce collapses at the cave front leading to periods of “no draw”. Figure 3.7 shows the draw profile along a production drift in which the collapse of the cave front was induced by a shallow angle of draw below 30 degrees.





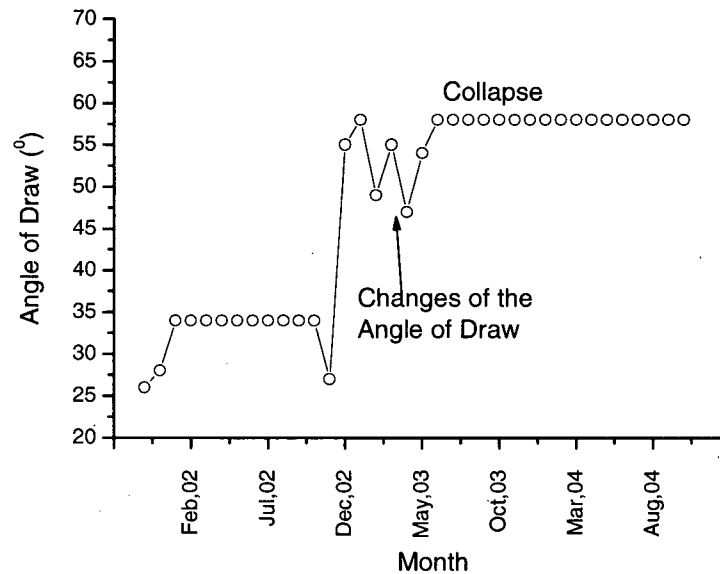
**Figure 3.7 Drift collapse due to a shallow angle of draw**

Figure 3.8 shows a case in which the collapse of the cave front was induced by a steep angle of draw over 60 degrees.



**Figure 3.8 Drift collapse due to a steep angle of draw**

Figure 3.9 shows the third mechanism of failure related to the sudden change of angle of draw from period to period. A theoretical explanation for this behaviour has not been found either in the literature. However it is believed that the stress tensor suffers several short-term changes as a result of modifying the angle of draw which would induce corresponding short-term changes in shear loads leading to rock mass failure.



**Figure 3.9 Drift collapse due to a sudden change on the angle of draw**

Based on the draw charts shown above it is possible to see that at this operation the range for the angle of draw should be in the interval 30 to 60 degrees. Obviously the ultimate range for the angle of draw is site dependent since this parameter is a function of in situ stress tensor, rock mass strength, undercutting method among others. Nevertheless the aim of this exercise was to show that production performance represented by the angle of draw may trigger geotechnical events that affect the stability of the cave front.

The cave front stability affects the undercutting process which influences the development rate. Araneda and Gaete (2004) derived an interesting relationship between development rate and block cave productivity

$$T(t) = D_v H \rho \left[ 1 - \exp\left(-\frac{v_d t}{\rho H}\right) \right] \quad (3.1)$$

The parameters of the model shown above are listed as follows:

$T(t)$	tonnage production per unit time
$D_v$	development rate in area per unit time
$H$	height of the economic draw column
$\rho$	the in situ specific gravity
$v_d$	the draw rate in tons/m <sup>2</sup> /day
$t$	the time variable

From the above relationship it is possible to see that any constraint on the development rate will affect the production tonnage and therefore the productivity of the mining system.

### *Induced stress on the production level*

Stress is redistributed on the production level as a function of the draw pattern performed across the production area. It is well established that even draw leads to a more uniform stress distribution on the production level than isolated draw. Isolated draw consists of performing excess ore extraction from a draw point or a group of draw points in isolation from the rest of the production area. Isolated draw leads to high concentration of stresses often resulting in large roof displacements. This phenomenon has been described by Verdugo and Ubilla (2004) who used a FLAC 2D model to represent the induced stress as a result of the arch effect produced in a hanged up draw point. Encina et al (2004) developed a model derived from first principles to analyze the effect of induced stress as a result of isolated draw. Also Rubio et al (2004) showed a discrete model constructed using PFC 2D to demonstrate the induced stress as a result of different draw strategies.

Although all this evidence presented in different papers it was desired to show the effect of production performance on the deformation of the major production apex pillar. Thus convergence observations, taken from mine M1, were used to study this phenomenon. Figure 3.10 shows the deformation of a draw point major apex pillar as a result of uneven draw. In this case the deformation led to the collapse of the production drift which later triggered closure of the entire production crosscut.



**Figure 3.10 Draw point minor apex pillar deformation as a result of uneven draw at mine M4**

Despite the empirical evidence and theoretical explanations for stress redistribution on the production areas of a block cave mine, none of the mines studied showed a clear indicator to assess the uniformity of the draw pattern. An indicator called “draw cycle” was developed as part of the research to represent the uniformity of a given draw pattern. The draw cycle of a production crosscut is defined as the time it would take to draw at least a certain number of buckets from every draw point of the crosscut. The longer the crosscut draw cycle, the more chance there is of areas of no draw within the crosscut leading to instability. An alternative definition of the draw cycle would be the fraction of the total number of draw points in a crosscut that are drawn in a given period of time.

The Mine M1 database was used to study the relationship between the convergence displacements observed at different places along the production drift and the draw cycle computed at this mine. The analysis was conducted in periods of four days given three years of production and convergence records. In this case the crosscut draw cycle was estimated as the fraction of the total number of draw points drawn (at least 500 tons) in a time period of four days. Figure 3.11 shows a relationship between the fraction of the production crosscut (XC) drawn in a four day period and the total convergence observed along the crosscut for the same period of time. Four days was used as the time period in order to obtain the whole range of

possible draw cycles. Figure 3.11 suggests a direct inverse correlation between crosscut draw cycle and convergence observed on the active production area of a block cave mine.

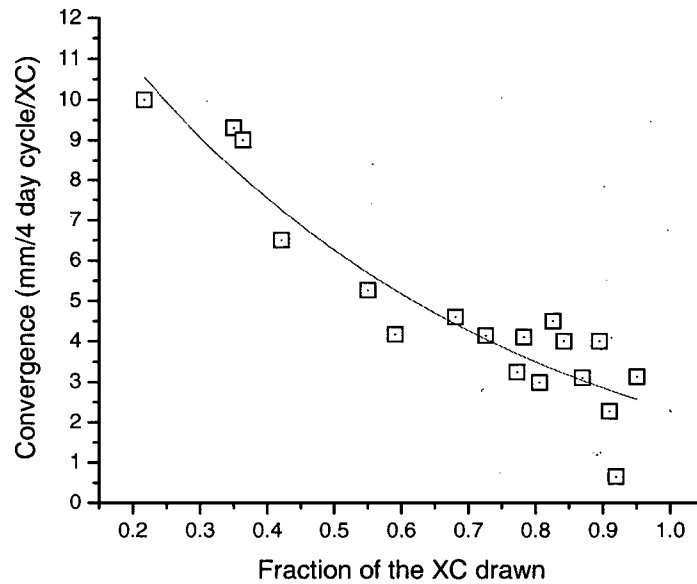


**Figure 3.11 Total crosscut deformation as a function of the draw cycle**

### 3.3 Failure of mining infrastructure

It has been shown that geotechnical events such as convergence and fragmentation affect the productivity of the mining system. In this section the failure characteristics of a draw point will be studied to achieve a better understanding of the relationship between failure and production performance. To begin the study, consider the draw point status recorded at mine M1 as shown on Figure 3.12.

Draw Point\ Day	1	2	3	4	5	6	7	8	9	10	11	12	13	14
D1	A	A	A	A	A	A	A	A	A	A/H	A/H	A/H	A/H	A/H
D2	B/H	B/H	B	B	B	B	B	B	B	B	B	B	B	B/H
D3	A	A	A	A	A	A	A	A	A	A	A	A	A	A
D4	A	A	A	A	A	A	A	A	A	A	A	A	A	A
D5	A	A	A	A	A	A	A	A	A	A	A	A	A	A
D6	A	A	A	A	A	A	A	A	A	A	A	A	A	A
D7	-	-	-	-	-	-	-	-	-	-	-	-	-	-
D8	-	-	-	-	-	-	-	-	-	-	-	-	0	0
D9	-	-	-	-	-	-	-	-	-	-	-	-	0	0
D10	-	-	-	-	-	-	-	-	-	-	-	-	0	0
D11	A/H	A/H	A	A	A/H	A/H	A/H	A/H	A	A/H	A/H	A/H	A/H	A/H
D12	C	C	C	C	C	C	C	C	C	C	C	C	C	C
D13	A/H	A/H	A/H	A	A/H	A/H	A/H	A	A/H	A	A	A/H	A/H	A
D14	A	A	A	A	A	A	A	A	A	A	A	A	A	A

**Figure 3.12 Operational records of draw point status data**

Note that in this case failure is recorded when the draw point status changes from active (A) to any of the other status such as oversize (B, B/H), temporarily closed due to high convergence (C) or hanged up (A/H). Table 3.12 shows the method that has been used to count the number of failures of a draw point. In this example draw point D54 is under analysis. Column “Code” contains a binary variable with value of 1 if the draw point is Active or 0 otherwise. Column “Failures” contains a binary variable with value of 1 if a draw point has changed its status Active to any other status within two consecutive days.

**Table 3.12 Counting failures as a function of the daily draw point status records**

Time (Days)	Draw Point Name	Status	Code	Failures
1	D54	A/H	0	
2	D54	A/H	0	0
3	D54	A/H	0	0
4	D54	A/H	0	0
5	D54	A/H	0	0
6	D54	A	1	0
7	D54	A/H	0	1
8	D54	A	1	0
9	D54	A	1	0
10	D54	A	1	0
11	D54	A/H	0	1
12	D54	A	1	0
13	D54	A	1	0
14	D54	A	1	0
15	D54	A	1	0
16	D54	A/H	0	1

Table 3.13 that shows the times during the life of a draw point at which failure occurs and the cumulative number of failures as a function of time,  $N(t)$ .

**Table 3.13 Counting process of failures for draw point D54**

Time of Failure (Days)	Cumulative Number of Failures $N(t)$
7	1
11	2
16	3
31	4
37	5
41	6
46	7
61	8
67	9
71	10
76	11
91	12
97	13
101	14
106	15
121	16

Figure 3.13 shows a plot of  $N(t)$  versus time. This plot is very relevant to the understanding of the evolution of failure in a draw point and the general mining infrastructure. For instance one can see that after 150 days of operation the tendency to failure changes reflected by the shape of  $N(t)$  which becomes more concave.

At the moment draw point failure has been related to time. However, mining infrastructure ages as a function of the tonnage that has been processed through it. For example two draw points could have been commissioned at the same time but one of them may have produced 150,000 tons and the second one only 40,000 tons. The first draw point would have been exposed to more wear and tear than the second draw point which is less mature (in terms of tonnage drawn). Therefore it is expected that the first draw point would have a greater tendency to fail than the second one. This suggests that time is not the correct indicator to represent the tendency of draw point failure.

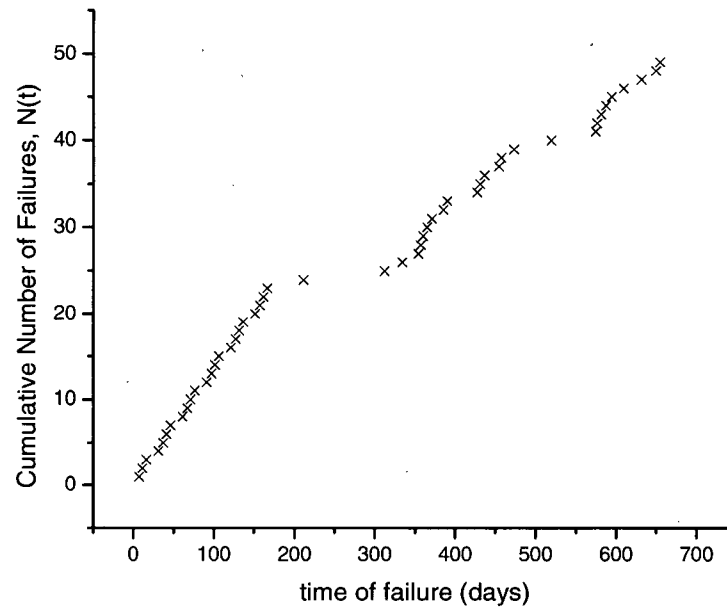


**Figure 3.13 Cumulative number of failures for a single draw point**

The production history of draw point D54 was taken from the tonnage production database and cross related with the failures recorded per month as shown on Table 3.14.

**Table 3.14 Estimation of Draw Point Rate of Occurrence of Failure**

Time of Failure (Days)	N(t)	Cumulative Tonnage (tons)	Incremental Tonnage (tons)	$\hat{w}(T)$ (Failures/tons)
31	4	6,623	6,623	0.0006
61	8	11,073	4,451	0.0009
91	12	18,492	7,419	0.0005
121	16	20,606	2,114	0.0019
151	20	28,949	8,343	0.0005
211	24	34,326	5,377	0.0007
312	25	42,884	8,558	0.0001
334	26	45,713	2,829	0.0004
427	34	55,065	9,352	0.0009
519	40	64,562	9,497	0.0006
574	41	73,069	8,507	0.0001
609	46	77,075	4,006	0.0012
631	47	79,254	2,179	0.0005

The first column of Table 3.14 shows the chronologic time at which the draw point failed. The second column shows the cumulative number of failures. The third shows the cumulative



tonnage drawn from the draw point at the time of failure. The fourth column shows the calculation of the incremental tonnages between times of failure. The last column shows the calculation of the draw point rate of occurrence of failure per tons.

The draw point rate of occurrence of failure (draw point ROCOF) represents the frequency at which a draw point fails in a given tonnage interval  $\Delta T$ . ROCOF is used rather than failure rate since a draw point is a repairable component that behaves as new after repair has been conducted. Failure rate is usually used to represent the failure behaviour of a non-repairable mechanical component (Hoyland and Rausand, 1994). The draw point ROCOF is given by:

$$w(T) = \frac{d}{dt} E[N(T)] \quad (3.2)$$

where  $w(T)$  is the draw point ROCOF after drawing  $T$  tons from the draw point,  $E[N(T)]$  is the expected value of the number of failures,  $N(T)$ , in the tonnage interval  $(0, T]$ . For a discrete tonnage interval  $\Delta T$  Equation 3.2 may be rewritten as follows:

$$w(T) = \lim_{\Delta T \rightarrow 0} \frac{E[N(T + \Delta T) - N(T)]}{\Delta T} \quad (3.3)$$

If  $\Delta T$  is small,  $E[N(T + \Delta T) - N(T)] = M(T, T + \Delta T)$ , the mean number of failures in the tonnage interval between draw point repairs. Then a natural estimator for  $w(T)$  would be

$$\hat{w}(T) \approx \frac{M(T, T + \Delta T)}{\Delta T} \quad (3.4)$$

Equation 3.4 will be used to estimate the draw point ROCOF for a given tonnage interval  $\Delta T$ . Table 3.14 shows the application of Equation (3.4) to estimate the draw point ROCOF during the production history of draw point D54.

Figure 3.14 shows a plot of draw point ROCOF against the cumulative tonnage drawn. From this plot is possible to see at least three areas in which the tendency of draw point D54 to fail changes. Between 0 and 20,000 tons drawn there is a decrease in the tendency of failure. Between 20,000 and 60,000 tons there is a relatively constant tendency to failure. Over 60,000 tons there is an increase in the tendency to failure. This behaviour could be explained by the nature of the mining method in which at the beginning of the life of the draw point there is a high probability of experiencing hang ups and oversize due to primary fragmentation with very little

or no influence of secondary fragmentation. Between 20,000 and 60,000 tons drawn the draw point enters a steady state regime in which there is an even probability of experiencing failure, most likely low probability of hang ups and medium probability of over size due to the influence of secondary fragmentation. Over 60,000 tons drawn in the case of D54 the draw point start to wear out showing damage on the concrete and the draw point brow tends to retreat towards the production drift.

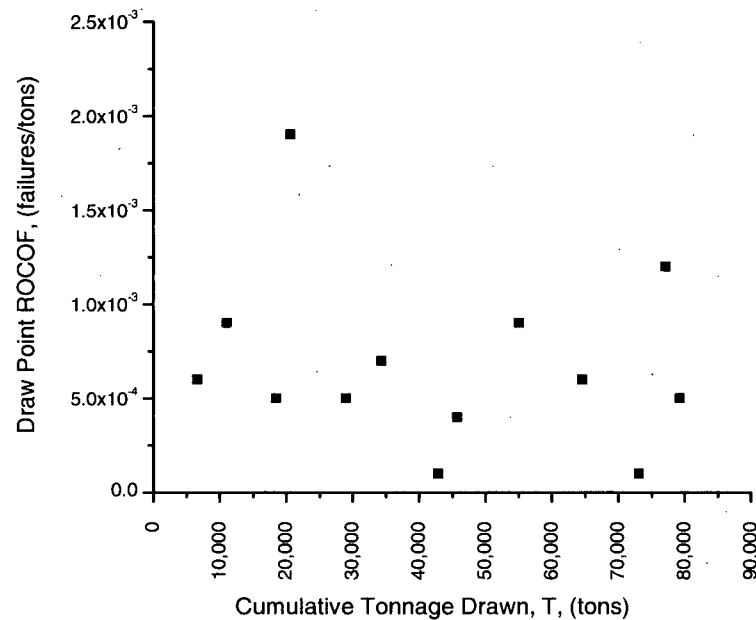


**Figure 3.14 Experimental draw point ROCOF for draw point D54**

The average draw point ROCOF curve of mines M1 and M2 was computed using the following procedure;

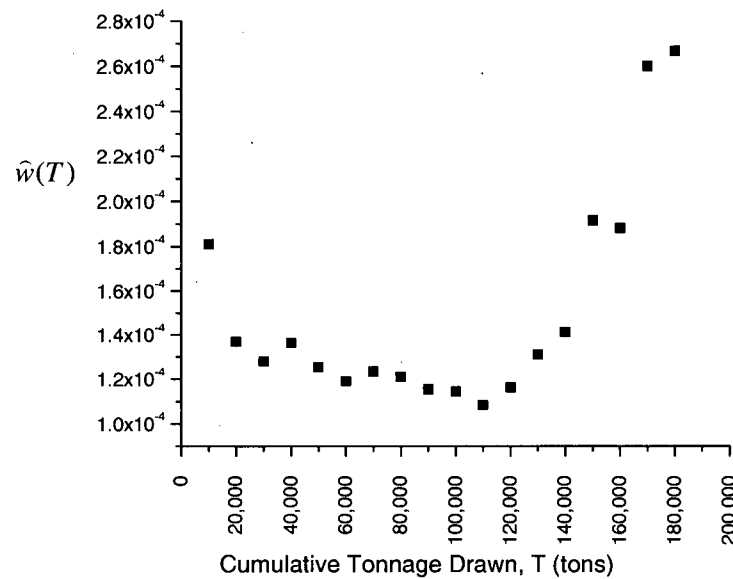
- 1) Compute the cumulative tonnage drawn per draw point per month for the time horizon under study.
- 2) Compute the number of failures of the draw points for each month during the time horizon under study
- 3) For each 10,000 ton interval of cumulative tonnage drawn, compute the average number of failures
- 4) Plot the computed average ROCOF versus the cumulative tonnage.

Table 3.15 shows a detailed calculation of average draw point ROCOF for mine M1. The second and the third columns represent the total number of draw points and the total number of failures of draw points with tonnage less or equal to the lower bound tonnage. The average number of failures per draw point is the ratio between the differentials of column 3 and 2. Finally the draw point ROCOF for different tonnage intervals is the result of dividing the 4<sup>th</sup> column by 10,000 tons.

**Table 3.15 Average draw point ROCOF for Mine M1**

Lower Bound Tonnage	Number of Draw Points	Number of failures	Average Number of Failures per Draw Point	$\bar{w}(T)$ (Failures/tons)
10000	327	592	1.81	1.8E-04
20000	666	1056	1.37	1.4E-04
30000	1002	1486	1.28	1.3E-04
40000	1338	1944	1.36	1.4E-04
50000	1650	2335	1.25	1.3E-04
60000	1965	2710	1.19	1.2E-04
70000	2273	3090	1.23	1.2E-04
80000	2554	3430	1.21	1.2E-04
90000	2807	3722	1.15	1.2E-04
100000	3010	3954	1.14	1.1E-04
110000	3201	4161	1.08	1.1E-04
120000	3342	4325	1.16	1.2E-04
130000	3445	4460	1.31	1.3E-04
140000	3513	4556	1.41	1.4E-04
150000	3548	4623	1.91	1.9E-04
160000	3565	4655	1.88	1.9E-04
170000	3575	4681	2.60	2.6E-04
180000	3578	4689	2.67	2.7E-04

Figure 3.15 shows the resulting draw point ROCOF curve for mine M1. This curve represents the evolution of the tendency of a representative draw point in Mine M1 to fail.



**Figure 3.15 Draw point ROCOF curve for mine M1**

Across an active layout there could be draw points that do not follow the same trend showed in Figure 3.15. More detailed analysis can treat these outlier draw points using a different draw point ROCOF curve representing the failure tendency of that subset of draw points.

The tonnage-dependent behaviour of failure of a draw point shown by the ROCOF curve is interesting. At the beginning of a draw point's production life, it is exposed to several factors that may induce it to fail such as poor construction quality, pillars left on the undercut level due to poor undercut blasting, or blast damage of the crown pillar due to poor design of the drilling and blasting at a draw bell. However the most serious geotechnical event would be the cave propagation after blasting the draw bell. After drawing the ore blasted as part of the undercutting a draw point moves to a regime in which the failure rate is relatively constant and dependent on secondary fragmentation and factors such as oversize and minimum hang up events. At the end of the productive life of a draw point the draw point brow will have been eroded. There will be a few steel arches lost, as a result of the constant friction between the concrete and the flow of rock, and the production drift will have experienced severe damage. These three behaviours are observed in Figure 3.15. At the beginning there is a high rate of failure which decreases until about 40,000 tons are drawn. Then the draw point moves to a stable rate of failure depending on

secondary fragmentation. Finally when the draw point reaches 120,000 tons drawn it starts to fail due to wear out of concrete and loss of steel arches on the draw point brow.

It is interesting to draw an analogy between the draw point ROCOF curve and a failure rate of a mechanical component as shown in Figure 3.16. The failure rate of a mechanical component, often called “bathtub” curve (Hoyland and Rausand, 1994) due to its characteristic shape, represents the evolution of the tendency of a mechanical component to fail during its life.

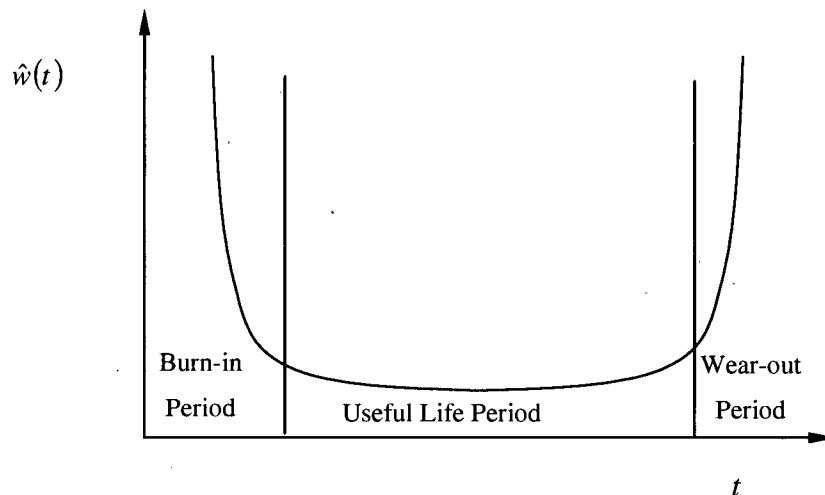


**Figure 3.16 Bathtub curve for a mechanical component (Hoyland and Rausand, 1994)**

There are three main areas on the bathtub curve. During the burn-in period there are undiscovered defects which usually manifest themselves when the units are activated. When the units have survived the burn-in period, the failure rate often stabilizes at a level where it remains for a certain period of time called the useful life period until it starts to increase as the unit begins to wear out. The similarity to the ROCOF curve of a mine is evident. This analogy is used to introduce the concept of draw point reliability later in this chapter.

### **3.3.1 Data Analysis for computing draw point ROCOF curve**

The estimation of ROCOF based on operational records of draw point status may be misleading as a result of noise contained on the raw data. For example it has been found at several operations that a draw point shuts down due to operational logistics rather than geotechnical problems. Also when a draw point has been cleared and is operational, the status of the draw point will change in the database only when the draw point has a LHD allocated to it. This could

be several days. Until that time, the draw point would still be in repair status. It is expected that in the future the allocation of secondary breakage equipment will be driven by the dispatch system which could enhance the way draw point status is recorded.

The methods used in this research to reduce the effect of noise in the recorded draw point status are summarized as follows:

- Disregard raw data outside the 95% confidence interval, that is data that is outside of the average plus or minus two times the standard deviation is ignored
- Crosschecks such as between draw point status and tonnage records for the same day, or between draw point status and production crosscut status.

### **3.4 Draw point ROCOF curve as a function of geotechnical domains**

The aim of this section is to study a possible relationship between the shape of the draw point ROCOF curve and the underlying geotechnical domain. The concept of the ROCOF curve would suggest that as the geotechnical characteristics of the rock mass become more adverse from a mining system point of view, the more failures a piece of mining infrastructure would experience. In the case of draw points and the main components of block caving infrastructure, as the rock mass becomes weaker, typically with a mining rock mass rating (MRMR) (Laubscher, 1989) less than 30, the draw point ROCOF curve should be shifted upwards as a result of high frequency of collapses experienced on the production level as a result of the low rock mass rating.. The same effect is observed when the rock mass is competent (MRMR greater than 70) the draw point ROCOF curve would be shifted upwards due to draw point fragmentation characteristics, resulting in high frequency of hang ups and oversize as a result of the high rock mass rating.

The relationship between draw point ROCOF curve and geotechnical domains has been tested by constructing the draw point ROCOF curve for every production crosscut. It was expected that eventually a crosscut would be developed in a different geotechnical environment (different MRMR) area respect to the rest of the crosscuts. This should be reflected by the shape of the draw point ROCOF curve. Figure 3.17 shows an analysis conducted using the data from mine

M1, in which the draw point ROCOF curve has been constructed for three different production crosscuts.

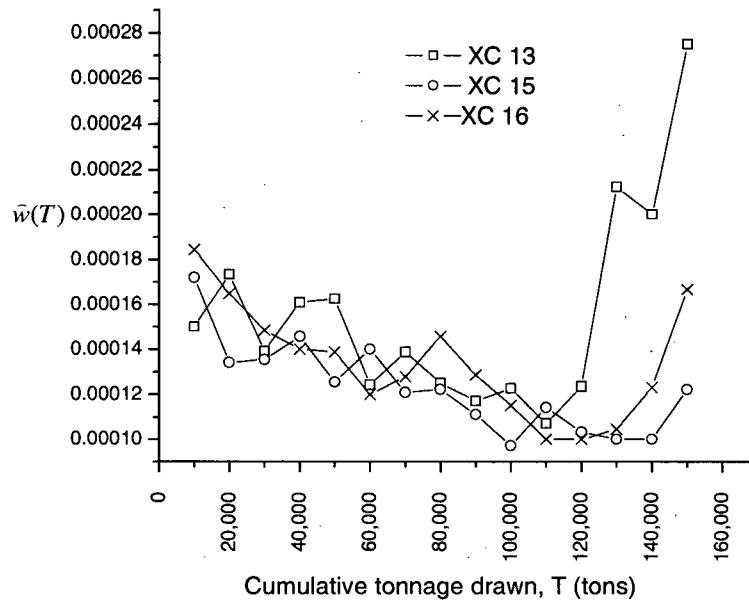


**Figure 3.17 Draw point ROCOF curve for different production areas of mine M1**

Based on Figure 3.17 the crosscut XC13 exhibits a higher likelihood of failure based on its draw point ROCOF curve. This agrees with the fact that the mine started undercutting in this area due to its weak rock mass characteristics. Hence, the same geotechnical characteristic that was used to decide the place where to start undercutting was harmful to the long term stability of the draw points. Therefore different draw point ROCOF curves have to be used to represent appropriately the draw point rate of failure of different geotechnical domains found across the mine.

A second test consisted in comparing the average draw point ROCOF curve of two different mines (M1 and M2) which happen to be operating in two different geotechnical environments. M1 operates in a rock environment that is considered to be the optimal for the use of block cave, since the rock is strong enough to sustain the production infrastructure but weak enough to produce the desired fragmentation for the mining method. On the contrary, M2 is developed in a competent rock mass environment that has delivered a very coarse fragmentation inducing a high rate of hang ups and oversize during the life of the mine. Figure 3.18 shows two different draw point ROCOF curves from mines M1 and M2.

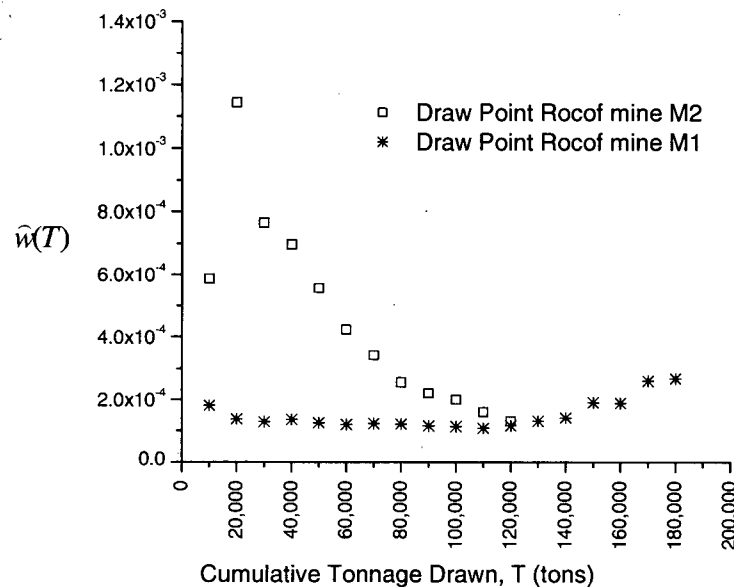


**Figure 3.18 Draw point ROCOF curve comparison between two operating block cave mines**

It is seen that mine M2 has a higher average draw point ROCOF curve than mine M1. In other words a M2 draw point fails more frequently than a M1 draw point. This is effectively reflecting the fact that M2 is operating in one of the most competent rock mass environments found in block cave mining today (MRMR=80). On the other hand, M1 operates in what is considered an ideal rock mass environment for block caving with a MRMR= 45 across the layout, facilitating cave propagation and fragmentation. In summary it is possible to see that both curves have similar shapes but the gap between them is related to the rock mass condition that triggers different geotechnical events and subsequent production losses.

Finally the draw point ROCOF curve has been identified as a very important caving performance indicator since it could provide insights as to how the production system will evolve in time without explicitly modeling the geotechnical behavior of the system. It is not suggested that geotechnical modeling should be excluded from the engineering process of designing a block cave mine. On the contrary, the author believes that such modeling may contribute a great deal to the understanding of the rock mass and its role in the mining system. Nevertheless the draw point ROCOF curve is a production control/planning tool that enables engineers to quantify the effect



of geotechnical events on the likelihood of mining infrastructure to achieve a desired production target.

The next step consists of introducing a tool that characterizes the life cycle of a draw point from a reliability point of view. This concept is important since it facilitates the implementation of draw point failure performance as part of a production scheduling process.

### **3.5 Draw Point Reliability as an Indicator of Geotechnical Events**

In the previous section, two geotechnical events were studied: hang ups and displacements along the production drift. It was shown that these two geotechnical events are correlated with draw point production performance. In this section, draw point reliability will be introduced as a planning parameter that could subsume the effects of at least these two geotechnical events. Draw point reliability is defined as the probability that the draw point will be available to produce certain amount of tonnage in a given period of time. Since the production capacity of a draw point will be determined in part by the underlying geotechnical events that induce failure on mining infrastructure, the failure characteristics of a draw point will determine the reliability of a draw point. The aim of this definition is to use the draw point reliability as a planning parameter that would facilitate the estimation of the mining system reliability by modeling the mine as if it were an aging mechanical component. Thus, concepts used in reliability engineering could be applied to better forecast the failure behaviour of a draw point, consequently enhancing the ability to forecast draw point production capacity.

Lakner and Anderson (1985) have defined reliability as the probability that an item will perform a required function under stated conditions for a stated period of time. Note that “functioning” implies that an item could be either in active operation or able to operate if required. In that context, reliability of a given component,  $r$ , is related to the probability of failure,  $p$ , through the equation

$$r = 1 - p \quad (3.5)$$

The reliability of a draw point is defined as the probability that the draw point does not fail to produce a certain tonnage  $\Delta T$ . This probability will be computed as a function of the draw point ROCOF curve which is the natural estimator of draw point tendency to failure.

### 3.5.1 Measurements of draw point reliability

An approach similar to that used by Ascher and Feingold (1984) can be used to define a relationship between the estimated ROCOF and an estimate of draw point reliability. The reliability of a draw point to produce  $T$  tons can be expressed as:

$$R(T) = 1 - F(T) = P(T_0 > T) \quad (3.6)$$

Then knowing that the rate of occurrence of failure is the probability that the draw point would fail within the tonnage interval  $(T, T + \Delta T]$ ,  $w(T)$  can be written as:

$$w(T) = \lim_{\Delta T \rightarrow 0} \frac{P(T < T_0 < T + \Delta T | T_0 > T)}{\Delta T} \quad (3.6)$$

Using Bayes theorem the conditional probability can be re-written as:

$$w(T) = \lim_{\Delta T \rightarrow 0} \frac{P(T < T_0 < T + \Delta T | T_0 > T)}{\Delta T} = \lim_{\Delta T \rightarrow 0} \frac{F(T + \Delta T) - F(T)}{\Delta T} \frac{1}{R(T)} \quad (3.7)$$

From Equation 3.6  $\dot{R}(T) = -F(T)$ . Substituting in Equation 3.8

$$w(T) = -\frac{\dot{R}(T)}{R(T)} \quad (3.8)$$

Integration of the above differential equation gives

$$\ln[R(T + \Delta T)] - \ln[R(T)] = - \int_T^{T+\Delta T} w(u) du \quad (3.9)$$

The draw point is functioning after drawing  $T$  tons, then  $R(T) = 1$ . Thus, equation (3.9) can be re-written as

$$R(T + \Delta T) = \exp \left[ - \int_T^{T+\Delta T} w(u) du \right] \quad (3.10)$$

In order to compute Equation 3.10 one would need to know the form of the function  $w(u)$ . Several models can be fit to this function such as the Poisson or renewal processes (Rigdon and Basu, 2000). In the following  $w(u)$  is read directly from the draw point ROCOF curve and it is assumed to be constant for the tonnage interval at which the production schedule is run. The tonnage interval for a typical long term production schedule run in a monthly basis would vary in the range of 3,000 to 8,000 tons which is less than 10,000 tons, the tonnage step for the construction of the draw point ROCOF curve. This assumes that the draw point tendency to

failure remains constant in a tonnage interval of 10,000 tons which is about 15m of draw column. This assumption is reasonable since in block cave mining system the rock mass is often very uniform. Thus, the draw point ROCOF curve will be replaced in Equation 3.11 resulting in the following expression for estimating the draw point reliability:

$$\hat{R}(T + \Delta T) = \exp[-\hat{w}(T)\Delta T] \quad (3.11)$$

The reliability per draw point per month was estimated for the mines M1 and M2 using the above formulation. Mines M3 and M4 were not analyzed since there were no records of draw point status per day or hang up frequency to construct the draw point bathtub curves. The estimation of historical draw point reliability was useful to compare against geotechnical factors such as hang up frequency and convergence. It is expected that this will show that draw point reliability could subsume the effects of geotechnical events that trigger operational upsets.

Note that the measurements of reliability have been made independent of the tonnage drawn per draw point or crosscut. This provides two independent variables: tonnage and reliability that aim to characterize the mining system at any given time.

To corroborate the estimation of draw point reliability as a function of the monthly ROCOF the draw point availability was computed. It was expected that there should be a direct correlation between draw point reliability computed using draw point monthly ROCOF and monthly draw point availability. The monthly draw point availability was computed as the ratio of the time that a draw point has been active to operate over a time period of a month. Figure 3.19 shows the average monthly draw point availability during the life of a draw point of mine M1. It is seen that the shape of the monthly draw point availability is the inverse of the draw point ROCOF curve. This will lead to a direct correlation between the draw point reliability derived from ROCOF and draw point availability as shown in Figure 3.20.

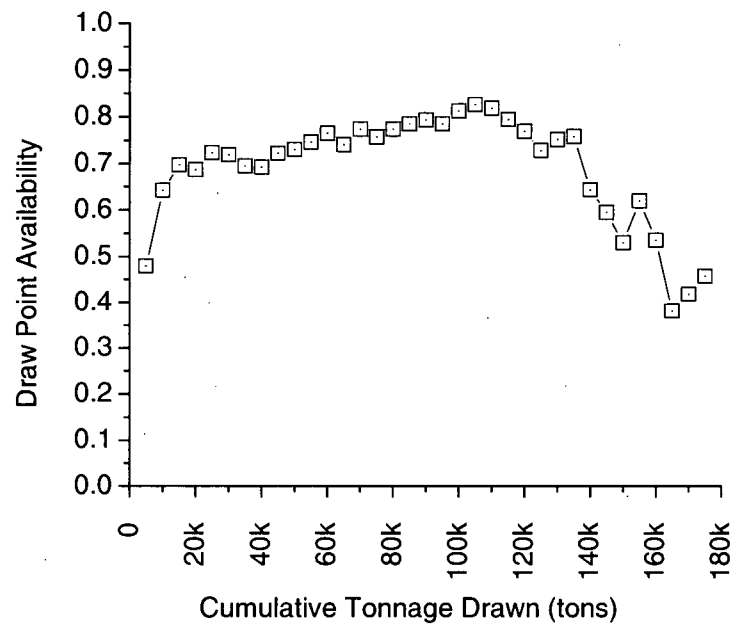


**Figure 3.19 Average monthly draw point availability from mine M1**

Figure 3.20 shows a close correlation (0.99) between draw point reliability and draw point availability. Therefore it would be possible to use Equation 3.11 within the production schedule to compute draw point reliability as a function of the draw point ROCOF curve.

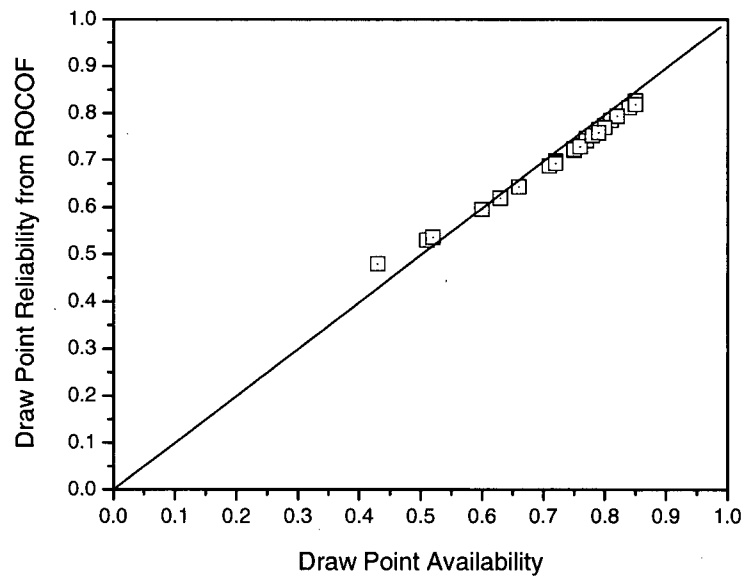


**Figure 3.20 Comparison of draw point reliability versus draw point availability**

### 3.5.2 Effect of hang up frequency on draw point reliability

Figure 3.21 shows a relationship between hang up frequency and draw point reliability at different stages of draw point maturity for mine M2. There is a negative correlation between hang up frequency and draw point reliability as a measure of its ability to provide the planned tonnage. Note that the available data is mainly in the interval of 2 to 10 hang ups/1000 t which results in a reduction of draw point reliability from 0.7 to 0.4.

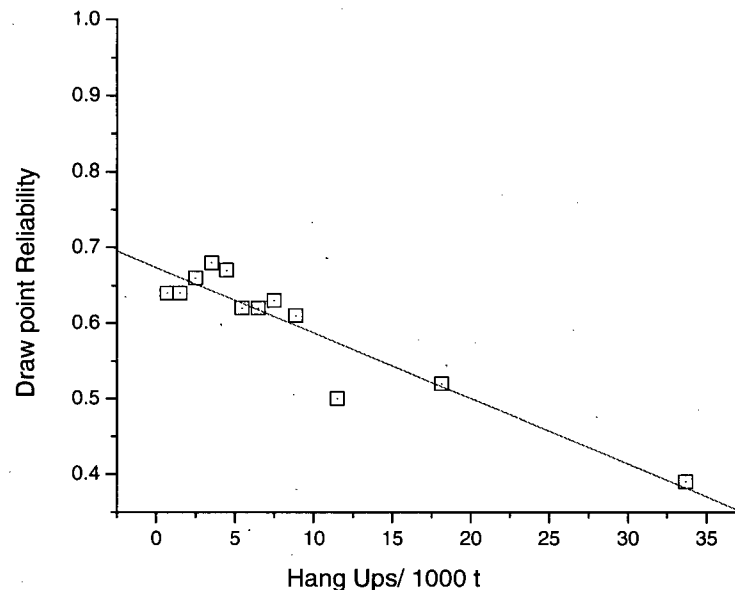


**Figure 3.21 Effect of hang up frequency on draw point reliability**

### 3.5.3 Effect of induced stress on draw point reliability

Induced stress across the active layout has been recognized as the second most important cause of draw point breakdown after draw point oversized and hanged up. Figure 3.22 shows also a negative correlation between measured convergence, as a result of stress redistribution, and draw point reliability for mine M1.

Based on the empirical charts constructed with data from mines M1 and M2, it was possible to conclude that draw point reliability does represent the most relevant geotechnical factors that trigger draw point failure with consequent loss in production. This conclusion is very important

since it implies that geotechnical factors can be represented by a simple operational measure such as the draw point reliability.

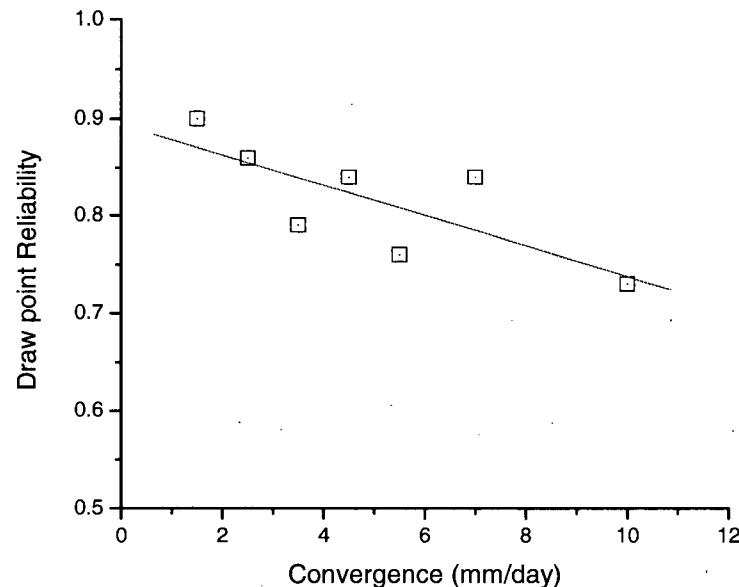


**Figure 3.22 Effect of convergence on draw point reliability**

The fact that hang up frequency and convergence observations correlate well with draw point reliability as shown on Figure 3.21 and Figure 3.22 respectively, indicates that draw point reliability could subsume the geotechnical events that lead to infrastructure failure. This result is of interest since draw point reliability, which is an operational indicator derived from empirical measurement of failures, would allow modeling the rock mass response to mining as a realization of the fundamental geomechanical models. The introduction of draw point reliability into a mine wide reliability model would facilitate the calculation of how realistic a production target is as a function of the system reliability. This will be further explained in the next chapter of the research.

## **4 PRODUCTION SCHEDULING INTRODUCING THE CONCEPT OF RELIABILITY**

One of the main objectives of the research presented in this dissertation is to compute the probability of success of a given production plan. This can be computed as the reliability of a production schedule, which represents the inherent uncertainty of the mining system to achieve a desired production target as a result of the geotechnical events that affect the availability of mining infrastructure. Chapter 3 showed how the draw point ROCOF can be used as an operational indicator of the likelihood of failure of a draw point. It was also shown that the draw point reliability, derived from the draw point ROCOF curve could subsume geotechnical events that trigger failure of the draw point. In this chapter the individual draw point reliabilities will be introduced in a mine wide reliability model to compute the system reliability. Then this model will be used to compute the probability of success of different production schedules as a function of planning variables such as production targets, draw point yield, and development rate.

### **4.1 Definition of System Reliability**

The concept of reliability applied to mining was first introduced by Dotson (1966), describing mainly the failure modes of equipment and its influence on productivity. Later Kumar and Granholm (1988) constructed reliability models to support the design, planning and operation mainly oriented to equipment performance. These authors concentrate on using reliability to identify the most unreliable subsystems and the economic implications of these subsystems.

Ramani, et al (1989) also discussed the application of the concepts of reliability, maintainability and availability to study the subsystems of longwall mining system. Kazakidis and Scoble (2002) used continuous distributions to model the reliability and hazard function of the mining system components presented in Figure 4.1. The authors used different probability distributions to model the failure rates of different mining infrastructure. Nevertheless, the authors stated that there was not enough operational data to support the use of a given set of distributions for different components of the mining system. Also this research does not consider whether the components of a mining system are non repairable or repairable components. As shown in Chapter 3 the components of the block cave mining system, particularly draw points, are repairable

components. This leads to a different formulation than the one presented by Kazakidis and Scoble (2002)

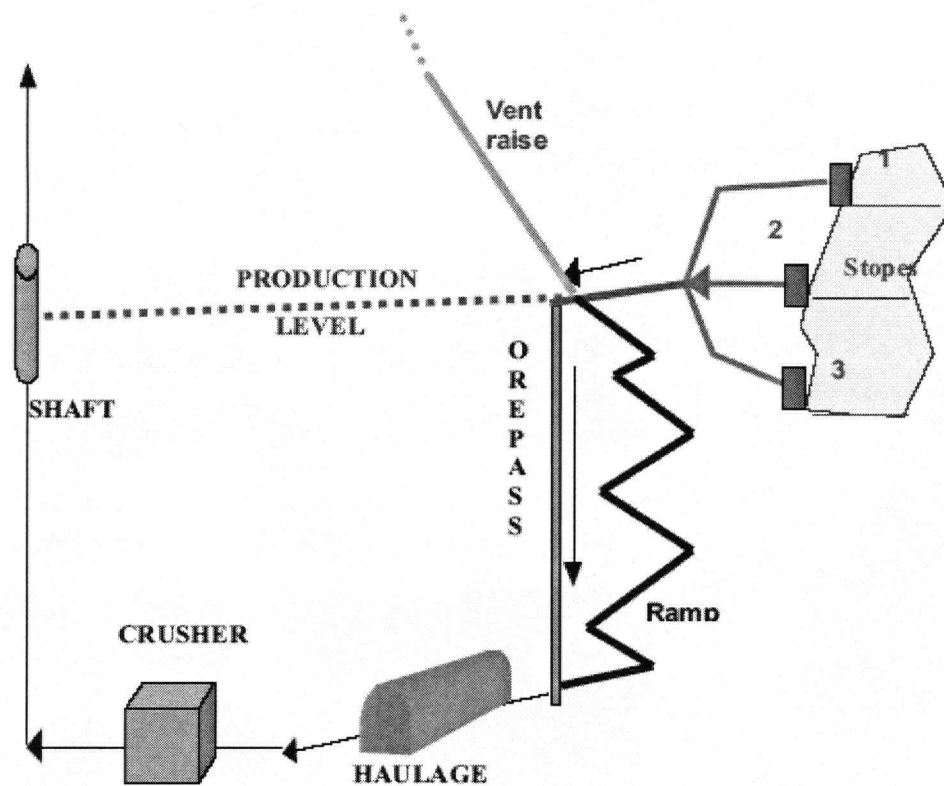


**Figure 4.1 Components of a traditional mining system (Kazakidis and Scoble, 2002)**

Reliability modeling of a system is based on the failure characteristics of the individual components of the system represented by the reliability of the system's component. To compute the reliability of a system based on the reliability of its components a "Reliability Block Diagram" (Hoyland and Rausand, 1994) is used to represent the hierarchical relationships among the different components of a system. Individual components of a system can be connected in series, parallel and series-parallel combinations, examples of such combinations are shown in Figure 4.2.



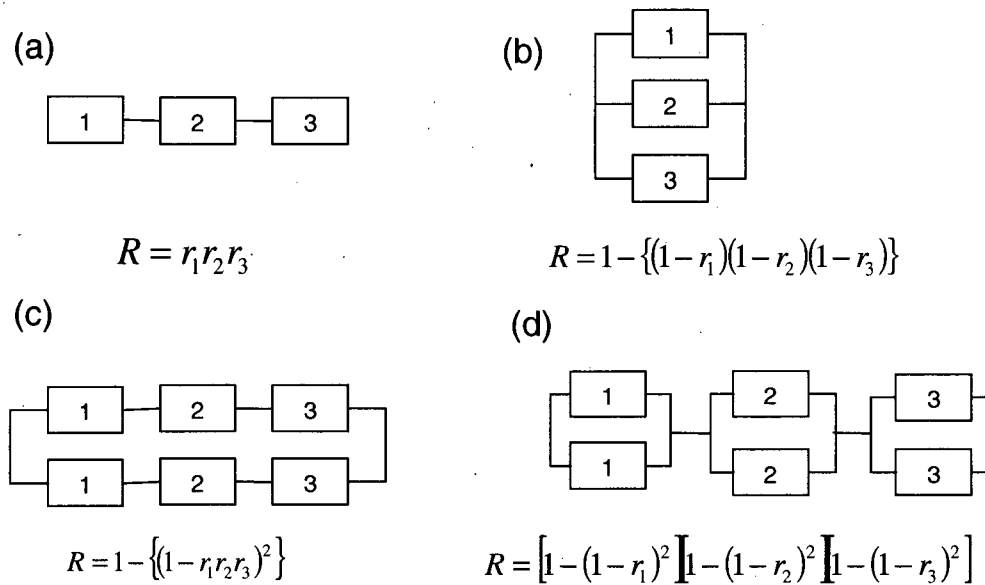


**Figure 4.2 System reliability based on the reliability of the components  $r_1, r_2, r_3$  (Hoyland and Rausand, 1994)**

The systems shown in Figure 4.2 show different levels of reliability and redundancy. The series system in Figure 4.2(a) is the least reliable since all components must function for the system to function. The parallel system in Figure 4.2(b) is more reliable since at least one component must function for the system to function. Figure 4.2(c) is a parallel-series system which has redundancy at the subsystem level while Figure 4.2(d) is a series-parallel system that has redundancy at the subunit level.

Figure 4.3 shows a comparison between the parallel-series system and a series-parallel system of three components with 100% component redundancy at the subunit level. From this figure is possible to see that the series parallel system is a more reliable system given the same amount of redundancy. This analysis leads to the statement that redundancy of components at the subunit level rather than at the subsystem level serves to increase system reliability.

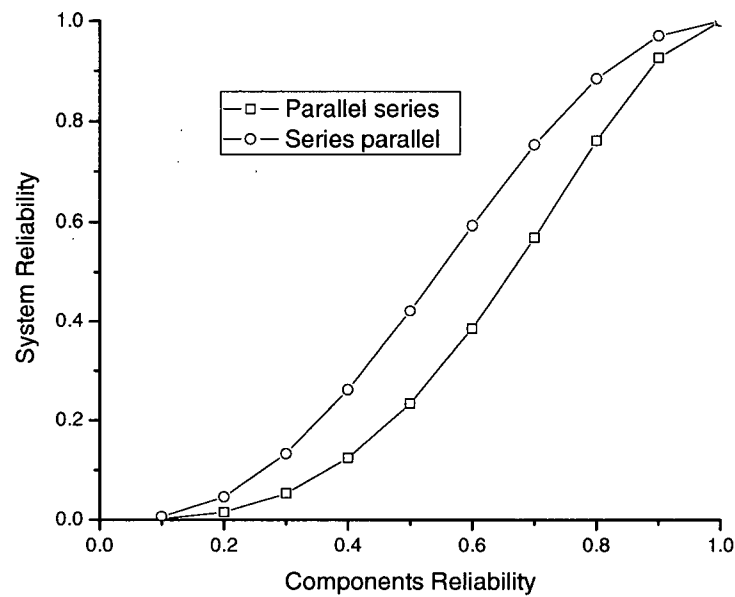


**Figure 4.3 Comparison between series parallel and parallel series for 3 components with 100% component redundancy**

If the block cave mining system is viewed as a mechanical system composed of different pieces of infrastructure with different reliabilities, the reliability of the mining system could be computed by linking its components in a manner similar to the examples shown in Figure 4.2.

#### 4.2 Reliability of a System with Redundancy at the Component Level

Another way of modeling systems that contain components redundancy is by using the *k-out-of-n* models. A *k-out-of-n* model consists of a system that has *n* components to perform a function that only needs *k* to function. This kind of models will be further study on the next section of the dissertation since they will be used extensively to model the reliability of the block cave production system.

A system that contains *n* independent components of which  $k < n$  are needed is redundant and is referred to as a *k-out-of-n* system. The system functions if and only if *k* of the *n* components function (Boland and Proschan, 1983). The quantity  $(n-k)$  is known as the system redundancy. The particular case of a parallel system would be a 1-out-of-*n* system and a series system would

be a *n-out-of-n* system. The reliability of a *k-out-of-n* system is computed by the following equation

$$R(k, n) = \sum_{i=k}^n C_{i,n} r^i q^{n-i} \quad (4.1)$$

where  $C_{i,n}$  is the number of combinations of  $i$  functioning components of  $n$  available given by

$$C_{i,n} = \frac{n!}{i!(n-i)!} = \binom{n}{i}$$

$r$  is the reliability of each component and  $q$  is the unreliability  $1-r$ . The product  $r^i q^{n-i}$  is the reliability of  $i$  components connected in series having  $n$  components available. Figure 4.4 shows a diagrammatic representation of system composed of 10 components connected in series to perform an activity and a second system with 50% of components redundancy whereby, there are 15 components available to perform an activity that just needs 10 components. The second system is called a 10 out of 15 system.

Figure 4.5 shows a comparison between a series system of 10 elements and a 10-out-of-15 system in which every component has the same reliability. It is clear that the system reliability increases by adding redundancy to the system. Certainly, to achieve this increased reliability, it must be physically possible to combine the  $k$  components. For a block caving system this is significant; it means that  $n$  draw points must be developed and available to provide all the possible combinations.

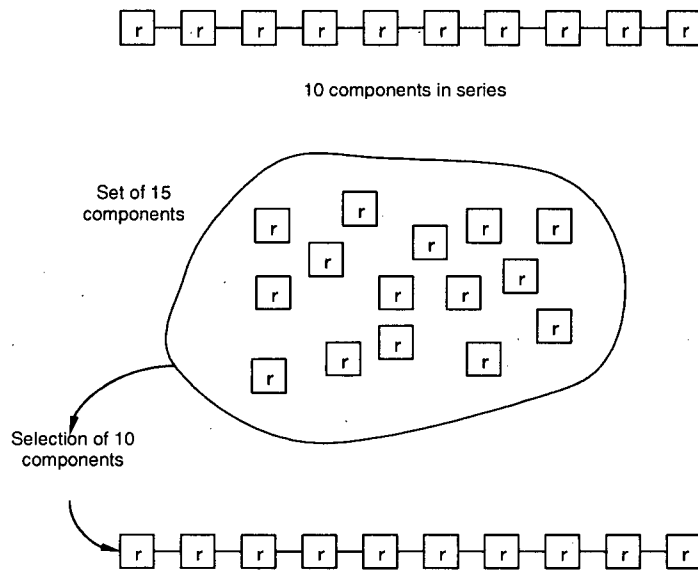


**Figure 4.4 Selection of 10 out of 15 components to compare with the performance of 10 components connected in series**

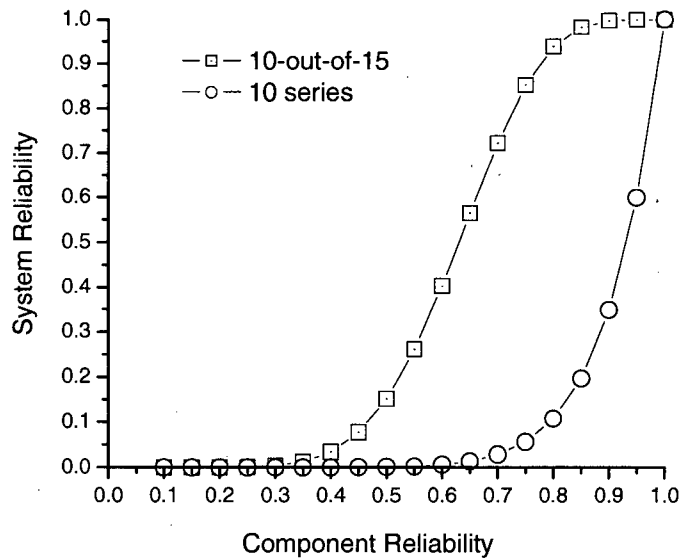


**Figure 4.5 Reliability comparison between a series and a  $k$ -out-of- $n$  system**

### 4.3 Block Cave Reliability Model

The reliability model associated to the block cave production system consists of production infrastructure components such as draw points, ore passes, crushers, tunnels. These components

are linked through different relationships depending on the goal of the mine plan. To improve the understanding of the model, the mining system has been divided into: production areas, production crosscuts and draw points as shown in Figure 4.6.

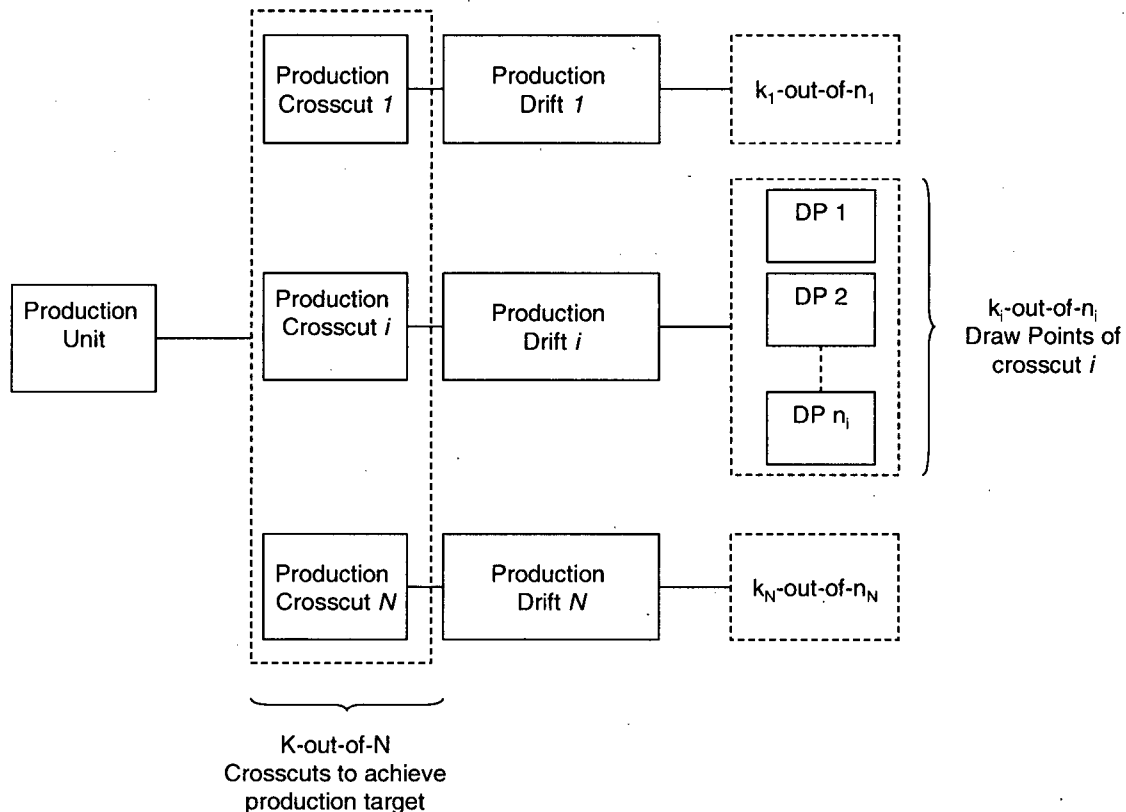


**Figure 4.6 Reliability block diagram of a block cave production system**

A production unit is an area of the mine that has a particular geology, geotechnical characteristics and the location facilitates the logistics of the mine. Every production unit is can be modeled as a k-out-of-n system composed of production crosscuts. Every production crosscut consists of one production drift connected in series with a k-out-of-n system of draw points.

Usually a production target is met by the tonnages produced from the different production crosscuts. Based on the nominal crosscut productivity there are usually more production crosscuts than needed to achieve a desired production target. This means that there is redundancy, more components than needed, at the crosscut level. The same can be observed at the draw point level. To achieve the crosscut nominal production target there are more draw points than needed based on the draw point nominal productivity. Thus the block cave mining system contains redundancy at the crosscut and draw point levels.

Usually  $k$ -out-of- $n$  systems in this dissertation consist of systems with identical components, i.e. all components have the same reliability. In block caving, the infrastructure components of the mining system such as draw points and drifts may have different reliabilities since they may be located in different geotechnical domains or may have different ages. For example in the case of a production crosscut there could be draw points at different stages of maturity that would lead to different draw point reliabilities along the production crosscut. The same can be observed at the crosscut level in which there are several crosscuts with different reliabilities yielding the production target. These systems are called  $k$ -out-of- $n$  system with independent and non-identical components. Computing the reliability of such systems is more complicated than systems with identical components. The notation used to compute the reliability of a  $k$ -out-of- $n$  system with independent and non identical components is presented below:

$n$	number of components in the system
$k$	minimum number of components that must function for the $k$ -out-of- $n$ system to function
$r_i$	reliability of component $i, i = 1, 2, \dots, n$
$r$	reliability of each component when all components are identical.
$q_i$	unreliability of component $i, q_i = 1 - p_i, i = 1, 2, \dots, n$
$q$	unreliability of each component when all components are identical $q = 1 - p$
$R_e(i, n)$	intermediate reliability entry which represents the probability that exactly $i$ out of $n$ components are functioning
$R(k, n)$	reliability of a $k$ -out-of- $n$ system or probability that at least $k$ out of the $n$ components are functioning, where $0 \leq k \leq n$ and both $k$ and $n$ are integers
$Q(k, n)$	unreliability of a $k$ -out-of- $n$ or probability that less than $k$ out of the $n$ components are functioning, where $0 \leq k \leq n$ and both $k$ and $n$ are integers, $Q(k, n) = 1 - R(k, n)$

Suppose that in a given crosscut there are  $n$  draw points available and depending on the average draw point yield and the crosscut production target,  $k$  out of the  $n$  draw points are needed to meet the target. Define a subset of  $i$  functioning in series out of  $n$  available as  $s_\tau^i$  with  $\tau = 1, 2, \dots, C_{i,n}$  and  $k \leq i \leq n$  ( $i < k$  will not be a feasible system). Then the reliability of a given subset  $s_\tau^i$  is

$$\begin{aligned}
 R(s_\tau^i) &= P(\text{components } t \in s_\tau^i \text{ available}) \times P(\text{components } t \in s_\tau^{n-i} \text{ unavailable}) \\
 &= \prod r_t(t \in s_\tau^i) \prod q_t(t \in s_\tau^{n-i})
 \end{aligned} \tag{4.2}$$

Denote the set of all  $s_r^i$  subsets is by  $S_r^n$ . Then the reliability of the  $k$ -out-of- $n$  system with non-identical and independent components is given by

$$R(k, n) = \sum_{i=k}^n \sum_{S_r^n} \left[ \prod_{t \in s_r^i} r_t \prod_{t \in s_r^{n-i}} q_t \right] \quad (4.3)$$

Incorporating the tunnel or production drift reliability  $R_T$ , the production crosscut reliability  $R_{CX}$  is defined as

$$R_{CX} = R_T R(k, n) \quad (4.4)$$

If explicit enumeration were to be used to compute Equation (4.4) 30,827 draw point combinations would be required to compute the reliability of a 5-out-of-15 system. However, a recursive algorithm developed by Barlow and Heidtmann (1984) is available to compute the intermediate entry reliabilities. (See Appendix B for a derivation of this algorithm.) The intermediate entry reliability  $R_e(i, j)$  is defined as the reliability of a system composed of  $i$  functioning components out of  $j$  available with  $i < j$ . Given the individual draw point reliabilities presented in Table 4.1, the intermediate reliabilities  $R_e(i, j)$  computed by the recursive algorithm are shown in Table 4.2.

**Table 4.1 Draw point reliabilities to compute the entries**

Draw Point	$r_i$
1	0.49
2	0.78
3	0.63
4	0.51
5	0.52
6	0.34
7	0.64
8	0.58
9	0.53
10	0.40

**Table 4.2 Intermediate entry reliability table,  $R_e(i, j)$**

$R_e(i, j)$	0	1	2	3	4	5	6	7	8	9	10
0	1.00	0.18	0.04	0.01	0.00	0.00	0.00	0.00	0.00	0.00	0.00
1	0.00	0.82	0.32	0.10	0.03	0.01	0.00	0.00	0.00	0.00	0.00
2	0.00	0.00	0.65	0.39	0.17	0.06	0.02	0.01	0.00	0.00	0.00
3	0.00	0.00	0.00	0.50	0.42	0.23	0.11	0.05	0.02	0.01	0.00
4	0.00	0.00	0.00	0.00	0.38	0.41	0.28	0.15	0.08	0.04	0.02
5	0.00	0.00	0.00	0.00	0.00	0.29	0.38	0.30	0.20	0.11	0.06
6	0.00	0.00	0.00	0.00	0.00	0.00	0.21	0.33	0.31	0.23	0.15
7	0.00	0.00	0.00	0.00	0.00	0.00	0.00	0.15	0.28	0.30	0.25
8	0.00	0.00	0.00	0.00	0.00	0.00	0.00	0.00	0.11	0.23	0.28
9	0.00	0.00	0.00	0.00	0.00	0.00	0.00	0.00	0.00	0.08	0.18
10	0.00	0.00	0.00	0.00	0.00	0.00	0.00	0.00	0.00	0.00	0.05

Based on the intermediate reliabilities presented in Table 4.2 the reliability of a 5-out-of-10 draw point system is computed by adding the rows 5 to 10 of column 10 of Table 4.2. Thus the system reliability would be 97.9%.

The intermediate entry reliability table is a useful result. This table could allow mine planners to analyze the effect of different amounts of redundancy added at the crosscut and draw point level on the overall reliability. Figure 4.7 shows a relationship between draw point redundancy and crosscut reliability for different draw point reliabilities. Clearly adding draw point redundancy increases crosscut reliability. However, the increase depends significantly on the individual draw point reliabilities.



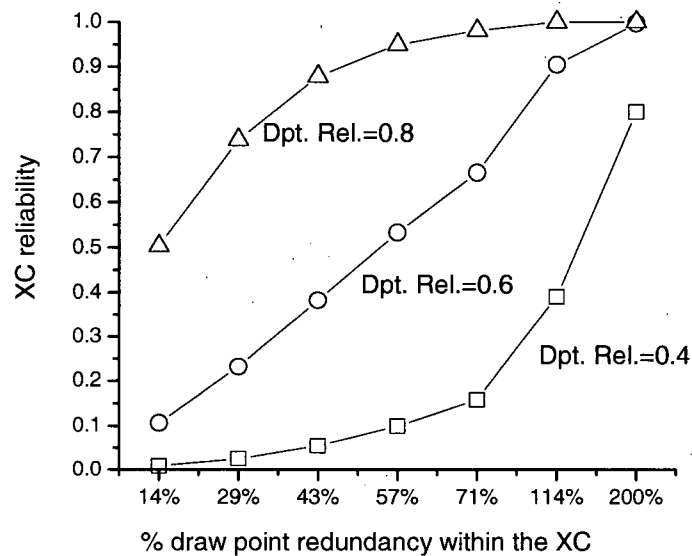


**Figure 4.7 Redundancy versus system reliability**

An aspect that has not been discussed so far in this section is how to select the  $n$  planned draw points within the open draw points available in the crosscut. Usually, this selection will be facilitated by the status of the draw points, i.e. there will be hang up, over size or repair draw points at any given time in the crosscut. Nevertheless, it has been found that usually all the available draw points should be used in a production schedule for all different planning horizons. This results in a robust estimation of the system reliability. Leaving active draw points out of the schedule over long periods (more than a week) is not realistic since even draw is required to minimize dilution entry as well as stresses. However, in daily or shift by shift planning horizons it is possible to select the draw points that should be in operation. This selection of draw points could be facilitated by the use of a priority system (Diering, 2004).

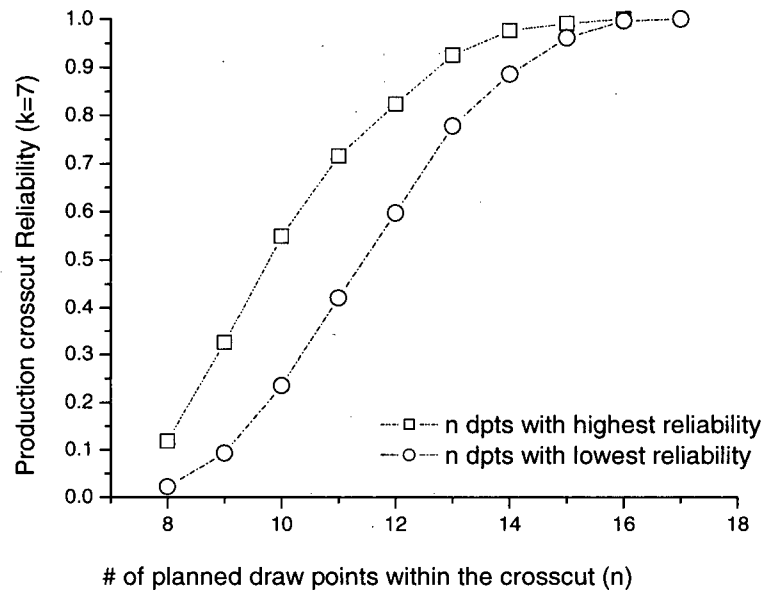


**Figure 4.8 Impact of draw point selection on crosscut reliability**

Figure 4.8 shows the effect on the system reliability of choosing  $n$  within the available draw points for a given number of required draw points ( $k=7$ ). It is possible to see that if the available draw points are sorted in descending order of individual reliability, the “highest reliability” performance is observed. If the draw points are sorted in ascending order of individual reliability, the “lowest reliability” behaviour is observed. Also, Figure 4.8 shows the impact of different  $n$  on the overall crosscut reliability. This criterion for draw point selection should be used together with other draw control rules such as angle of draw and maximum differential draw to avoid isolated draw in the production area of the mine.

#### **4.3.1 Draw point productivity as a function of draw point yield and draw cycle**

An important component of the reliability model is the estimation of the number of draw points  $k$  needed to achieve the crosscut production target. This estimation is performed using the average nominal draw point productivity within the crosscut. The following will explain how this parameter is computed.

The draw point productivity is a function of the draw point yield which is defined by the particle size distribution at the draw point, LHD bucket size and production cycle time. The particle size

distribution of a draw point will affect the bulk density of the loose material at the draw point. As the draw point matures, the secondary fragmentation together with the mixing along the draw column will lead to a wide distribution of particle sizes which will result in an increase in the bulk density of the rock. Thus, the draw point yield would be a function of the draw point maturity as shown in Figure 4.9 which has been constructed from raw data taken from mine M2. Note that the curve has been constructed without including the hang ups or oversize that may have occurred at the draw points.

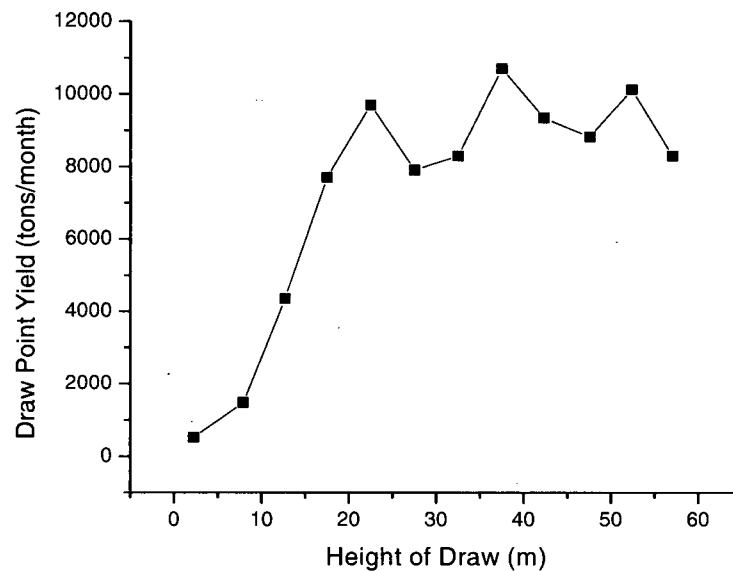


**Figure 4.9 Draw point yield as a function of height of draw**

Production cycle time also affects draw point productivity. The production cycle time is a function of the speed of the LHD and the average distance that the LHD has to travel in a time period. The average distance that the LHD has to travel to achieve a given production call would be a function of the number of draw points that the LHD has to muck in the call within the crosscut. If the whole crosscut had to be drawn, the productivity of the LHD will be less than if only the closest draw points to the ore pass had to be drawn to fulfill the crosscut production call. Therefore there is an inverse relationship between the LHD productivity and the number of draw points to be drawn within a crosscut. Consequently a highly productive schedule would tend to use less draw points to meet the crosscut target, concentrating the mucking activity on those draw points close to the ore passes or crushers. Nevertheless if just a few draw points are drawn within a crosscut the draw cycle would increase and trigger convergence as shown in Chapter 3

Figure 3.11. For a given amount of acceptable convergence a draw cycle can be computed. This computed draw cycle can be used to estimate the minimum number of draw points that need to be drawn in a given period of time using as shown in Figure 4.10.

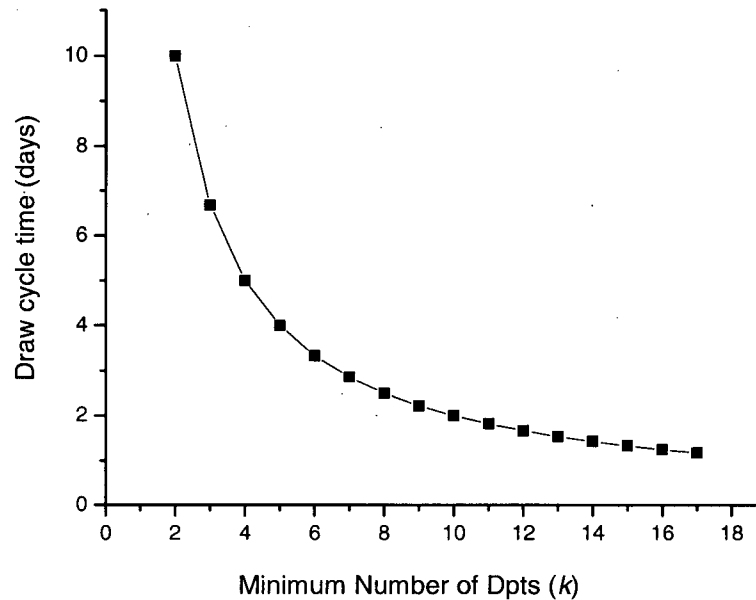


**Figure 4.10 Draw cycle time as a function of  $k$**

The draw point yield curve and the minimum number of draw points to be drawn per period will be used to compute the number of draw points needed to achieve the crosscut production call. This number is computed per crosscut and per every period of the production schedule during a given planning horizon.

#### **4.4 Production Scheduling Integrating Draw Point Reliability**

It is important to define what is meant by production schedule reliability. The reliability of a production schedule is defined as the probability of achieving a given production target. This probability can be assumed to be directly proportional to the probability that there will be enough mining infrastructure available to produce a given production target. This probability will be time dependent since the production targets as well as the failure characteristics of mining infrastructure change from period to period. Thus the reliability of a production schedule will not be represented by a single number but rather a vector of reliabilities, one for each period of the schedule. Equation 4.5 illustrates the definition of reliability

$$R[TT(t)] = P[TA(t) \geq TT(t)] \quad (4.5)$$

where  $R[TT(t)]$  is the reliability of achieving the tonnage target  $TT(t)$  at time  $t$ ,  $TA(t)$  is a random variable representing the actual tonnage produced from the mine at a given time. Figure 4.11 shows the expected variation of tonnage distribution for different times during the life of the mine. Note that the lower the tonnage target the greater the probability of achieving it. From this figure it is possible to see that the tonnage distributions change over time since the slope of the curves shown in Figure 4.11 varies from period to period.

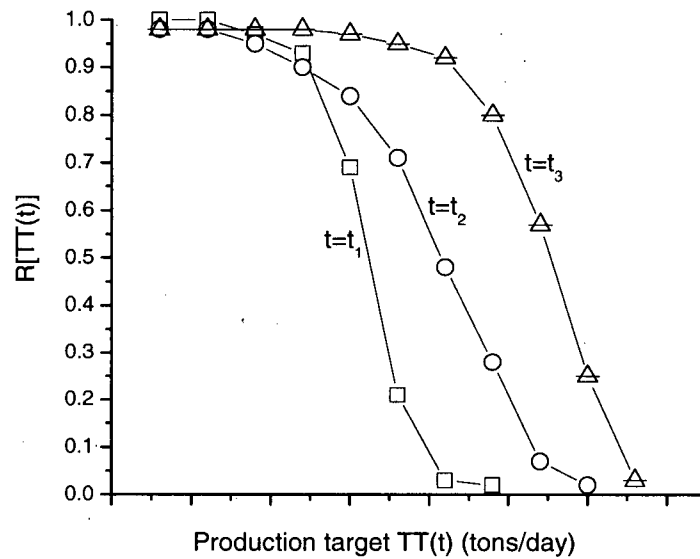


**Figure 4.11 Expected evolution of actual tonnage distribution**

Consequently the aim of this chapter is to present a method to compute the reliability of a production schedule together with the methods to compute the tonnage distribution curve throughout the life of a mine.

The mining system reliability model described in the previous section of this research will be used to compute the reliability of a given production plan as a function of the reliability of the mining infrastructure. Figure 4.12 shows the proposed mine planning model including the reliability model.

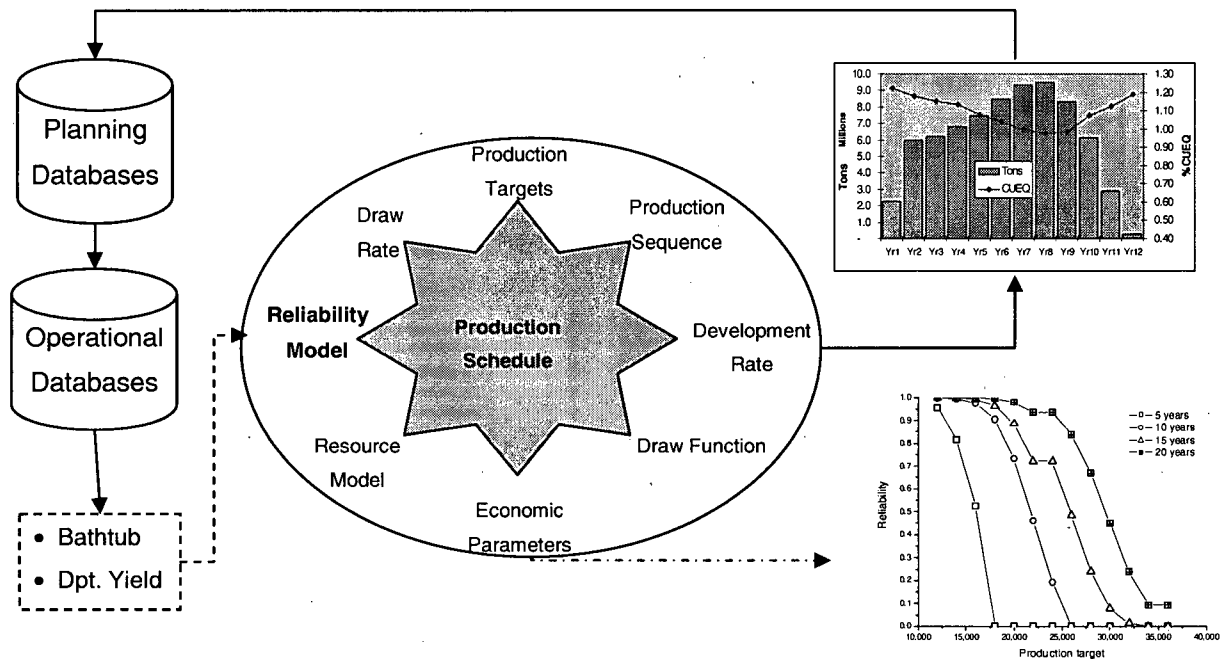


**Figure 4.12 Proposed mine planning model including reliability model**

There are two main operational indicators used in the reliability model: the draw point ROCOF curves and the draw point yield curves. Both of these parameters should be computed using the operational records of the mine. The derivation of the draw point yield will be explained later.

A prototype production scheduler was constructed to integrate characteristics of the draw points, production targets, crosscut relationships, ROCOF curves and draw point yields. The parameters used in the model are presented below

- $T(t)$  production target for period  $t$
- $T_i(t)$  tonnage target for crosscut  $i$  at time  $t$
- $K(t)$  minimum number of crosscuts needed to achieve the production target at period  $t$
- $k_i(t)$  minimum number of draw points needed in crosscut  $i$  to achieve  $T_i(t)$
- $k_i^c$  minimum number of draw points needed to achieve a given draw cycle to control convergence of crosscut  $i$ . Computed from relationship shown in Figure 4.10
- $N(t)$  available crosscuts at period  $t$
- $n_i(t)$  available draw points in crosscut  $i$  at period  $t$
- $M(t)$  nominal production capacity of a crosscut at period  $t$
- $d_i(t)$  average productivity of draw points in crosscut  $i$  at period  $t$
- $r_i^j(t)$  draw point reliability of draw point  $j$  of crosscut  $i$  at period  $t$

$CT_i^j(t)$	cumulative tonnage of draw point $j$ of crosscut $i$ at period $t$
$w[CT_i^j(t)]$	ROCOF curve for draw point $j$ of crosscut $i$
$R_i(t)$	reliability of crosscut $i$ at time $t$ for $k_i(t)$ draw points needed and $n_i(t)$ draw points available in crosscut $i$
$\hat{T}_i(t)$	Expected production from crosscut $i$ at period $t$
$\hat{T}(t)$	Expected total production capacity at period $t$

The minimum number of draw points to achieve the production target of crosscut  $i$  is

$$k_i(t) = \max \left\{ \frac{T_i(t)}{d_i(t)}, k_i^c \right\} \quad (4.5)$$

There are  $n_i(t)$  draw points available and only  $k_i(t)$  draw points are needed to achieve the crosscut  $i$  production target,  $T_i(t)$  at time  $t$ . The minimum number of draw points to achieve a desired draw cycle per crosscut,  $k_i^c$ , is assumed constant during the production schedule to simplify the model. Nevertheless it is possible that  $k_i^c$  is time dependent reflecting the dynamic stress conditions during the life of the mine.

The production crosscuts form one  $k$ -out-of- $n$  system with non identical components and result in the crosscut reliabilities,  $R_i(t)$ ,  $i = 1, \dots, N(t)$ , as a function of the draw point ROCOF curves,  $r_i^j(t)$ .

Once the crosscut reliabilities,  $R_i(t)$ , have been computed another  $k$ -out-of- $n$  system is formed among the crosscuts. The minimum number of crosscuts needed to achieve the production target,  $T(t)$ , is  $K(t)$  which is computed using the following procedure:

- Sort crosscuts in ascending order of crosscut production capacity,  $T_i(t)$
- Add the crosscut production targets,  $T_i(t)$  until the production target  $T(t)$  is reached. This determines the number of crosscuts  $K(t)$  needed.

Note that this approach is very conservative since it will always compute the worst possible production scenario. If priorities are used to quantify the minimum number of crosscuts needed

to achieve the production target, the crosscuts should be sorted in descending order of priority before computing  $K(t)$ .

The final part of the algorithm computes the total system reliability by computing the reliability of a  $k$ -out-of- $n$  system with non identical production crosscuts with reliabilities,  $R_i(t)$ , in which there are  $N(t)$  crosscuts available and  $K(t)$  crosscuts needed to achieve the production target,  $T(t)$ . Figure 4.13 shows a scheme of how the different components of the production schedule as well as the availability of mining infrastructure are linked to compute the production schedule reliability.

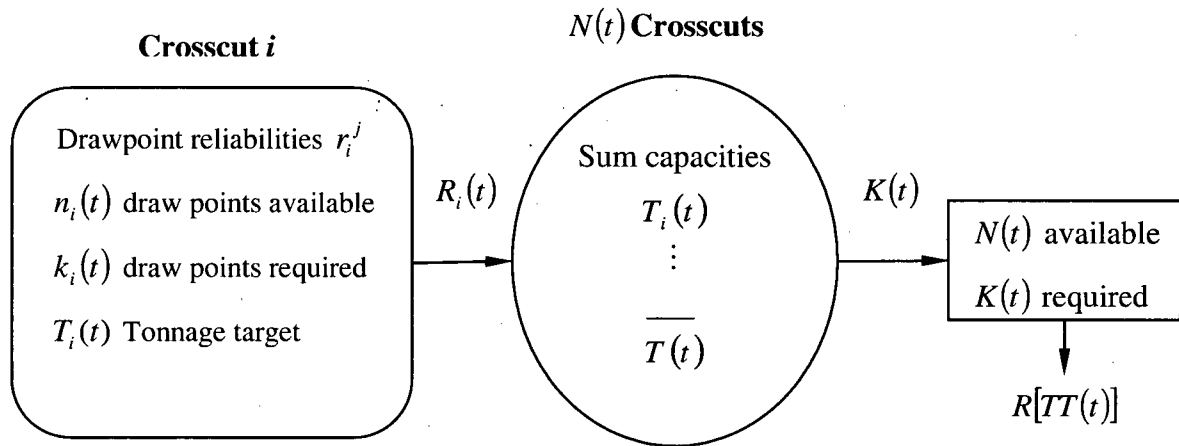


**Figure 4.13 Scheme to compute the reliability of a given production schedule**

The second output of the reliability model is the expected tonnage  $\hat{T}(t)$ . The estimation of the expected crosscut production,  $\hat{T}_i(t)$ , is performed by embedding a sampling procedure into the  $k$ -out-of- $n$  model. A number of draw points  $z$ ,  $k \leq z \leq n$ , in a crosscut (sub indices have been dropped to simplify the notation) are chosen from the  $n$  available draw points using a random sampling process. The productivity of these  $z$  draw points is computed by adding their draw point productivities. The sampling of the  $z$  draw points is repeated a fixed number of times. At the end the productivity of the  $z$  draw points,  $\hat{T}^z(t)$ , is estimated by taking the average of all



samplings. This procedure is repeated for all  $k \leq z \leq n$ . Then the expected production of crosscut  $i$ ,  $\hat{T}_i(t)$ , is estimated using the intermediate reliability entries  $R_e(z, n)$  as shown below:

$$\hat{T}_i(t) = \sum_{z=k}^n \hat{T}_i^z(t) R_e(z, n) \quad (4.6)$$

Table 4.3 shows the method to compute crosscut productivity based on reliability measures. Note that in this example the nominal crosscut productivity was 80,000 tons/month. Then the expected crosscut productivity should be  $80,000 \times 0.4$  tons/month assuming a deterministic behavior of the draw point productivity. Nevertheless by incorporating the stochastic behaviour of tonnage together with the reliability of different draw point configurations the expected tonnage is computed to be 29,141 tons/ month as shown below. The former estimation is more realistic since it represents the stochastic behaviour of draw points active rather than the deterministic traditional approach.

**Table 4.3 Estimation of crosscut production capacity based on reliability estimates**

$$k_i = 9$$

$$n_i = 12$$

$z$	$R_e(z, n)$	$\hat{T}_i^z(t)$
9	0.215	67,500
10	0.131	75,000
11	0.049	82,500
12	0.008	90,000

$$\hat{T}_i(t) \quad 29,141$$

Finally to compute the expected production capacity of the mine the same procedure as illustrated in Table 4.3 is followed. In this case the components are the production crosscuts with estimated productivities  $\hat{T}_i(t)$ . Appendix C shows the details of the data flow related to the proposed scheduler algorithm shown in this section.

#### 4.5 Production Schedule Reliability

The first application of the reliability model consists of estimating the reliability of a given production schedule. In order to compute the reliability of a production schedule the draw point

ROCOF and draw point yield curves must be computed. Another input for the reliability model consists of the production schedule which specifies the amount of tonnage to be produced per period and the draw point opening sequence as shown in Appendix C. The final input for the reliability model is the crosscut production target per period. These targets can be computed either from the production schedule or from the maximum haulage capacity of a crosscut. After setting up the inputs the reliability model is run to compute the reliability per period as shown in Figure 4.14.

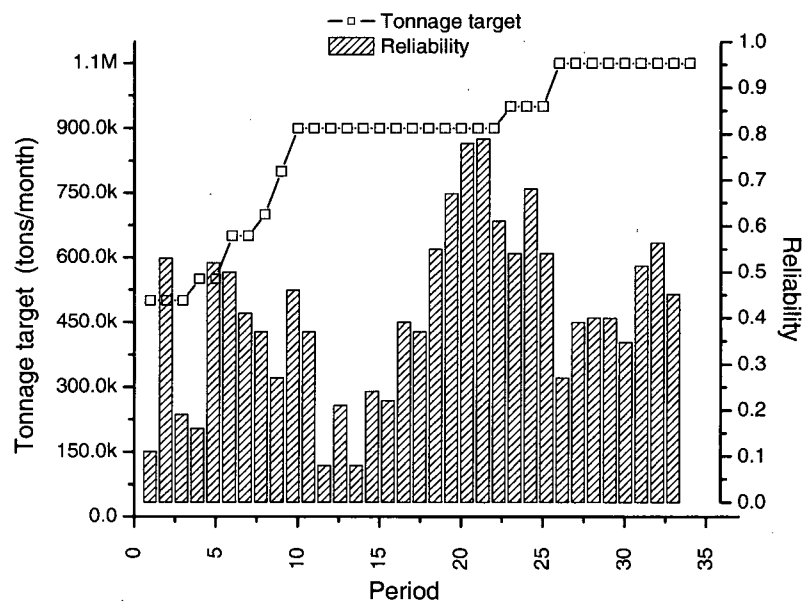


**Figure 4.14 Assessment of reliability based on a computed production schedule**

In the example shown in Figure 4.14 the reliability per period is fairly low during the production schedule. The variance of the reliability per period is due to the draw point and crosscut availability per period, which depends on the draw point sequence used in the production schedule.

Once the reliability of a production schedule is known the model can be used to recommend changes to the draw point opening sequence and to the production target per period that could improve the overall reliability during the production schedule. For example Figure 4.15 shows the reliability for different production targets of a mine, maintaining all the production schedule related parameters constant. Evidently lower production targets will produce more reliable

production schedules as a result of the amount of redundancy contained in the mining system. The redundancy in the mining system is reflected by the number of draw points and crosscuts commissioned in a given period of the production schedule.

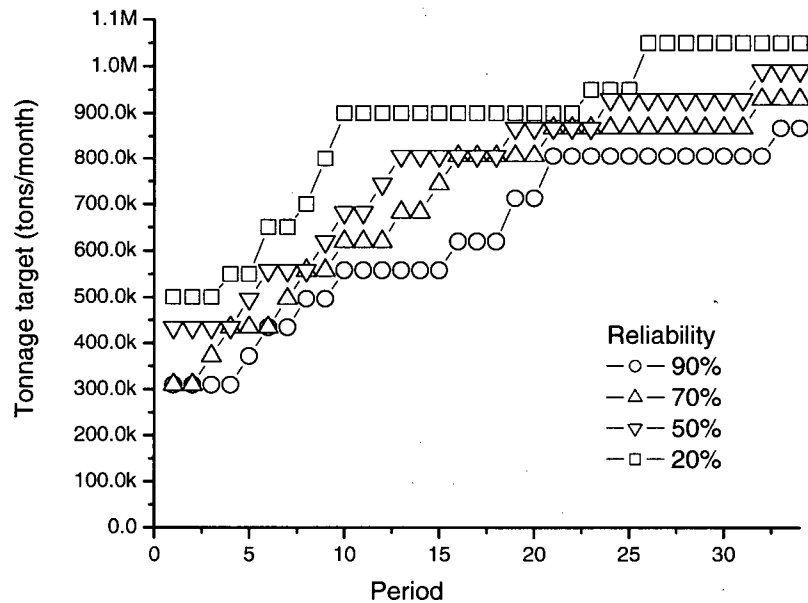


**Figure 4.15 Production schedules including reliability as a target**

An analytical tool resulting from applying the reliability model to production scheduling is the production forecast as a function of reliability. Figure 4.16 shows an example in which the reliability model has been used to forecast production capacity. In this case the reliability has been computed to assess the maximum production capacity at different periods during the life of the mine.

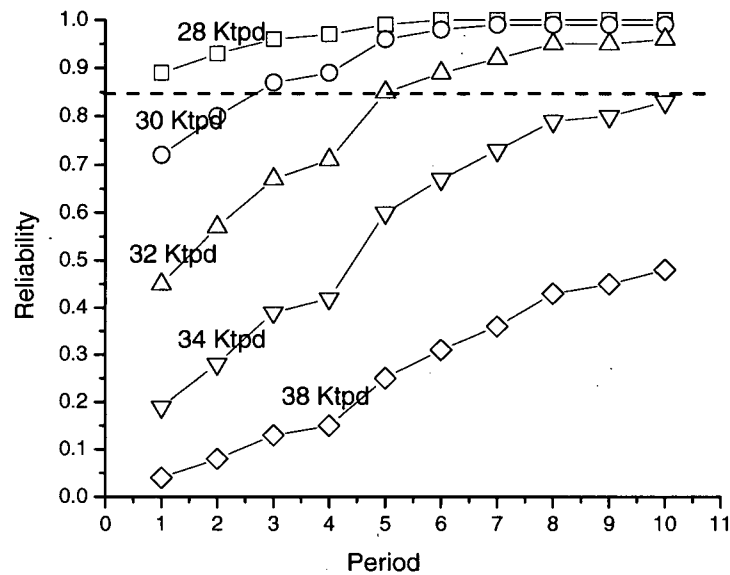


**Figure 4.16 Production schedules with integrated reliability**

If 85% was the desired reliability for the mine shown in Figure 4.16. The recommended production profile is shown in Table 4.4.

**Table 4.4 Production profile at 85% reliability**

Period (year)	Target (tons/day)
1	28,000
2	29,000
3	30,000
4	31,000
5	32,000
6	32,000
7	32,000
8	33,000
9	33,000
10	34,000

Another analytical tool developed as a result of applying the reliability model to production scheduling is presented in Figure 4.17, which shows the effect of redundancy on production schedule reliability, adding redundancy at the crosscut and draw point level. This chart is important since it allows mine planners to assess the benefits of allocating redundancy at the crosscut and the draw point level. The ultimate amount of redundancy to introduce in the mining system can be planned in order to balance the reliability of the production schedule with the amount of capital cost needed to support the production schedule.

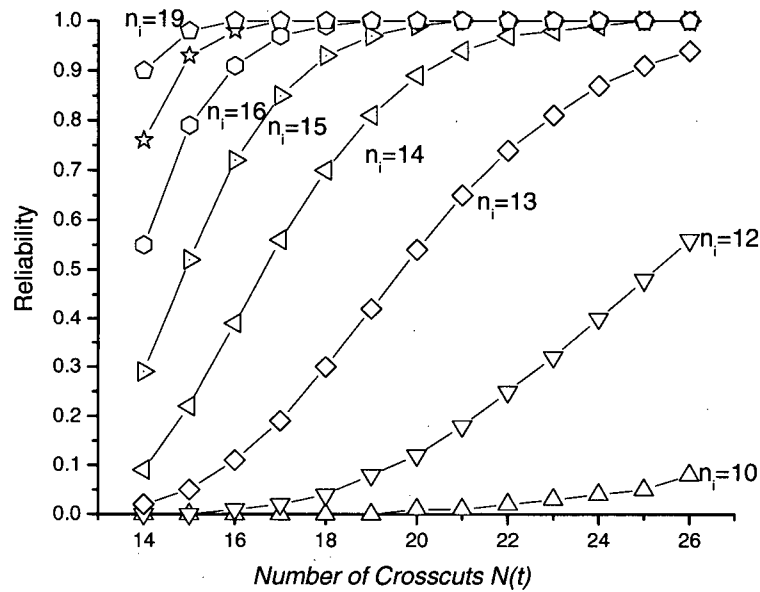


**Figure 4.17 Effect of redundancy at the draw point and crosscut level**

#### 4.6 Sensitivity of Different Inputs to the Reliability Model

A sensitivity analysis was performed in order to understand how the reliability model would behave in different applications. Figure 4.18 shows the reliability profile of a production schedule for different draw point ROCOF curves. To analyze the impact of different ROCOF curves in the reliability model, three different curves with constant values of rate of occurrence of failure 0.1, 0.2 and 0.3 were used to represent the effect of the draw point tendency to failure in the production schedule reliability. The resulting reliabilities were compared to the reliability profile using the actual draw point ROCOF curve obtained from mine M1. The production target was set to be 360,000 tons/month constant during the life of the mine. Figure 4.18 shows that the ROCOF curve affects not only the absolute reliability value but also the shape of the reliability profile.

The second parameter that has a tremendous influence on the reliability model is the nominal productivity of a crosscut. For the same production target as used above and the actual draw point ROCOF curve of mine M1 the crosscut nominal productivity has been changed in the

range of 60-150 K tons/day. Figure 4.19 shows the effect of this parameter on the performance of reliability during the life of a mine.

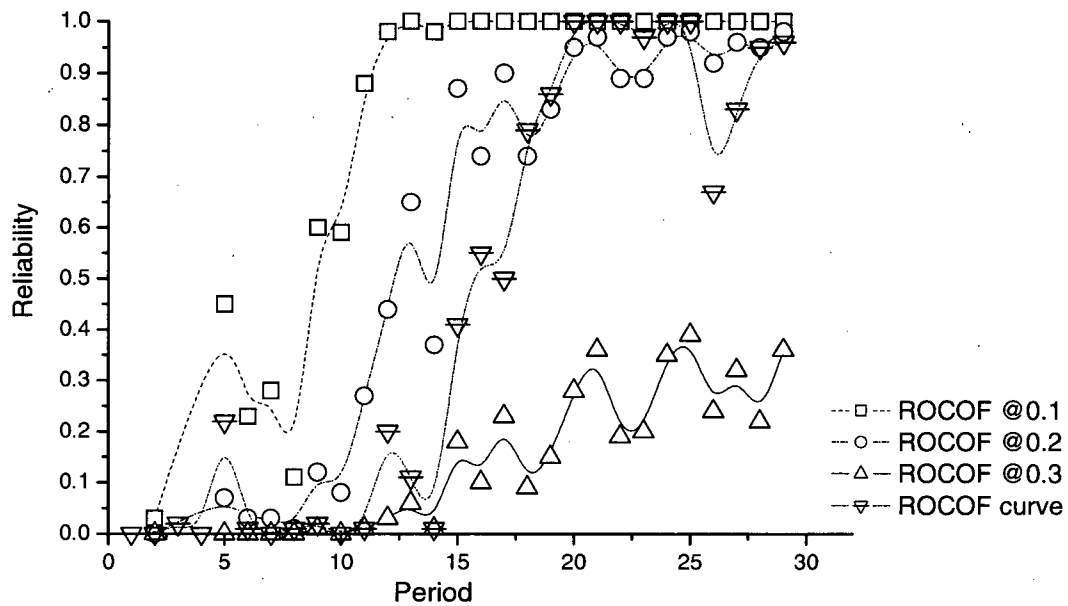


**Figure 4.18 Sensitivity of the reliability model to the ROCOF curve**

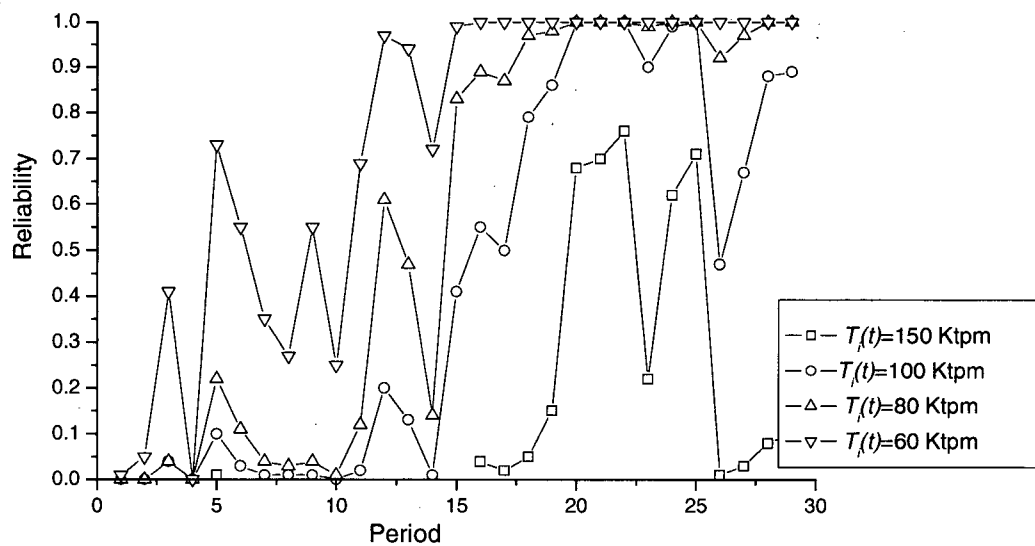


**Figure 4.19 Sensitivity to crosscut productivity**

#### **4.7 Using the Reliability Model to Assess the Value of Overdrawn Draw Points**

Overdrawn draw points are defined as those draw points that have depleted their mining reserves according to the long term model but are still producing grade above the predictions made with the long term model. This behaviour has been observed at several block cave mines. When this situation arises at an operation the fundamental question is whether to consider this resource as part of the short term plans, 2 to 4 months, or simply exclude this material from the planning model. It is often found that the overdrawn draw points will be included in the plan since this action will bring some flexibility to the operation which may be under pressure to achieve the production target. If the overdrawn draw points are considered in the plan, the question is what strategy should be followed in order to maintain the mine throughput stability. Usually there is a trade off between a short term increase in production rate versus a medium term steady state production rate.

Mine M1 faced the issue of deciding what strategy to use to treat the overdrawn draw points. The challenge was to find a production strategy to mine 23 overdrawn draw points in a time horizon of 9 months. The strategies studied were: mine the 23 draw points at their fastest capacity so there could be a production increase in the following 2 months, or mine a few of those 23 draw points at their maximum capacity and save the rest of the draw points to offset an eventual loss of future scheduled production due to an unstable production crosscut, called XC GU.

The reliability model was used to quantify the number of overdrawn draw points needed to offset an expected loss in production due to a potential unstable production crosscut. In this example the draw points located in the potential unstable crosscut have been assigned a reliability of 0.2. The overdrawn draw points have been included in the plan with a reliability of 0.35. Figure 4.20 shows how the reliability model has been used to evaluate the different options and the throughput that is supported by every one of these options. The base case scenario is shown by the line labeled "with XC GU" which shows a reliability of 0.8 to produce 36,000 tons/day. The reliability of 36,000 tpd drops to 0.65 if XC GU collapses, as shown by the line labeled "without XC GU". However, in the event that crosscut XC GU collapses, by adding 23 overdrawn draw points to the medium term plan the reliability of 36,000 tons/day target increases to 0.9, which is represented by the line tagged "wo XC GU, 23 acc". In the event that crosscut XC GU collapses

and just 10 overdrawn draw points are added to the medium term plan the reliability of a 36,000 tons/day target increases to 0.75, which is represented by the line tagged “wo XC GU, 10 acc”. The analysis presented here was used to support the decision regarding the number of overdrawn draw points that can be used to increase short term production and maintain the reliability of the medium term production schedule when faced with the potential collapse of a production area.

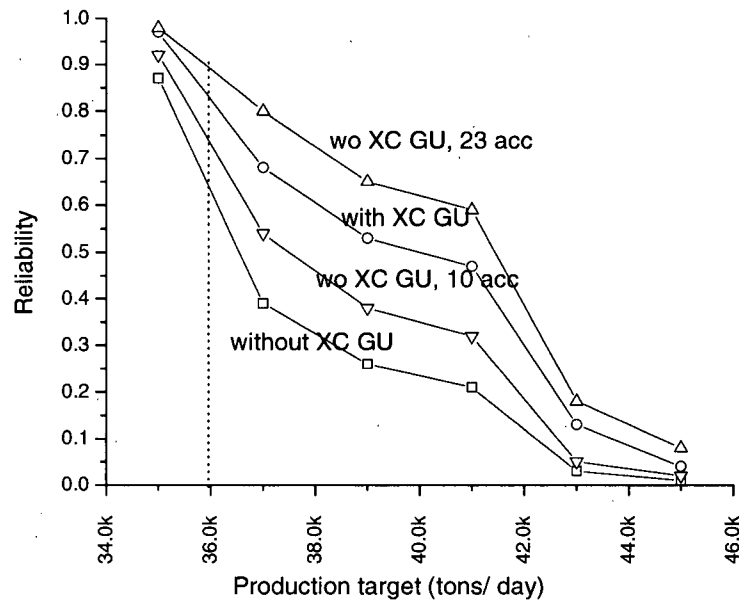


**Figure 4.20 Assessing the effect of overdrawn draw points in the production schedule**

#### 4.8 Using the Reliability Model to Support Tactical Decisions

One of the tactical decisions that affects the productivity of a block cave mine is the allocation of secondary breakage resources, crews and equipment, to different production crosscuts. This decision is usually left to operators to accommodate the tasks of production and secondary blasting. Yet it has been noticed at operating block caves that placing a draw point or a crosscut on hold for secondary blasting has tremendous production implications (Dessureault et al, 2000). Then mine planners are starting to include the secondary blasting chart as part of the daily production call. Nevertheless there has been no study of the best strategies for allocating secondary breakage resources in an operating environment. A method to allocate secondary breakage resources based on the production crosscut reliability is proposed.



As draw points within a crosscut begin to hang up, the draw point redundancy decreases with the number of available draw points approaching the minimum required draw points  $k$  at which point the crosscut is sent to secondary breakage and then returned to operation. Figure 4.21 shows how the reliability model can be used to monitor the reliability of the crosscut as a function of the draw points reliabilities and the crosscut redundancy. When a crosscut reaches a secondary breakage threshold it will be put on secondary breakage status.

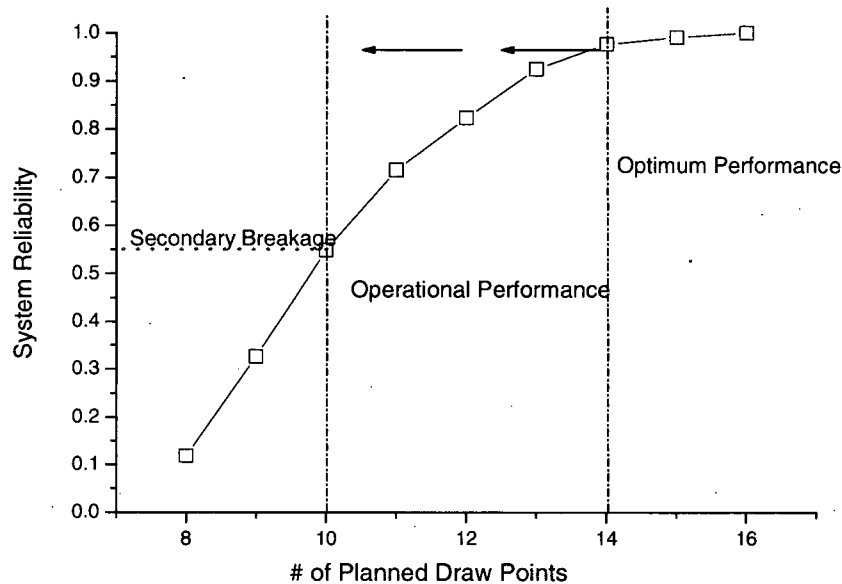


**Figure 4.21 Reliability model used to prioritize secondary blasting**

#### **4.9 Definition of Production Capacity of a Block Cave Mine using Reliability**

The traditional approach to define production capacity in block caving has been by constructing a curve that shows the tonnage profile during the life of the mine. The use of the reliability model in production planning allows estimation of the uncertainty associated with a production profile. The reliability profile produced by the reliability model can be interpreted as an estimator of the uncertainty of a production profile for a given available mining infrastructure. If several production profiles are simulated and passed through the reliability model, a family of curves relating tonnage to reliability could be plotted in which a single curve would represent the expected tonnage distribution of that period. Figure 4.22 shows an example of defining

production capacity by introducing the probability of different production profiles during the life of the mine.

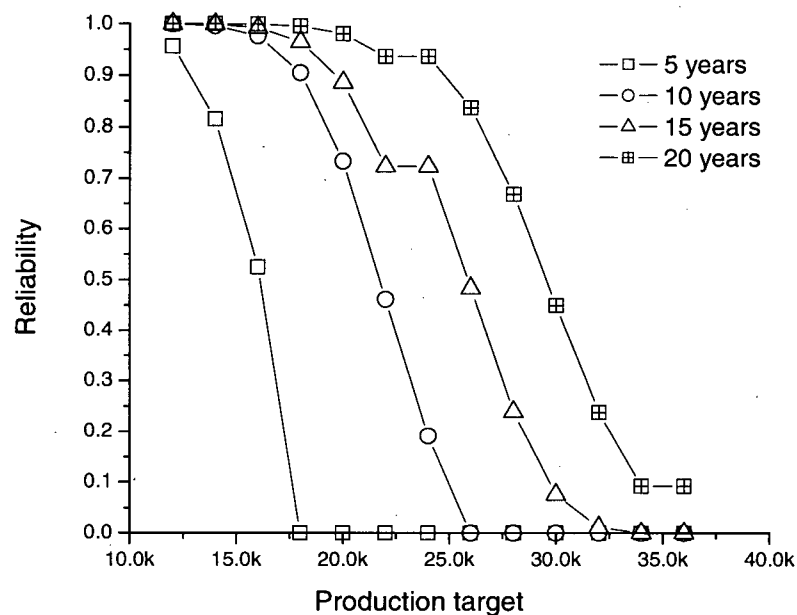


**Figure 4.22 Evolution of the production capacity distribution throughout a production schedule**

Figure 4.22 shows the distribution of the production capacity throughout the life of the mine for a given draw point opening sequence and development rate. However if several planning strategies are under evaluation the mine planner could be able to plot every strategy as a surface in which the X axis is the production target, Y axis the time and Z axis the reliability. Figure 4.23 shows the distribution of the production capacity for a given strategy in a surface format.

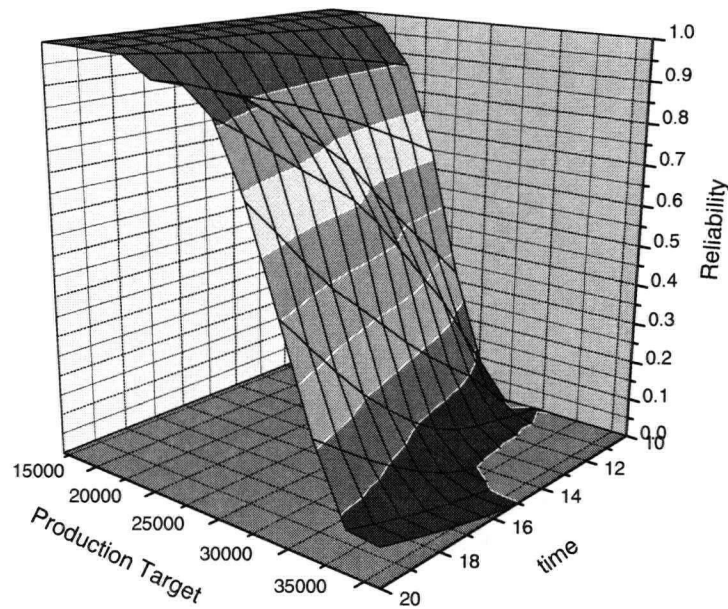


**Figure 4.23 Stochastic definition of production capacity of a block cave mine**

Based on Figure 4.23 a production strategy could be defined as a surface rather than a curve.

#### **4.10 Expected Tonnage versus Adjusted Draw Rate to Assess Production Capacity**

One possible result of this research could be to use the estimated draw point reliability to adjust the draw point yield to achieve a more realistic prediction of draw point productivity. In fact at the moment several of the mines visited as part of the research were using different kinds of “fudge factors” to adjust draw point productivity, based on the availability of the area, the status of the draw point and even sometimes “engineering judgment”. At some other operations the final production forecast was adjusted without a clear criterion to accommodate historical performance. It is important to understand how use of reliability per draw point alone can lead to an erroneous estimate of mine productivity. Figure 4.24 shows a comparison among the actual tonnage drawn from mine M2, the expected production capacity from the reliability model and the expected production capacity using an adjusted draw point productivity.

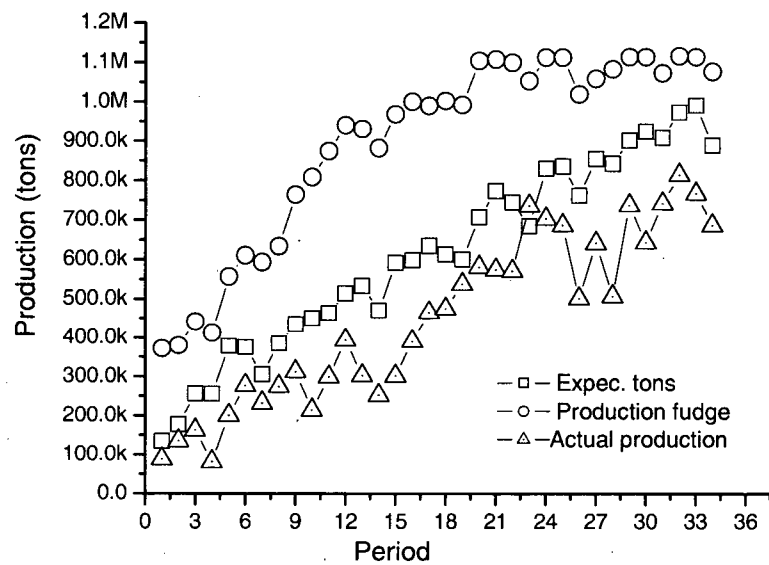


**Figure 4.24 Expected tonnage computed using the reliability model and the fudge factor approach**

From Figure 4.24 is seen that by adjusting the draw rate by a factor such as the draw point reliability the production capacity of the mine is excessively overestimated. There is a much better agreement between the actual production and the expected production capacity derived from the reliability model than using the draw point reliability as a fudge factor.

In summary the reliability model produces two main outputs: the reliability of the system and the expected tonnage per period. The system reliability per period has to do with the minimum number of days in which the tonnage target would be achieved within the period. The expected tonnage would be the most likely tonnage that would be produced in a given period of the production schedule. In the next chapter of the dissertation both of these parameters will be calibrated using data from mines M1 and M2 in order to validate the approach proposed in this thesis.

## 5 MODEL VALIDATION

Validation of the model was considered to be significant because it would demonstrate that the introduction of reliability measures related to mining infrastructure in a production scheduling algorithm could facilitate the estimation of the system reliability as previously defined in Chapter 4. In order to perform this analysis several methods of validation were tested using the production databases from mines M1 and M2.

The validation process started with the construction of the draw point ROCOF curves of both mines M1 and M2. This construction was performed using the draw point status available from the operational databases. The original production targets used at mines M1 and M2 were also estimated using the historical draw point sequence. Then all the inputs: draw point ROCOF curves, draw point yield curves and original production targets were used to compute the reliability of these targets. Figure 5.1 shows the data flow to compute the system reliability based on operational data.

The methods used to estimate the actual reliability obtained at mines M1 and M2 respect to their original production targets are listed below:

- As the ratio between the actual total production and the original production target per period.
- As the probability of achieving the production target based on the actual tonnage distribution curve per period. In this case every period was set up to be 60 days of production.

The following sections will review in detail the validation process in detail based on estimates of actual reliability mentioned above.

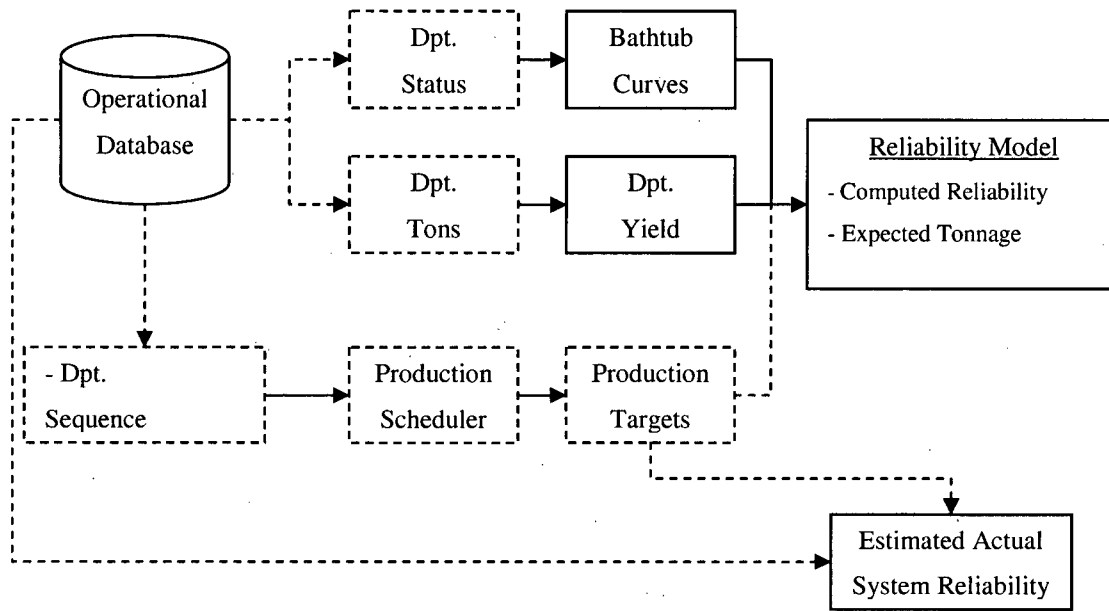


**Figure 5.1 Data flow to compute the reliability of the original production schedules of mines M1 and M2**

### 5.1 Reliability Model Calibration Using Absolute Reliability

The first method of calibration consisted in estimating the actual reliability as the ratio between the actual tonnage drawn and the tonnage target at time  $t$

$$R'(t) = \frac{AT(t)}{T(t)} \quad (5.1)$$

The actual reliability,  $R'(t)$  was plotted against the reliability computed by the model. The aim of this first analysis was to estimate how well the computed reliability can represent the dispersion of the actual tonnage with respect to the plan. This first analysis was performed using a nominal crosscut production capacity,  $T_{cx}(t)$ , of 85,000 tons per month. Figure 5.2 shows the result of this first analysis.

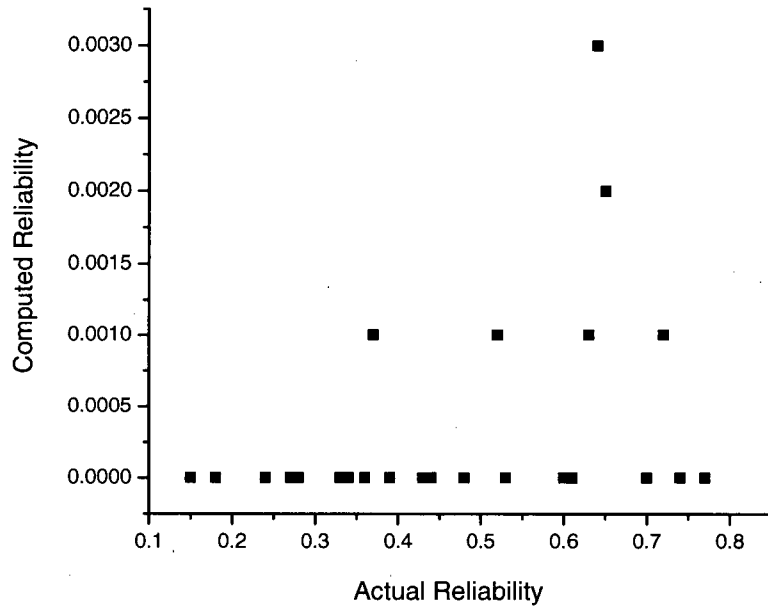


**Figure 5.2 Calibration of computed reliability using a constant crosscut production capacity**

The results shown on Figure 5.2 were very disappointing since there was no correlation between the actual and computed reliability. However, it was discovered that the nominal crosscut capacity should not be constant since the number of draw points constructed per crosscut evolves together with the production schedule. Crosscuts that are not developed fully at the beginning of the periods used in the calibration will not have the draw points to reach their nominal capacity. Thus it was decided to introduce a production target per crosscut,  $T_i(t)$  which was computed as a function of the actual number of draw points commissioned at time  $t$ . The following equation shows how the production target per crosscut is computed as

$$T_i(t) = \frac{h_i(t)}{f_i} T_{cx}(t) \quad (5.2)$$

Where  $h_i(t)$  is the number of draw points that have been commissioned at time  $t$  in crosscut  $i$ ,  $f_i$  is the total number of designed draw points in crosscut  $i$ , and  $T_{cx}(t)$  is the nominal crosscut production capacity at time  $t$ . Figure 5.3 shows how the calibration is improved by making the nominal crosscut production capacity variable during the production schedule.

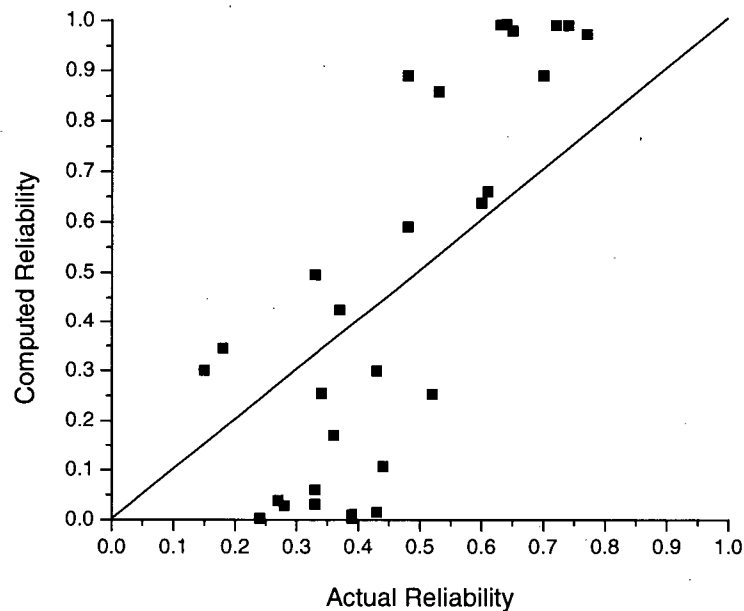
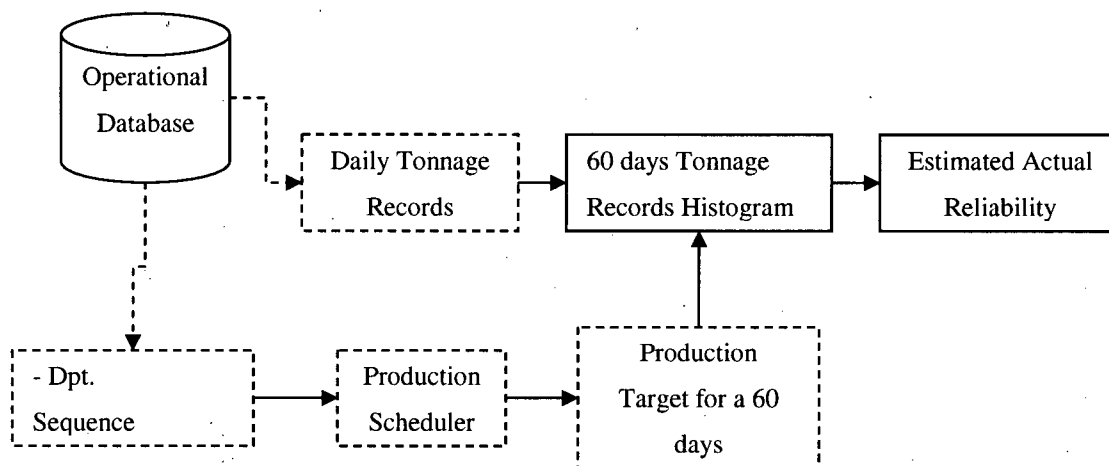


**Figure 5.3 Calibration of computed reliability using variable crosscut production capacity across the active layout**

## **5.2 Reliability Model Calibration Using Tonnage Distribution**

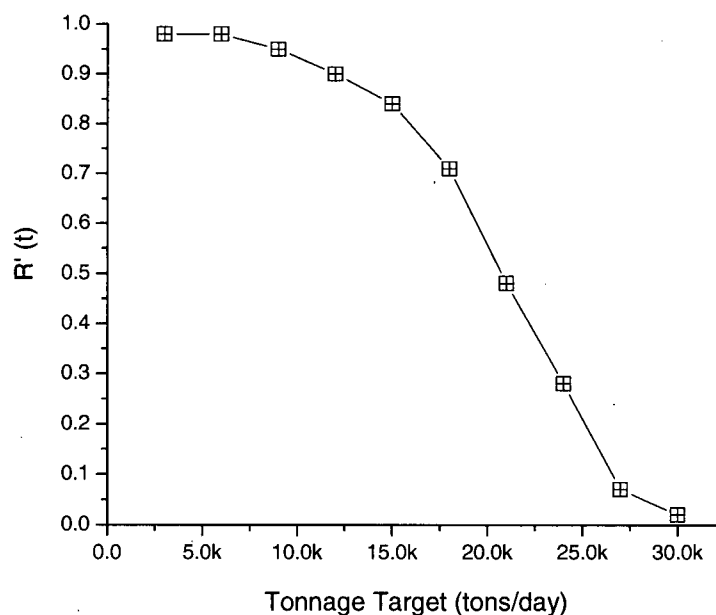
The second method to estimate actual reliability was based on a production tonnage histogram which was constructed based on the daily tonnage records. For each mine, M1 and M2, the actual daily production records were divided into two month periods in order to have enough information (60 data points) to construct the tonnage distribution within a period. One year of Mine M1 production data and almost three years of Mine M2 production data were used. The actual reliability for a given period was computed from the histogram as the probability of achieving at least the target defined for that period. Figure 5.4 shows a schematic dataflow that illustrates how the daily production records were used to compute the actual reliability of a period of 60 days.





**Figure 5.4 Dataflow used to estimate actual reliability of a 60 days period based on the tonnage distribution curve**

Figure 5.5 shows a relationship between tonnage target and actual reliability for a period of 60 days.



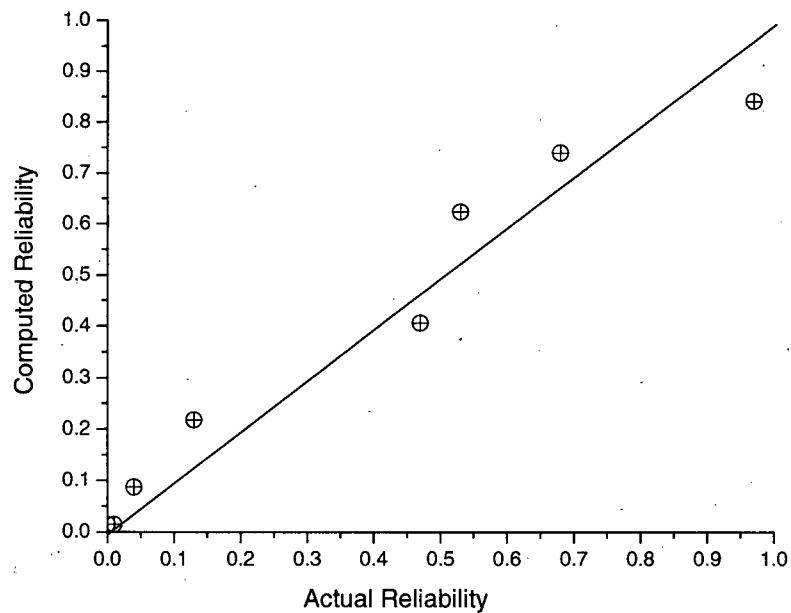
**Figure 5.5 Actual reliability as a function of actual tonnage distribution for a period of 60 days**

Table 5.1 shows a comparison between the actual versus computed reliability for a given production profile using data from mine M1.

**Table 5.1 Comparison of actual versus computed reliability**

Period	Target (tons/day)	Computed. Reliability	Actual. Reliability
1.00	35000	0.97	0.84
2.00	37000	0.68	0.74
3.00	39000	0.53	0.62
4.00	41000	0.47	0.41
5.00	43000	0.13	0.22
6.00	45000	0.04	0.09
7.00	47000	0.01	0.01
8.00	49000	0.00	0.01

The validation of the reliability model using actual reliability from the tonnage distribution curve for mine M1 is presented in Figure 5.6. The correlation coefficient for this validation was 0.97 for 8 points.



**Figure 5.6 Reliability model calibration using mine M1 data set**

Similar results for mine M2 are presented in Figure 5.7. The correlation coefficient found in this comparison was 0.98 for the 40 compared points.

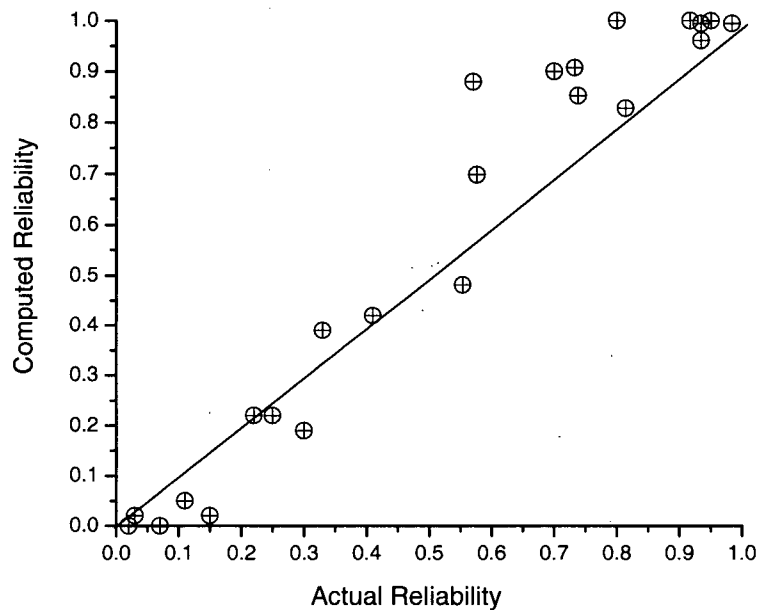


**Figure 5.7 Reliability model calibration using mine M2 data set**

The results shown in Figure 5.6 and Figure 5.7 are very encouraging since it demonstrates that for the actual mine production from operations M1 and M2, the reliability model does reproduce the reliability obtained at these mines for a given set of production targets.

### 5.3 Calibration Based On Expected Tonnage per Period

A different way of validating the reliability model was to compare the expected tonnage computed by the reliability model versus the actual tonnage mined in a given period of time. In this case the draw point ROCOF curves, the draw point yield curves and the tonnage target per period are input to the reliability model. The production targets in this case were set to be the same as the actual tonnage mined per period. In this case the model should produce a reliability equal to one for every period of the schedule since the production target has been set to be the same as the actual tons. The expected tonnages are supposed to be greater than or equal to the actual tons according to the definition of reliability introduced in Chapter 4. Figure 5.8 shows a comparison between the actual production and the expected tonnage computed from the reliability model. The correlation coefficient found between expected tonnage and actual tonnage is 0.87 for 32 periods. There is one outlier (circled) which is the result of a very low production

caused by a problem related to an underground crusher. Disregarding this point the correlation between actual tons and expected tons increases to 0.92.

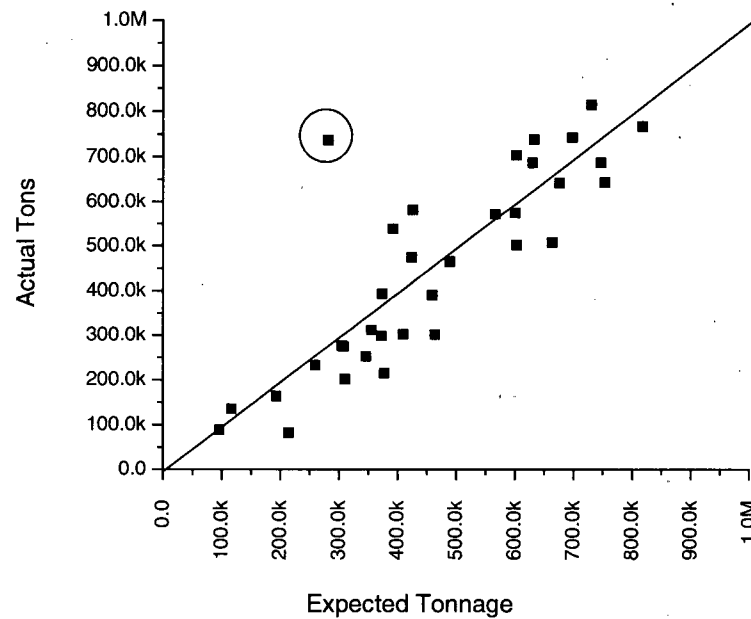


**Figure 5.8 Comparison between expected tonnage versus actual tons mined from mine M2**

Figure 5.8 Comparison between expected tonnage versus actual tons mined from mine M2 shows that the shape and the tonnage distribution for the production schedule is reproduced by the expected tons computed by the reliability model which can be used to forecast mine production capacity. In an application of the reliability model to a pre-feasibility study of a mine the actual tons will be unknown. Then the reliability model will have to run until a reliability of 1.0 is achieved for every period of the production schedule. The expected tonnage profile estimated by the reliability model will become the best estimate of the production profile for this mine.

Although the calibration results have exhibited some scatter between actual reliability and computed reliability at this stage of development it is considered that the correlation coefficients are acceptable given the available input to the model. The model has shown to be a valid tool to assess the tonnage distribution per period of a block cave mine and could be applied to an industrial application.

## 6 DISCUSSION AND CONCLUSIONS

### 6.1 Discussion

A mine plan defines the production promise of a mine operation. Its main outcome, the production schedule, is a bankable document that will support the ultimate decision of whether to pursue the mining venture or not. The block cave mining method has gained tremendous popularity in recent years due to its production capacity and low operating cost. Nevertheless, it has been observed that the recently developed block cave mines have not been able to reach their initial production targets. Even though there are several computer based applications that enable mining engineers to compute a production schedule none of them integrates the fundamental geotechnical models that sustain the process of caving the rock mass. The lack of geotechnical models in the planning process leads to unrealistic production targets that do not take into account the operational upsets such as hang ups, over sizes, wet muck and rock instability that affect mining infrastructure. As a consequence the real value of the mine is hidden together with the real potential of the mining system to deliver a given production plan.

The integration of geotechnical models in production schedules would require a reformulation of the existing scheduling packages. However, even if the current geotechnical models were integrated there would still uncertainty related to the parameters involved in those models and their ability to represent the actual rock mass behavior would still exist. The other factor is the ability of the current geotechnical models to simulate the actual caving behavior in highly stressed and competent rock masses. Therefore, as discussed in Chapter 3, using the actual performance of mining infrastructure as the main indicator that reflects the geotechnical events that take place in a block caving operation seems to be the most appropriate approach based on the current knowledge and technologies available to plan a block cave mine.

The concept of rate of occurrence of failure (ROCOF) has been successfully implemented to represent the performance of mining infrastructure as part of the thesis presented in this dissertation, in particular draw point ROCOF, related to their tendency to fail. The estimation of draw point reliability has a function of the draw point ROCOF has lead to the conclusion that it could subsume the effect of geotechnical effects on production performance. The reliability of a draw point as a function of the Rate of Occurrence of Failure (ROCOF) was investigated and

tested with two set of operational databases. It was also found that a more detailed record of the failures could perhaps enhance the estimation of draw point reliability by introducing time to repair as a random variable. It was found that the draw point ROCOF curve represents well the failure behaviour of a draw point during its operating life. It was observed that different draw point ROCOF curves could represent the behavior of mining infrastructure to different rock masses and stresses. Therefore for different geotechnical domains different draw point ROCOF curves could be used to represent the effect of rock mass and stress level on failure performance of different components of mining infrastructure. In this dissertation, two examples of draw point ROCOF curves have been presented representing two extremes of geotechnical behavior in block cave mining. This motivates novel research to develop a comprehensive database that could support the choice associate to the shape of a draw point ROCOF curve for a given geotechnical domain. The results of this proposed research could be used by mines facing feasibility studies or operating mines that do not know the draw point failure behaviour of a given area of the mine.

The initial stage of the draw point ROCOF curve could represent the interaction of a draw point and the undercut blasting activity since it could reflect the geotechnical events that tend to retard the undercut blasting. At the moment undercutting usually is seen as an activity independent of production. However it was shown that the traditional, advanced and pre undercutting methods show a strong relationship between undercut and production level. Commissioning of draw point to production will depend upon the undercut front position and its ability to progress in the short term. Therefore, the burn in region of the curve could be affected by the performance of the undercutting. If the undercutting is retarding the commissioning of a draw point the starting point on the curve will be raised. Consequently, it may be possible to include the uncertainty of undercut construction and stability as part o the production system.

In terms of the way that the ROCOF is estimated using draw point status, tactical problems that induce draw point closure should not affect draw point status but rather draw point productivity. There is a trend to think that draw points fail due to tactical decisions such that status is driven by tonnage. However a draw point that is idle due to tactical reasons is still available to be mined so this should not affect the shape of the draw point ROCOF curve.

Based on the reliability of the mining system components, the reliability of the mining system was estimated as a measure of the ability of the mining system to produce a given production target. The reliability of the block cave mining system was defined as the probability of the system to achieve a given production target at a given time. A *k-out-of-n* model was constructed to compute the reliability of the block cave mining system. It was found that the mining system could be divided into: production areas, production feeders and production crosscuts. A production crosscut is a *k-out-of-n* system composed of independent and non identical draw points. At the same time a production feeder is a *k-out-of-n* system composed of independent and non identical production crosscuts. Therefore the block cave reliability system consists of a dual redundancy model at the draw point and the crosscut level. Every one of the *k-out-of-n* systems is solved using a recursive algorithm. Finally the reliability model would produce a reliability profile associated with a production schedule as an indicator of the ability to achieve a given production target. The reliability profile would depend on the draw point reliabilities and the general distribution of redundancy across the active layout.

The reliability center mine planning model provides a tool to compute production targets integrating the potential infrastructure failures that may affect the viability of achieving a given production schedule. Redundancy at the draw point and crosscut level has been added as a planning variable to mitigate the geotechnical uncertainty. Therefore redundancy should be carefully included in the mining system to maximize reliability at the minimum capital and operating cost.

Several discussions related to how operators should deal with the redundancy contained in the mining system have taken place during this research. The actual concept is that by introducing redundancy in the medium and long term plans, logistical problems will be introduced to the operation of the plan by having more resources than needed. Consider *n-k* redundant draw points in a long term production plan. When the time comes to operate the plan there will be a need to decide which draw points shall be mined, since there are going to be more draw points than needed to fulfill the production target. If the reliability model has been properly implemented in terms of draw point ROCOF curves and draw point yield this should not happen. Redundancy is introduced in production planning to mitigate uncertainty. Therefore at the time the plan is

implemented there shall be just  $k$  draw points available since the rest will be unavailable as a result of the geotechnical events. In the event that there is redundancy in the operation of the mine an analysis such as the one shown in Chapter 4 needs to be conducted to plan the best usage of redundancy in terms of delivering the medium and long term plans.

Fudge factors are widely used in the mining industry usually to reconcile the results of numerical models to the actual performance of the mine. There could be the temptation to use the reliability of a draw point as a fudge factor to adjust draw point productivity. It was demonstrated as part of the thesis that this practice should be avoided since the actual productivity of a block cave depends upon the amount of redundancy built in at the draw point and crosscut level rather than the simple sum of the adjusted draw point productivity. The relationship between redundancy and draw point reliability is non linear and varies over time. Consequently the expected tonnage as a result of the reliability model should be understood as the best estimator of block cave productivity since it is a function of the reliability model which subsumes the geotechnical model that sustains the block cave mining system.

The approach to mine planning presented in this dissertation challenges the traditional approach in which design and planning of a mine operation are seen as individual and independent processes taking place as part of engineering a mine. The reliability approach to planning assists mining engineers and geologists to estimate the probability of achieving a given production schedule. To mitigate the periods of low reliability within the production schedule the mine planners would introduce more infrastructure such as ore passes, draw points, production crosscuts as means of redundancy to enhance the system reliability. Therefore the amount of mining infrastructure to introduce in a plan would be seen as a planning decision rather than a design decision. Thus when using the reliability approach to planning, mine design becomes part of the mine planning process.

## **6.2 Conclusions**

An empirical approach which uses observations of the behaviour of mining infrastructure has been employed to provide a guide for the planning of such infrastructure so as to attach reliability to a production schedule. It is believed this is a better measure of future performance.



Specific conclusions are as follows:

- The low compliance shown by current production schedules can be attributed to the way production schedules are computed and the way the fundamental models are integrated in the process of computing these production plans
- The estimation of the rate of occurrence of failure (ROCOF) of mining infrastructure based on operational status was shown to be appropriate to represent the geotechnical events that affect the availability of mining infrastructure.
- The ROCOF of mining infrastructure has been shown to be time-dependent, behaving as a mechanical component whose performance is well defined by the rate of occurrence of failure of a draw point.
- The mining infrastructure exposed to different rock mass and stresses environments will have different ROCOF curves associated with their likelihood of failure.
- The estimation of mining infrastructure reliability was successfully implemented as a function of the ROCOF. The time to repair was showed to have a larger impact on the low reliability components than on the high reliability ones.
- The reliability of mining infrastructure was shown to be highly correlated with the geotechnical events that affect productivity. Consequently, the concept of using reliability measures to subsume geotechnical events on mining infrastructure was shown.
- Block cave system reliability was defined as the ability of the mining system to achieve at least a given production target at a given time within the production schedule.
- The production profile was redefined using the reliability profile which was computed as a result of the block cave system reliability.
- Block cave system reliability was validated using two of the operational databases obtained as part of the research. The expected tonnage as well as the system reliability was shown to exceed a correlation coefficient over 0.85 when compared to actual production performance.
- The reliability of a production schedule is an indicator of the technical uncertainty contained in the mining system as a function of the balance between unknown rock mass behavior and redundancy of mining infrastructure.

- The definition of production capacity in a block cave mine goes beyond computing accurately the draw point productivity. This capacity depends highly on the relationship between draw point productivity, crosscut production capacity and the amount of redundancy at the draw point and crosscut level.

### **6.3 Recommendations**

It is important to construct a wide operational database that could store the distribution parameters for different infrastructure components of a block cave mining system under different rock mass and stress environments. This is seen as an important step forward in the development of the theory presented in this thesis. It is envisioned that in the future there would be a set of empirical charts that could support the estimate of the ROCOF shape depending upon the geotechnical variables that sustain the mining system.

The reliability method should be used as a main tool to quantify the quality of the reserves supported by a given production plan. The reliability model could be used to assist engineers to classify different production schedules according to the international standards that relate mining reserve estimation. Mining reserves must be classified according to technical uncertainty involved not only in the resource estimation process but also as a result of the mining process.

A chart as shown in Figure 4.15 could be imported to a financial model to determine the extent one could optimize reliability by lowering production targets particularly during the ramp up period of the schedule. This is a fundamental question that needs to be answered in the process of assessing the value of a block cave operation. Different levels of reliability of a production schedule will need different amounts of “insurance” (Vergara, 2004) to compensate for the effect of a potential failure of the original production promise. Thus the value of a block cave mine must be derived as a function of the geotechnical uncertainty since the nature of the mining system relies entirely on the rock mass. Consequently the reliability model will facilitate the estimation of technical uncertainty to be fed into a financial model that could derive the true value of a caving venture.

In this research the concept of redundancy has been used to enhance the reliability of a production schedule. Nevertheless the research presented in this dissertation does not address the optimal reliability of a production schedule. There is a clear correlation between redundancy and production capacity. The production schedules computed using the traditional methods would disregard the reliability of those schedules leading to an erroneous estimation of the mine value. The optimal value of a mine should be supported by a financial tool such as real options that allows the integration of production schedule reliability in order to represent the uncertainty involved in the production planning process. The optimal production schedule should be such that allows return to the share holders under a predefined level of uncertainty.

The fact that the raw data used to construct the draw point ROCOF curves and draw point yield curves contain noise leads to model every one of the inputs of the reliability model as a random variable with an underlying probability distribution. By integrating the probability distribution of the inputs of the reliability model could lead to quantify the probability associated to a certain level of reliability which opens a whole new area of research. It is recommended that further research should be conducted on this area in order to quantify levels of certainty of different reliability estimates.

## REFERENCES

Aguayo A., Campos C., Mansilla M., Sougarret J., Susaeta A., 2004. LHD versus Mechanized Grizzly in III panel of Andina. In *Proceedings, MassMin 2004*, Santiago, pp. 415-420. Santiago, (Ed: A Karzulovic and M Alfaro).

Araneda O. and Gaete S., 2004. Continuous Modeling for Caving Exploitation. In *Proceedings, MassMin 2004*, Santiago, pp. 415-420. (Ed: A Karzulovic and M Alfaro).

Ascher, H. and Feingold, H., 1984. *Repairable Systems Reliability*, Marcel Dekker Inc., New York.

Barraza M. and Crorkan P., 2000. Esmeralda Mine Exploitation Project. In *Proceedings, MassMin 2000*, Brisbane, pp. 267-278. The Australasian Institute of Mining and Metallurgy: Melbourne.

Barraza M., San Martín J. F., Montecino M., 2004. Mine Technology and its Implementation and Control, Reservas Norte – Sub 6, El Teniente. In *Proceedings, MassMin 2004*, Santiago, pp. 681-685. (Ed: A Karzulovic and M Alfaro).

Barlow, R.E. Heidtmann, K.D., 1984. Computing k-out-of-n System Reliability, *IEEE Trans. on Reliability*, Vol. R-33, Oct, 322 - 323.

Bartlett, P. J., 1992. The Design and Operation of Mechanized Cave at Premier Diamond Mine. In *Proceedings, MassMin 1992*, Johannesburg, South African Institute of Mining Metallurgy: Johannesburg

Barlett, P.J., Nesbitt K., 2000. Draw Control at Premier Mine. In *Proceedings, MassMin 2000*, Brisbane. The Australasian Institute of Mining and Metallurgy: Melbourne.

Boland, P.J. and Proschan F., 1983. The Reliability of K out of N Systems. *The Annals of Probability*, Vol. 11, pp. 760-764.

Brown, E T, 2003. Block Caving Geomechanics. *JKMRC Monograph Series on Mining and Mineral Processing*. Vol 3, 515 p. Julius Kruttschnitt Mineral Centre, University of Queensland: Brisbane.

Cacceta, L and Giannini, L M, 1988. The Generation of Minimum Search Patterns in the Optimum Design of Open Pit Mines. In *Proceedings, Australasian Institute of Mining and Metallurgy*, Vol. 5, N 293, pp. 57-61.

Carew T., 1992. The Casiar Mine Case Study. In *Proceedings, MassMin 1992*, Johannesburg, Journal of the South African Institute of Mining Metallurgy: Johannesburg.

Chacón J., Göpfert H., Ovalle A., 2004. Thirty Years Evolution of Block Caving in Chile. In *Proceedings, MassMin 2004*, Santiago, (Ed: A Karzulovic and M Alfaro).

Chanda E C K, 1990. An Application of Integer Programming and Simulation to Production Planning for a Stratiform Ore Body. *Mining Science and Technology*, Vol. 11, pp. 165-172

De Nicola, R., Fishwick, M., 2000. An Underground Air Blast - Codelco Chile Division El Salvador. In *Proceedings, MassMin 2000*, Brisbane. The Australasian Institute of Mining and Metallurgy: Melbourne.

Dessureault, S., Scoble, M., Rubio, E, 2000. Simulating Block Cave Secondary Breakage - An Application of Information and Operations Management Tools in Mass Mining Systems. In *Proceedings, MassMin 2000*, Brisbane, pp. 893-896. The Australasian Institute of Mining and Metallurgy: Melbourne

deWolf, V., 1981. Draw Control in Principle and Practice at Henderson Mine. In *Design and Operation of Block Caving and Sub Level Stoping Mines* (Ed: D R Steward), pp. 729-735. Soc Min Engrs, AIME: New York.

Didyk M. and Vasquez, G., 1981. Draw Behaviour in El Salvador Mine. In *Design and Operation of Block Caving and Sub Level Stoping Mines* (Ed: D R Steward), pp. 737-743. Soc Min Engrs, AIME: New York.

Dimitrakopoulos, R., Farrelly, C.T. and Godoy, M.C., 2002. Moving Forward from Traditional Optimisation: Grade Uncertainty and Risk Effects in Open Pit Mine Design. *Transactions of the IMM, Section A Mining Industry*, Vol. 111, pp. A82-88.

Diering T, 2000. PC-BC: A Block Cave Design and Draw Control System. In *Proceedings, MassMin 2000*, Brisbane, pp301-335.. The Australasian Institute of Mining and Metallurgy: Melbourne

Diering T, 2004. Computational Considerations for Production Scheduling of Block Cave Mines. In *Proceedings, MassMin 2004*, Santiago, Chile. (Ed: A Karzulovic and M Alfaro).

Doepken, W. G, 1982. The Henderson Mine. In *Underground Mining Methods Handbook* (Ed: W A Hustrulid), Vol. 1, pp. 990-997. Soc Min Engrs, AIME: New York.

Dolipas R. S., 2000. Rock Mechanics as Applied in Philex Block Cave Operations. In *Proceedings, MassMin 2000*, Brisbane. The Australasian Institute of Mining and Metallurgy: Melbourne.

Dotson, J. C., 1966. Reliability Engineering and Its Application in Mining, *Mining Congress J.*, pp. 68-78.

Dunbar, W. S., Dessureault S., Scoble M., 1998. Modeling of Flexible Mining Systems, In *Proceedings Can Inst Min Metall, Annual General Meeting*, Montreal, 8p.

Dunlop R and Gaete S, 1995. Seismicity at El Teniente Mine: A Mining Process Approach. In *Proceedings, 4th International Symposium on Mine Planning and Equipment Selection*. October 31 –November 03, Calgary, Canada.

Encina V., Fuentes C., Palma M., 2004. Study of interaction between ellipses of extraction in a physical model of granular material in 2-D. In *Proceedings, MassMin 2004*, pp. 141-149. (Ed: A Karzulovic and M Alfaro).

Esterhuizen G. S., Rachmad L., Potapov A. V., Nordell L. K., 2004. Investigation of Swell Factor in a Block Cave Draw Column. In *Proceedings, MassMin 2004*, Santiago, pp 215-219 (Ed: A Karzulovic and M Alfaro).

Esterhuizen, G S, 1994. A program to predict block cave fragmentation. Technical reference and user guide, version 2.1.

Febrian I., Yudanto W., Rubio E., 2004. Application of Convergence Monitoring to Manage Induced Stress by Mining Activities at PT Freeport Indonesia Deep Ore Zone Mine. In *Proceedings MassMin 2004*, pp. 269-272, Santiago, (Ed: A Karzulovic and M Alfaro).

Flores, G, Karzulovic, A and Brown, E T, 2004. Current Practices and Trends in Cave Mining. In *Proceedings, MassMin 2004*, Santiago, (Ed: A Karzulovic and M Alfaro).

Flores, G, 2004. Geotechnical Challenges of the Transition from Open Pit to Underground Mining at Chuquicamata Mine. In *Proceedings, MassMin 2004*, Santiago, (Ed: A Karzulovic and M Alfaro)

Gershon, M, 1987. Heuristic Approaches for Mine Planning and Production Scheduling. *Int J of Min and Geol Eng*, Vol. 5, pp. 1-13.

Glazer, S. and Hepworth, N., 2004. Seismic Monitoring of Block Cave Crown Pillar – Palabora Mining Company, RSA. In *Proceedings, MassMin 2004*, pp 565-569, Santiago, (Ed: A Karzulovic and M Alfaro).

Guest A. R., Van Hout G. J., Von Johannides A., Scheepers L. F., 2000. An Application of Linear Programming for Block Cave Draw Control. In *Proceedings, MassMin 2000*, Brisbane. The Australasian Institute of Mining and Metallurgy: Melbourne.

Heslop T. G. and Laubscher, D. H., 1981. Draw Control in Caving Operations on Southern African Chrysotile Asbestos Mines. In *Design and Operation of Block Caving and Sub Level Stopping Mines* (Ed: D R Steward), pp. 755-774. Soc Min Engrs, AIME: New York.

Hoyland, A., and Rausand, M., 1994. *System Reliability Theory: Models and Statistical Methods*. The Norwegian Institute of Technology. Wiley New York.

Hustrulid, W., 2000. Method Selection for Large-Scale Underground Mining. In *Proceedings, MassMin 2000*, Brisbane, pp. 29-56. The Australasian Institute of Mining and Metallurgy: Melbourne.

Kear, R. M., 2000. The Use of Evaluation Surfaces to Assist in the Determination of Mine Design Criteria. In *Proceedings, MassMin 2000*, Brisbane, pp. 29-56. The Australasian Institute of Mining and Metallurgy: Melbourne.

Kajner, L. and Sparks G., 1992. Quantifying the Value of Flexibility When Conducting Stochastic Mine Investment Analysis, *Bulletin Can Inst Min Metall*, 85, NO 964, pp. 68-71

Kaufmann, A., Grouchko, D. & Cruon, R., 1977. *Mathematical Models for the Study of the Reliability of Systems*. New York: Academic Press.

Kazakidis, V.N. and M. Scoble, 2002. Accounting for Ground-Related Problems in Planning Mine Production Systems, *Mineral Resources Engineering*, Vol. 11, N 1, pp. 35-57.

Kazakidis, V.N., and Scoble, M., 2003. Planning for Flexibility In Underground Mine Production Systems, SME Publications Dept. prior to Nov. 30, 2003.



Krantz, D., and Scott, T., 1992. Hard Rock Mining: Method Selection Summary, *SME Mining Engineering Handbook* 2nd edition.

Kraushacer, D. E., 1987. Long Term Planning of Coal Mines by Statistical Evaluation of Databases in Existing Mines. In *Proceedings APCOM 1987: International Symposium on the Application of Computers and Operations Research in the Minerals Industries*.

Kumar, U. and Granholm S., 1988. Reliability Technique – A Powerful Tool for Mine Operators. *Mineral Resources Engineering*, Vol 1, No 1, pp. 13-28.

Kvapil R., 1965. Gravity Flow of Granular Materials in Hoppers and Bins. Part I and II, *Int. J. Rock Mech. Mining Sci.* Vol 2, pp.35-41.

Lakner, A. A., and Anderson, R. T. 1985. *Reliability Engineering for Nuclear and Other High Technology Systems*. Elsevier Applied Science, London.

Laubscher, D. H., 1990. A Geomechanics Classification System for the Rating of Rock Mass in Mine Design. *Journal of the South African Institute of Mining Metallurgy*, Vol 90, No 10, pp 257-273.

Laubscher, D. H., 1994. Cave Mining- The State of the Art, *Journal of the South African Institute of Mining Metallurgy*, Vol. 94, pp. 279-292.

Lewis, R. S. and Clark, G. B., 1964. *Elements of Mining*, 3<sup>rd</sup> edition, 768 p. John Wiley & Sons: New York

McClennan F. W., 1930. Mining Copper Co. Method of Mining Low-grade Ore Body, Vol 91 p 39.

McKinnon, S D and Lorig, L J, 1999. Considerations for Three Dimensional Modelling in Analysis of Underground Excavations. In *Distinct Element Modelling in Geomechanics* (Ed: V W Sharma, X R Saxena and R D Woods), pp. 145-166. Oxford and IBH Publishing: New Delhi.

Moss A., Russel F., Jones C., 2004. Caving and Fragmentation at Palabora: Prediction to Production. In *Proceedings, MassMin 2004*, Santiago, pp. 585-590. Santiago, (Ed: A Karzulovic and M Alfaro).

Moyano A. F. and Vienne J. C., 1993. Remote Operation of LHD and Pick Hammers in Rock Burst Conditions, Innovative Mine Design for the 21<sup>st</sup> Century. In *Proceedings of the International Congress on Mine Design*, Kingston, Ontario, A A Balkema, Rotterdam, pp 579-591.

Owen, K. C. and Guest, A. R., 1994. Underground Mining of Kimberlite Pipes. In *Proceedings, XV CMMI Congress* (ed: HW Glen), 1, pp 207-218. South African Institute of Mining Metallurgy: Johannesburg.

Prasetyo R., Flint D. C., Setyoko T. B., Samosir E., 2004. Use of the Modular Dispatch System to Control Production Operations at the DOZ Block Cave Mine. In *Proceedings, MassMin 2004*, Santiago, pp. 696-701. Santiago, (Ed: A Karzulovic and M Alfaro).

Peele, R., 1941. *Mining Engineers' Handbook*, 3<sup>rd</sup> edition. John Wiley & Sons: New York.

Rahal, D., Smith, M., van Hout, G., and von Johannedis, A., 2003. The Use of Mixed Integer Linear Programming for Long-Term Scheduling in Block Caving Mines. In *Proceedings, APCOM 2003: 31st International Symposium on the Application of Computers and Operations Research in the Minerals Industries*, May 14-16, 2003, Cape Town, South Africa.

Ramani, V. R., Bhattacharjee A., Pawlikowski R. J., 1989. Reliability, Maintenance, And Availability Analysis of Longwall Mining Systems. *Mineral Resource Engineering*, Vol 2, No 1, pp. 3 – 17.

Rech W. and Keskimaki, K. W., Stewart D. S., 2000. An Update on Cave Development and Draw Control at the Henderson. In *Proceedings, MassMin 2000*, Brisbane, pp. 495-505. The Australasian Institute of Mining and Metallurgy: Melbourne.

Riddle, J., 1976. A Dynamic Programming Solution of a Block – Caving Mine Layout. In *Proceedings APCOM 1976: International Symposium on the Application of Computers and Operations Research in the Minerals Industries*.

Rojas E., Molina R., Bonani A., Constanzo H., 2000. The Pre-Undercut Caving Method at the El Teniente Mine, Codelco Chile. In *Proceedings, MassMin 2000*, Brisbane, pp. 261-266. The Australasian Institute of Mining and Metallurgy: Melbourne.

Ross J. G. et al., 1934. Block Caving at King Asbestos Mine, Quebec, *Trans Can Inst Min & Met*, Vol 37 p 209. Ibid, Vol 39 (1936) pp. 441.

Rubio, E, Cáceres, C, Scoble, M., 2004. Towards An Integrated Approach To Block Cave Planning. In *Proceedings, MassMin 2004*, Santiago, pp. 128-134. Santiago, (Ed: A Karzulovic and M Alfaro).

Rubio, E, Diering, T., 2004. Block Cave Production Planning Using Operations Research Tools. In *Proceedings, MassMin 2004*, pp. 141-149. (Ed: A Karzulovic and M Alfaro).

Rubio, E, Dunbar W S, Scoble M, 2001. Scheduling in Block Caving Operations Using Operations Research Methods. In *Proceedings Annual General Meeting, Can. Inst. Min & Metall.* : Montreal, Quebec, Canada, May 2001.

Russel, F. M., 1987. Application of A PC-Based Network Analysis Program to Mine scheduling. In *Proceedings APCOM 1987: International Symposium on the Application of Computers and Operations Research in the Minerals Industries*.

Rushdi, A. M., 1987. Efficient Computation of k-out-of-n System Reliability, *Reliability Engineering*, Vol 17, 1987 Feb, pp. 157-163

Samis, M. and R. Poulin, 1998. Valuing Management of Flexibility: A Basis to Compare the Standard DCF and MAP Valuation Framework. *Bulletin Can. Inst. Min. Metall.*, Vol. 91, No 1019, pp.69-74.

Singh, A. and Skibniewski, M. J., 1991. Development of Flexible Production Systems for Strip Mining. *Mining Science and Technology*, Vol.13, pp. 75-88.

Smith M L, 1999. The Influence of Deposit Uncertainty on Mine Production Scheduling, *International Journal of Surface Mining*, Vol. 13, pp.173-178

Summers, J., 2000. Analysis and Management of Mining Risk. In *Proceedings, MassMin 2000*, Brisbane, pp. 63-82. The Australasian Institute of Mining and Metallurgy: Melbourne.

Tobie, R. L. and Julin, D. E. 1982. Block Caving: General Description. *Underground Mining Methods Handbook*, pp.967-972. SME Mining Engineering.

Tota, E. W., 1997. Northparkes Mines – New Performance Benchmarks for Underground Mining. In *Proceedings 1997 AusIMM Annual Conference*, pp. 57-64 (The Australasian Institute of Mining and Metallurgy: Melbourne).

Trigeorgis, L., 1990. A Real Options Application in Natural Resource Investments. *Advances in Future and Options Research*, Vol 4, pp153-164.

van Hout G., Allen S., Breed M., Singleton J., 2004. Status of Draw Control Practice and Waste Management at Cullinan Diamond Mine. In *Proceedings, MassMin 2004*, pp. 491-497. (Ed: A Karzulovic and M Alfaro).

Verdugo R., Ubilla J., 2004. Geotechnical Analysis of Gravity Flow During Block Caving. In *Proceedings, MassMin 2004*, pp. 141-149. (Ed: A Karzulovic and M Alfaro).

Vergara, L., 2004. Personal communication. El Teniente Codelco - Chile

Wilke, F L, Mueller, K, and Wright, E, 1994. Ultimate Pit and Production Scheduling Optimization. In *Proceedings, APCOM 1994*, pp 499-505 (IMM: London).

Xiaotian S., 1989. Caving Process Simulation and Optimal Mining Sequence At Tong Xuang Yu Mine, China. In *Proceedings APCOM 1989: International Symposium on the Application of Computers and Operations research in the Minerals Industries*.

## **APPENDICES**

### **A Proposed Operational Database in Block Cave Mines**

The operational database stores a collection of production and monitoring data that is recorded as the operation of the mine takes place. Usually this database is composed of different component such as the production module, equipment module, and geologic module. The production module stores tonnages drawn from the draw points per day, the ore passes and haulage system activity, secondary breakage activity, draw point status. The equipment module stores the location of equipment every hour, the equipment availability, maintainability indexes. The geologic module stores draw point sampling, geologic mappings, geotechnical monitoring. In this research the most relevant component of the operational database consists of the production module that contains tonnages records and draw point status.

The production module of the operational database will be used for two different purposes in this research; the first purpose would be to compute a set of key indicators related to caving performance such as, draw points, ore passes, cross cuts, the second purpose would be to compute the rate of failure occurrence of the mining components.

The key caving performance indicators have been defined in order to summarize the status of the caving. It is proposed that this performances would be used to compare a given block cave against its initial feasibility study or other block caves in order to explain production drops or any special unexpected behaviour happening in the operation. A summarized list of the key performance indicators recommended to be derived out of the production database is presented as follows:

- Production performances, this involves curves of tons versus draw points, production crosscuts, ore passes, crushers, trains, etc. Also these indicators are usually measured in a time range such as shift, day, week, month or year, then they are linked to cave maturity (height of draw), geology, structural patterns, etc.
- Fragmentation, this involves curves that could represent the evolution in time of hang ups and oversize. Usually these indicators will be cross checked against production performances.

- Operational status, store different kinds of status associated to the draw points such as hang up, oversize, not used, wet muck. Often is found that just the change on status is stored rather than the daily draw point status. Also the crosscut, ore passes, crushers and trains status is often missing from the production database. This piece of data is fundamental to compute the reliability of the mining components.
- Mean time to failure and mean time to repair are both indicators derived from the reliability system theory that can be used to analyse the performance of secondary breakage activities. Nevertheless the most important application of these indicators is the relationship between mean time to failure and the geotechnical factors triggering the failures.
- Draw point priority is a historical record of the sequence how the draw points were drawn. This is important to back analyse the relationship between this sequence and the efficiency of secondary breakage.

A representation of the workflow to derive mining components reliability from the operational database is presented in Figure A.1.

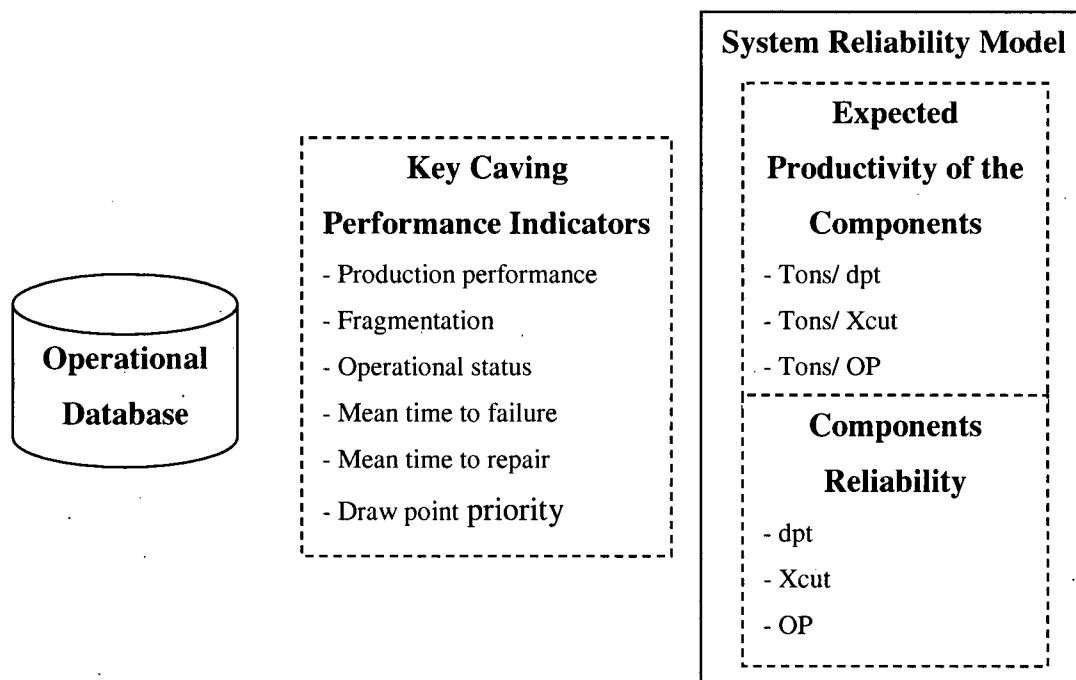


**Figure A.1 The reconciliation model**

It is interesting to note that most of the mines visited did not have a comprehensive design of their operations database including tonnage records, draw point status, hang up frequency, convergence, stress monitoring, equipment information, etc. The operations database was evolving as new data was collected. Also it was noted that some of the important data such as explosive consumption and undercut records were kept in spreadsheets and often that information was corrupted and consequently useless. Usually there were no records regarding repair efficiencies such as time and resources allocated to infrastructure repair or even cross cut rework. Almost all the operations visited had a draw point status classification for however this classification was usually useless or difficult to interpret. At some operations for example the draw point status was recorded when there was a change on it. At some other operations the draw point status was measured using the Modular Mine dispatch system which did not record accurately enough the factors happening at the draw points, mainly because the secondary blasting crews and equipment were not connected to the dispatch system. The Tamrock automated dispatch system also did not record the status of the draw point accurately since they were looking at the LHD mechanical behavior rather than the mining system. Therefore there is a fair amount of work to be done in order to establish a comprehensive, dynamic and a centralized database to store monitoring data.



## B Recursive Algorithm for the Reliability of a k-out-of-n System

The recursive algorithm to compute a *k-out-of-n* system begins by computing the intermediate reliability entries  $R_e(i, j)$  which are defined as follows:

$$R_e(i, j) = q_j R_e(i, j-1) + p_j R_e(i-1, j-1) \quad 0 \leq i \leq n, 0 \leq j \leq n \quad (\text{B.1})$$

The boundary conditions applied to B.1 are shown below

$$R_e(0,0) = 1; R_e(-1, j) = R_e(j+1, j) = 0 \quad 0 \leq j \leq n \quad (\text{B.2})$$

The derivation of the recursive algorithm considers the generation function presented by Barlow and Heidtmann (1984)

$$g_n(z) = \prod_{i=1}^n (q_i + p_i z) = \sum_{i=0}^n R_e(i, n) z^i \quad (\text{B.3})$$

The above generating function can be rewritten as the following recursive relationship

$$g_{j-1}(z) = \prod_{i=1}^{j-1} (q_i + p_i z) = \sum_{i=0}^{j-1} R_e(i, j-1) z^i \quad (\text{B.4})$$

From B.3,  $g_j(z) = (q_j + p_j z) g_{j-1}(z)$  and the right hand side of B.3 can be rewritten as follows:

$$\sum_{i=0}^j R_e(i, j) z^i = (q_j + p_j z) \sum_{i=0}^{j-1} R_e(i, j-1) z^i \quad (\text{B.5})$$

By introducing the terms inside the total sum of Equation B.5 the following equation can be derived:

$$\sum_{i=0}^j R_e(i, j) z^i = \sum_{i=0}^j [q_j R_e(i, j-1) + p_j R_e(i-1, j-1)] z^i \quad (\text{B.6})$$

$R_e(i, j)$  is derived by comparing both sides of Equation B.6. Rushdi (1987) directly linked the intermediate *k-out-of-n* probabilities,  $R_e(i, n)$ , with the total reliability as follows:

$$R(k, n) = \sum_{i=k}^n R_e(i, n) \quad (\text{B.7})$$

To better understand the above formulation an analytical derivation of the recursive algorithm will be explored in the following sections. Consider the definitions shown below.

$$\begin{aligned} p_i &= \text{reliability of component } i \\ q_i &= 1 - p_i = \text{unreliability of component } i \end{aligned}$$

First a system of 2 components functioning out of 3 available will be computed as follows:

$$R_e(2,3) = p_1 p_2 q_3 + p_1 q_2 p_3 + q_1 p_2 p_3 \quad (\text{B.8})$$

By grouping the terms Equation B.8 can be written as follows:

$$R_e(2,3) = (p_1 q_2 + q_1 p_2) p_3 + p_1 p_2 q_3 \quad (\text{B.9})$$

Compute the exact probabilities of having 1 and 2 components functioning out of 2 available as shown below

$$R_e(1,2) = p_1 q_2 + q_1 p_2 \quad (\text{B.9})$$

$$R_e(2,2) = p_1 p_2 \quad (\text{B.10})$$

By substituting Equations B.11 and B.10 in B.9, the exact probability of 2 components functioning out of 3 available can be rewritten as shown below

$$R_e(2,3) = R_e(1,2) p_3 + R_e(2,2) q_3 \quad (\text{B.11})$$

Equation B.12 suggests a recursive algorithm to compute the exact probability of having  $i$  components functioning out of  $j$  available with  $i \leq j$ :

$$R(i, j) = R_e(i, j-1) q_j + R_e(i-1, j-1) p_j \quad (\text{B.12})$$

Mathematical induction will be used to show the above recursive algorithm. First the algorithm will be tested for  $j = 1$

$$R_e(1,1) = R_e(1,0) q_1 + R_e(0,0) p_1 \quad (\text{B.13})$$

By definition  $R_e(1,0) = 0$  and  $R_e(1,1) = p_1$ , which is the trivial solution when there is only one component available with reliability  $p_1$ . If the probability of having  $i$  components functioning out of  $n$  available,  $R_e(i, n)$ , is known the induction will be used to construct the  $R_e(i, n+1)$  scenario. The  $j = n+1$  scenario means that an extra component is added to the system as means of redundancy. Therefore this component  $n+1$  could be either functioning or broken.

The probability of the subsystem composed of  $n+1$  components in which the  $n+1$  component is broken and there are  $i$  components functioning can be written as  $R_e(i, n) q_{n+1}$ .

The probability of the subsystem composed of  $n+1$  components in which the  $n+1$ st component is functioning can be written as  $R_e(i-1, n) p_{n+1}$  where  $R_e(i-1, n)$  is the probability of having  $i-1$

components functioning out of  $n$  available since the  $n+1$  component is functioning. Then the probability of having  $i$  components out of  $n+1$  available can be written as

$$R_e(i, n+1) = R_e(i, n)q_{n+1} + R_e(i-1, n)p_{n+1} \quad (\text{B.14})$$

Equation B.15 is the same as applying the recursive algorithm shown in Equation B.13 to the problem of finding the exact probability of having  $i$  components functioning out of  $n+1$  available.

The table below shows how the recursive algorithm works in matrix form.

	0	1	2	3	4
0	1	$q_1$	$q_1q_2$	$q_1q_2q_3$	$q_1q_2q_3q_4$
1		$p_1$	$p_1q_2+q_1p_2$	$q_1q_2p_3+(p_1q_2+q_1p_2)q_3$	$q_1q_2q_3p_4+(q_1q_2p_3+[p_1q_2+q_1p_2]q_3)q_4$
2		0	$p_1p_2$	$p_1p_2q_3+(q_1p_2+p_1q_2)p_3$	$[p_1p_2q_3+(q_1p_2+p_1q_2)p_3]q_4+[q_1q_2p_3+(p_1q_2+q_1p_2)q_3]p_4$
3			0	$p_1p_2p_3$	$p_1p_2p_3q_4+[p_1p_2q_3+(q_1p_2+p_1q_2)p_3]p_4$
4		0	0	0	$p_1p_2p_3p_4$

**Figure B.1 Intermediate reliability calculation**

The above recursive algorithm was programmed to test whether or not it would be suitable to be used to compute the reliability of a crosscut and consequently the block cave mining system. The individual draw points reliabilities presented in Table B.1 were used to test the initial algorithm. The resulting intermediate entries reliabilities are shown in Table B.2.

**Table B.1 Draw point reliabilities to compute the entries  $R_e(i, j)$**

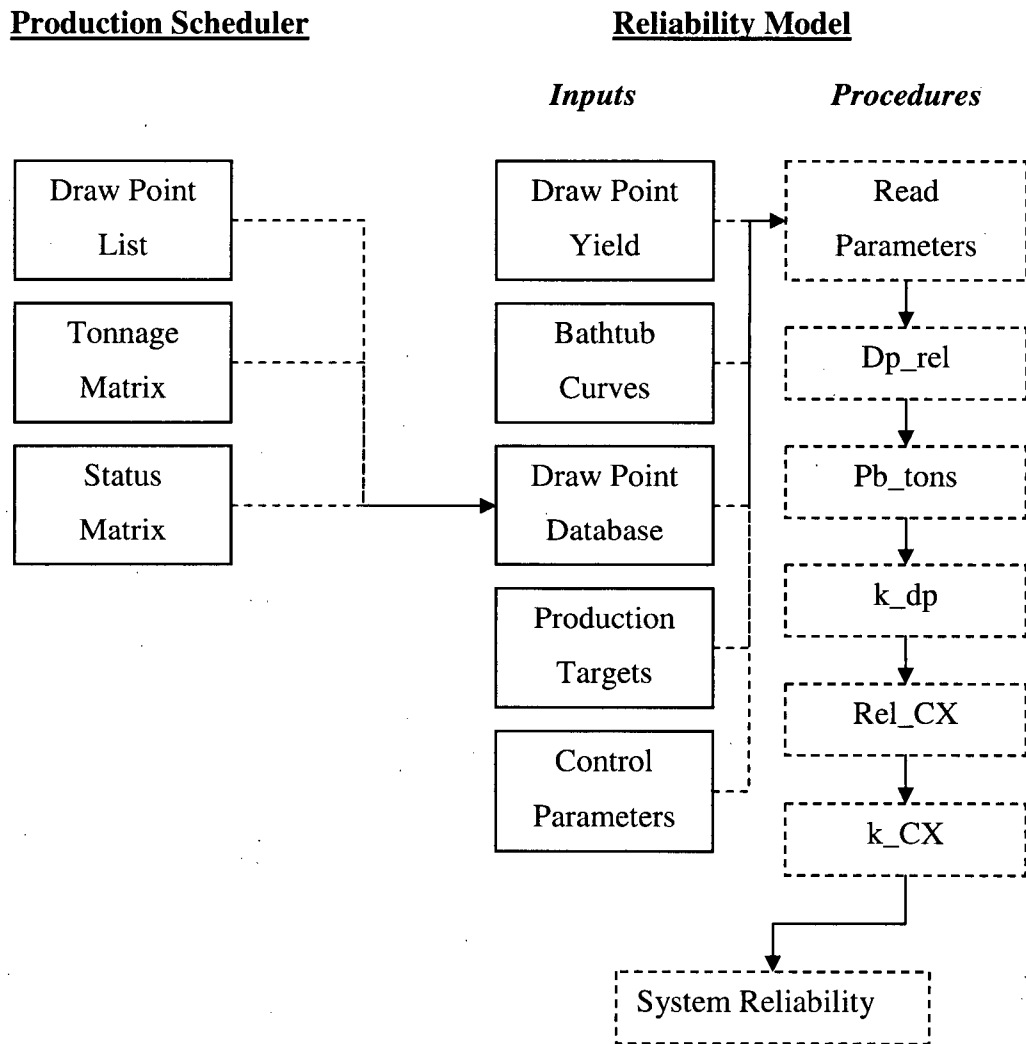
Dpt	Ri
1	0.82
2	0.79
3	0.77
4	0.76
5	0.75
6	0.73
7	0.73
8	0.72
9	0.70
10	0.67

**Table B.2 Intermediate entry reliabilities  $R_e(i, j)$**

$R_e(i, j)$	0	1	2	3	4	5	6	7	8	9	10
0	1.00	0.18	0.04	0.01	0.00	0.00	0.00	0.00	0.00	0.00	0.00
1	0.00	0.82	0.32	0.10	0.03	0.01	0.00	0.00	0.00	0.00	0.00
2	0.00	0.00	0.65	0.39	0.17	0.06	0.02	0.01	0.00	0.00	0.00
3	0.00	0.00	0.00	0.50	0.42	0.23	0.11	0.05	0.02	0.01	0.00
4	0.00	0.00	0.00	0.00	0.38	0.41	0.28	0.15	0.08	0.04	0.02
5	0.00	0.00	0.00	0.00	0.00	0.29	0.38	0.30	0.20	0.11	0.06
6	0.00	0.00	0.00	0.00	0.00	0.00	0.21	0.33	0.31	0.23	0.15
7	0.00	0.00	0.00	0.00	0.00	0.00	0.00	0.15	0.28	0.30	0.25
8	0.00	0.00	0.00	0.00	0.00	0.00	0.00	0.00	0.11	0.23	0.28
9	0.00	0.00	0.00	0.00	0.00	0.00	0.00	0.00	0.00	0.08	0.18
10	0.00	0.00	0.00	0.00	0.00	0.00	0.00	0.00	0.00	0.00	0.05

Finally to compute the  $k$ -out-of- $n$  system reliability, the rows  $k$  to  $n$  of column  $n$  are summed up. For example for the system 5-out-of-10 the system reliability is computed by adding up the shaded rows of Table B.2 resulting in a reliability of 97.9%.

A flow chart of the proposed procedure to compute the system reliability embedded in the production schedule is shown in Figure C.1.



The components of the proposed system to compute block cave production schedules reliability are separated into two categories components on the production scheduler side and components on the reliability model

- **Draw point list** corresponds to the list of the draw points including their names, crosscuts at which they belong, default draw rate, priority based on the draw strategy. Figure C.2 shows an example of the draw point list generated on the production scheduler

Draw Point	XC
P13-01E	P13
P13-01W	P13
P13-02E	P13
P13-02W	P13
P13-03E	P13
P13-03W	P13
P13-04E	P13
P13-04W	P13

**Figure C.2 Draw point list used in the reliability model**

- **Status matrix** corresponds to the detailed draw point/period report of status as an output of a production schedule simulation. Every row of this report represents a draw point and every column a period of the production schedule. Figure C.3 shows an example of the status matrix generated as an output of the production scheduler.

Draw Point	May,03	Jun,03	Jul,03	Aug,03	Sep,03	Oct,03	Nov,03	Dec,03
L01W01	C	C	C	C	A	A	A	A
L01W02	C	C	C	C	C	A	A	A
L01W03	C	C	C	C	A	A	A	A
L01W04	C	C	C	C	C	A	A	A
L01W05	C	C	C	C	C	C	A	A
L01W06	C	C	C	C	A	A	A	A
L01W07	C	C	C	C	C	A	A	A
L01W08	C	C	C	C	A	C	A	A
L02E01	C	C	C	A	A	A	A	A
L02W01	C	C	C	A	A	A	A	A
L02E02	C	A	C	A	A	A	A	A
L02W02	A	C	C	A	A	A	A	A
L02E03	C	C	C	A	A	A	A	A
L02W03	C	C	C	A	A	A	A	A
L02E04	C	C	C	A	A	A	A	A
L02W04	A	C	C	A	A	A	A	A
L02E05	A	C	C	A	A	A	C	A
L02W05	C	C	C	A	A	A	A	A
L02E06	C	C	C	A	A	A	A	A
L02W06	A	C	C	A	A	A	A	A
L02E07	C	C	C	A	A	A	C	A

**Figure C.3 Status matrix used in the reliability model**

- **Tonnage matrix** corresponds to the detailed draw point/ period report of tonnage as an output of production schedule simulation. Every row of this report represents a draw point and every column a period of the production schedule. Figure C.4 shows an example of the tonnage matrix generated as an output of the production scheduler.

Draw Point Name	Oct,02	Nov,02	Dec,02	Jan,03	Feb,03	Mar,03	Apr,03	May,03
L01W01	0	0	0	0	0	0	0	0
L01W02	0	0	0	0	0	0	0	0
L01W03	0	0	0	0	0	0	0	0
L01W04	0	0	0	0	0	0	0	0
L01W05	0	0	0	0	0	0	0	0
L01W06	0	0	0	0	0	0	0	0
L01W07	0	0	0	0	0	0	0	0
L01W08	0	0	0	0	0	0	0	0
L02E01	0	0	0	0	0	0	0	0
L02W01	0	421.3821	0	386.6383	0	0	0	0
L02E02	0	0	0	322.1986	37.13389	0	0	0
L02W02	0	144.157	2886.905	4216.199	0	244.8	173.2407	47.51491
L02E03	0	0	0	211.7305	0	0	10.19063	0
L02W03	0	44.35601	1931.679	2899.787	0	1020	0	0
L02E04	0	0	0	4354.284	0	0	0	0
L02W04	0	1053.455	774.7942	386.6383	0	367.2	81.52501	38.01193
L02E05	0	0	0	478.695	0	0	0	114.0358
L02W05	170.7322	898.2092	2504.814	193.3191	0	1060.8	30.57188	0
L02E06	0	0	0	0	0	10.2	0	0

**Figure C.4 Tonnage matrix used in the reliability model**

There are two categories of components on the reliability model of the proposed system: input data and procedures to actually compute the system reliability.

- **Draw point yield** corresponds to the curve that defines the maximum productivity of a draw point as function of its maturity, measured in cumulate tonnage drawn to date. Several draw point yield curves can be input in the reliability model to represent the swell factor and fragmentation characteristics of different sectors of the mine. Figure C.5 shows an example of a yield curve

Dpt Maturity	Yield
0	7,500
2,493	7,500
8,774	7,500
14,082	7,500
19,416	7,500
24,939	7,500
30,546	7,500
36,060	7,500
41,605	7,500
46,960	7,500
52,753	7,500
58,084	7,500
63,275	7,500
109,732	7,500
200,000	7,500

**Figure C.5 Draw point yield curve used in the reliability model**

- **Draw point ROCOF curve** corresponds with the evolution of the ROCOF over time for a given draw point or group of draw points. Different areas of the mine may have different ROCOF curves as it has been shown in previous section of this dissertation. Therefore the system allows several ROCOF curves to be input as part of the initial set up. Figure C.6 shows an example of ROCOF curve used as part of the reliability model.

Dpt Maturity	Fail rate
0	0.59
10000	0.59
20000	0.53
30000	0.50
40000	0.48
50000	0.47
60000	0.46
70000	0.45
80000	0.44
90000	0.43
100000	0.43
110000	0.42
120000	0.42
130000	0.41
140000	0.41
150000	0.40

**Figure C.6 Draw point ROCOF curve used in the reliability model**

- **Draw point database** corresponds with the integration of the draw point list generated as part of the production scheduler, cumulative tonnage before starting the run per draw point, draw point ROCOF curve, draw point yield curve per draw point, default ROCOF per draw point. Figure C.7 shows an example of how the draw point information is integrated to make it available for the reliability model.

Draw Point	XC	CumTJan02	Priority	ROCOF	Status	Tons	Bathtub	Yield
P13-01E	P13	101,071	278	0.16	A	8000	1	1
P13-01W	P13	91,177	279	0.18	A	8000	1	1
P13-02E	P13	109,168	280	0.15	A	8000	1	1
P13-02W	P13	94,541	281	0.18	A	8000	1	1
P13-03E	P13	120,914	282	0.20	C	8000	1	1
P13-03W	P13	125,169	283	0.24	A	8000	1	1
P13-04E	P13	157,887	284	0.37	C	8000	1	1
P13-04W	P13	145,910	285	0.40	C	8000	1	1

**Figure C.7 Draw point database used as part of the reliability model**



- **Production targets matrix** corresponds to the total tonnage target per period and the production per crosscut as percentage of the total tonnage per period. Figure C.8 shows an example of the production targets imported in the reliability model.

Period	Target	P13	P14	P15	P16	P17
1	1,085,000	0.03	0.02	0.01	0.02	0.03
2	1,147,000	0.03	0.02	0.01	0.02	0.03
3	1,209,000	0.03	0.02	0.01	0.02	0.03
4	1,271,000	0.03	0.02	0.01	0.02	0.03
5	1,333,000	0.03	0.02	0.01	0.02	0.03
6	1,395,000	0.03	0.02	0.01	0.02	0.03
7	1,457,000	0.03	0.02	0.01	0.02	0.03
8	1,519,000	0.03	0.02	0.01	0.02	0.03

**Figure C.8 Tonnage targets per period used in the reliability model**

- **List of Control parameters** corresponds with the settings to achieve even draw performance such as the minimum number of draw points per crosscut per call, periods to compute reliability, nominal tonnage production per crosscut, number of draw point ROCOF curves, number of draw point yield curves, switch to use or not production per crosscut instead of the nominal production per crosscut, switch to run past historical tonnages or forward estimation.
- **Read parameters** corresponds with the procedure to actually read all the input information and store it in different arrays.
- **Dp\_rel** corresponds with the procedure to compute draw point reliability based on ROCOF
- **Pb\_tons** corresponds with the procedure to compute crosscut production target based on proportions
- **k\_dp** corresponds with the procedure to compute the number of draw points per CX to achieve crosscut production target
- **Rel\_CX** corresponds with the procedure to compute crosscut reliability
- **k\_CX** corresponds with the procedure to compute the number of crosscuts to achieve total production target
- **R\_Sys** corresponds with the procedure to compute the system reliability

The procedure to compute crosscut reliability and system reliability is the same since both systems are *k-out-of-n* non identical components. It is important to note that as a result of

**Rel\_CX** and **R\_Sys** procedures the reliability as well as the expected tonnage of the system is computed. For the general case of crosscut reliability the **Rel\_CX** procedure simulates a number of different scenarios of  $i$  draw points working out of the  $n$  available. In fact there is an input parameter called *samples*, which corresponds with the number of random numbers used to compute the most likely crosscut productivity.